≋USGS
science for a changing world

The Phosphoria Formation at the Hot Springs Mine in Southeast Idaho: A Source of Selenium and Other Trace Elements to Surface Water, Ground Water, Vegetation, and Biota[1]

By D.Z. Piper[2], J.P. Skorupa[3], T.S. Presser[4], M.A. Hardy[5], S.J. Hamilton[6], M. Huebner[4], and R.A. Gulbrandsen[7]

Open File Report 00-050

2000

U.S. DEPARTMENT OF THE INTERIOR
U.S. GEOLOGICAL SURVEY

[1] Prepared as part of the Western U.S. Phosphate Project and in collaboration with U.S. Bureau of Land Management, U.S. Forest Service, Agrium U.S. Inc., FMC Corporation, J.R. Simplot Company, Rhodia Inc., Solutia Inc.
[2] U. S. Geological Survey (M/S 902), 345 Middlefield Road, Menlo Park, CA 94025
[3] U.S. Fish and Wildlife Service, 2800 Cottage Way, Sacramento, CA., 95825
[4] U. S. Geological Survey (M/S 435), 345 Middlefield Road, Menlo Park, CA 94025
[5] U.S. Geological Survey, 230 Collins Road, Boise, ID 83702.
[6] U.S. Geological Survey, 31247 436th Ave., Yankton, SD 57078
[7] 3815 Fourth Avenue South, Great Falls, MT 59405

CONTENTS

FIGURE CAPTIONS

1. Location map of the northwest United States, showing the extent of the Phosphoria Formation, location of evaporite deposits to the east, and paleolatitudes during Permian time. In the land areas of Montana and central Wyoming, deposits include red beds. The Hot Springs Mine and location of other sections analyzed earlier are shown by closed squares (Medrano and Piper, 1995, Piper, 2000). Figure is adapted from Sheldon (1964).

2. Stratigraphic column of the Meade Peak Member of the Phosphoria Formation at the Hot Springs Mine. Thicknesses (0 to 5236) are in centimeters; sample numbers give level at which samples (53-series and 75-series) were collected. Each sample represents about a 10 to 25 cm interval. Position of

ore and waste zones are only approximate. However, the upper ore zone seems to extend higher into the section here than at other sites. No distinction has been made between calcite and dolomite, although the carbonate is predominantly dolomite (Table 3). Lithologies are based on report by Gulbrandsen (1979) and on chemical analyses given in Table 4 and in Gulbrandsen (1979).

3. Relation between CO_2 measured and CO_2 calculated, which is based on the stoichiometry and concentration of each carbonate-bearing component (Tables 2 and 3).

4. Relation between La measured by ICP-AES and ICP-MS in the 75-series of samples.

5. Relation between U and apatite. Measured values are plotted in (a) and $\log_{10}$ of values are plotted in(b). Sample symbols are the same as in Figure 3>

6. Relations between Al_2O_3 and SiO_2 (a), CaO (b), K_2O (c), and Fe_2O_3 (d). Solid curves represent best estimate of relations, based on analyses at other sites (Medrano and Piper, 1995).

7. Relations between detritus and selected trace elements. Sample symbols and curves are the same as in Figure 6.

8. Relations between detritus and a selected group of those trace elements that show a strong enrichment above the detrital contribution, which is listed in Table 5. Sample symbols and curves are the same as in Figure 6. The minima at this site are different than those for the other sites. This is seen most strongly in frame "f", for which the As minimum at Hot Springs Mines (not shown) extrapolates to an As value in detritus of 10 ppm (Table 5), less than at the other sites, where the minimum (solid curve) gave a value of 32 ppm As in detritus (Medrano and Piper, 1995)

9. REE patterns of samples with less than 25% apatite (frames a through d) and greater than 25 percent apatite (frames e through h). See Figure 2 for identification of zones. Y-axis is 3-cycle in each frame. Note grouping in frame (g).

10. Relation between detritus and selected REE. Sample symbols and curves are the same as in Figure 6.

11. Relation between apatite and CaO (a), Ce anomaly (b), F (c), and La (d). Sample symbols and curves are the same as in Figure 6, except in frame (d), in which samples from the ore and waste zones are shown. The broken curve is the least-squares best-fit for the center waste only.

12. Relation between height above the base of the Meade Peak Member, the Ce anomaly, and normalized Yb:Sm ratios of samples with greater than 25 percent apatite. Ore zones are shown by shading (Fig. 2).

13. Relation between CO_2 and CaO (a) and MgO (b). Curves represent stoichiometric relations as defined in Table 2. Sample symbols are the same as in Figure 6.

14. Relation between the sum of carbonate minerals and the Ce anomaly for the 75-series of samples. Note that the relation divides the samples into two distinct populations.

15. Relations between organic matter, sulfur, nitrogen, and selected trace elements. Solid curves give relations in modern plankton, broken curves give least-squares best-fit, along with standard deviation. A heteroscedastic distribution of residuals is evident in essentially all trace-element plots. Sample symbols are the same as in Figure 6.

16. Distribution of selected components and trace elements versus depth, i.e., height above the base of the Meade Peak Member of the Phosphoria Formation at the Hot Springs Mine. The approximate position of the two ore zones, seen at other sites in SE Idaho, is shown by shading.

17. Preliminary results of selenium in coot eggs and associated water. Site A is at the lower reservoir northwest of Conda: sites B are at the upper reservoir east of Smoky Canyon Mine; site C is at South Pond, Rasmussen Valley. The upper broken curve gives the Se concentration in duck eggs above which 100% teratogenesis in embryos is observed; the lower curve gives the Se concentration above which

2

the incidence of teratogenesis increases with increase in concentration. The two values are based on this and other studies. Se was analyzed by fluorescence-based microdigestion. Water samples were unfiltered. The aim of the method is to ascertain the form of Se in different media. Although the data are preliminary, they compare well with data collected by various other methods used by the U. S. Fish and Wildlife Service.

TABLE TITLES

1. Summary of detection limits, accuracy, and precision for elements analyzed by the different analytical techniques, as determined by repeated analysis of rock standards. All procedures are discussed in detail by Baedecker (1987).

2. Formulas used to calculate the normative components and total CO_2, based on measured concentrations of major-element oxides (Table 4). See Table 5 for the trace-element concentrations of the detrital component. The amount of H_2O in organic matter was selected to give a carbon concentration of 71.6% and is not intended to imply a concentration of hydrogen or oxygen in the organic component as shown.

3. Major components (in percent) of samples from the Hot Springs Mine, based on element-oxide compositions. Lithology is taken from Gulbrandsen (1979). Identification of major units is based on lithology of all 304 samples collected by Gulbrandsen and approximate thicknesses as compared to those at the Enoch Valley Mine (Piper 2000).

4. (a)Major-elements and oxides (in percent) and trace elements (in parts per million) in the 75-series of samples. Thicknesses (in meters) are cumulative. Blanks indicate no analysis. Numbers in () give detection limits in cases for which concentrations were less than the detection limit. Such values are then listed as mid-values to zero. (b) Major elements and oxides, in per cent, and minor elements, in parts per million, in the 53-series of samples. Thicknesses are cumulative, in meters. Blanks indicate no analysis

5. Major-oxide composition (in percent) and trace-element composition (in parts per million) of terrigenous, detrital fraction. Blanks in column 5 indicate that the concentration of an element was determined by a means other than the use of a minimum curve. Blanks elsewhere indicate that no value was listed, or that it could not be determined.

6. Varimax orthogonal transformation solution, principal component factor extraction method, using Statview[tm]II software. Log_{10} of measured values was used rather than raw data. Values greater than 0.5 are in bold. Table 6a gives the values for the 75-series of samples and 6b values for the 53-series of samples. The two are given separately because of the format of Statview[tm]II; it cannot handle blanks in a table.

7. Concentrations of trace elements in marine plankton (in parts per million) and in seawater (in parts per billion) at approximately 2000-m depth in the Pacific Ocean (Martin and Knauer, 1973; Boyle and others, 1976, 1977; Boyle, 1981; Elderfield and others, 1981; Bruland, 1983; Collier, 1984, 1985; de Baar and others, 1985; Palmer, 1985; Brumsack, 1986).

8. Selenium in source rocks, soil, water, sediment, vegetation, and biota in southeast Idaho. Concern levels and levels at which selenium in solids and water extract constitute a hazardous waste and water quality standards are also given. Sample designations are taken from reports cited, with only minor changes.

Abstract

Major-element oxides and trace elements in the Phosphoria Formation at the Hot Springs Mine, Idaho were determined by a series of techniques. In this report, we examine the distribution of trace elements between the different solid components—aluminosilicates, apatite, organic matter, opal, calcite, and dolomite—that largely make up the rocks. High concentrations of several trace elements throughout the deposit, for example, As, Cd, Se, Tl, and U, at this and previously examined sites have raised concern about their introduction into the environment via weathering and the degree to which mining and the disposal of mined waste rock from this deposit might be accelerating that process. The question addressed here is how might the partitioning of trace elements between these solid host components influence the introduction of trace elements into ground water, surface water, and eventually biota, via weathering? In the case of Se, it is partitioned into components that are quite labile under the oxidizing conditions of subaerial weathering. As a result, it is widely distributed throughout the environment. Its concentration exceeds the level of concern for protection of wildlife at virtually every trophic level.

INTRODUCTION

The Phosphoria Formation in the northwest United States, a marine sedimentary deposit of Permian age (Mansfield, 1916; Sheldon, 1957; McKelvey and others, 1959; Gulbrandsen, 1966; Murata and others, 1972; Maughan, 1976), extends over thousands of square kilometers (Fig. 1). During the last half of this century, it has provided approximately five percent of the world's annual demand for phosphate. Several trace elements exhibit high concentrations, relative to their concentrations in most sedimentary deposits. Their partitioning (1) into a residuum of the original marine organic matter, carbonate fluorapatite, less so calcite, dolomite, chert, and possibly sulfide minerals—the marine source fraction—and (2) into quartz/aluminosilicate debris—the terrigenous detrital source fraction—can be clearly ascertained.

The aim of this study is to examine the partitioning of trace elements between these host solids and how that might contribute to trace-element dispersal in the environment at the present time under oxic conditions of weathering. We have show in earlier reports (Piper and Medrano, 1994; Piper, 2000) that interelement relations of trace elements in the Phosphoria Formation identify their sources as (1) detrital debris derived from the terrestrial environment, (2) planktonic debris that settled out of the photic zone of the water column and onto the sea floor, and (3) a hydrogenous fraction derived largely from bottom water of the basin via inorganic reactions. In contrast to these Permian sources, however, present-day partitioning of trace elements into their

host phases, which was achieved largely following deposition, should contribute to trace-element reactivities during weathering. Trace elements hosted by labile components, e.g., Se in organic matter (Piper, 1999), pyrite, and sphalerite, and as elemental Se (Grauch and others, 1999), might quickly enter ground and surface water as mining exposes increasing amounts of waste rock to the oxic conditions of subaerial weathering. Because Se (and possibly other trace elements) can be highly toxic (Presser, 1994; Skorupa, 1998; USDOI, 1998) and it is now present throughout the ecosystem of this mining region, the weathering of mine waste may pose a hazard to livestock and wildlife in southeast Idaho (Anonymous, 1999).

SAMPLING AND PHYSIOGRAPHIC SETTING

Sample Selection

The underground Hot Springs Mine is located at 42° 13.109´ N and 111° 24.745´ W (Fig. 1). Samples were collected from a mine adit at the northern end of Bear Lake. The samples come from the Meade Peak Phosphatic Shale Member of the Phosphoria Formation, the major phosphate-bearing member of the formation in this general area of Idaho. Samples were collected at approximately 10-cm intervals and analyzed initially by semi-quantitative techniques (Gulbrandsen, 1979). Samples examined in this study were taken from this collection, at approximately a 1-m interval, and analyzed by quantitative techniques. A stratigraphic section (Fig. 2) shows sample positions.

Geologic and Oceanographic Setting

The Phosphoria Basin was located in what is now eastern Idaho, western Wyoming, northern Utah, northeastern Nevada, and southwestern Montana. Paleomagnetic data (Sheldon, 1964) indicate that the basin was at 3° to 9° N latitude in Permian time (Fig. 1), along the western margin of the North American craton. Palinspastic reconstruction of Mesozoic and Early Cenozoic shortening might extend the basin in an east-west direction, but extension during Late Cenozoic and Tertiary time apparently compensated for much of this shortening (Levy and Christie-Blick, 1989). Deposition occurred over 10 my (Wardlaw and Collinson, 1984; Murchey and Jones, 1992), in this expansive, epicratonic basin. The Meade Peak Member of the formation, the most

phosphatic enriched member and the unit examined in this study, accumulated over a period of approximately 7.2 my. Paleontologic evidence further shows that deposition occurred at an ocean depth of a few hundred meters, possibly as shallow as 200 meters (Yochelson, 1968).

This member of the formation now consists of organic-carbon-enriched phosphatic mudstone, siliceous mudstone, phosphorite, limestone, dolomite, and chert (McKelvey and others, 1959). At other sites examined for their geochemistry (Medrano and Piper, 1995), Conant Creek, the easternmost site in central Wyoming (Fig. 1), is a carbonate-enriched facies, possibly of shallow-water origin. Mud Spring, the westernmost site, is largely a siliceous mudstone facies, possibly deposited in deeper water (McKelvey and others, 1959). The formation at the Hot Springs Mine and at other intermediately located sites consists of these units plus relatively thick phosphorite units. The lithology has suggested to some that the deposit accumulated under conditions of intense primary productivity, typical of the coast of Peru. However, this conclusion has been based solely on the current composition of the deposit, rather than on an interpretation of the oceanographic conditions at the time of deposition, which incorporates rates of reactions. In the case of the Meade Peak Member, for example, its average accumulation rate suggests that primary productivity in the basin was no more than moderate, in the range of 0.5 g carbon m^{-2} per day (Piper, 2000), which is typical of ocean-margin basins of today (Berger and others, 1988). A major difference with modern basins was an extremely low rate of accumulation of terrigenous debris in the Phosphoria Basin, resulting in only slight dilution of the seawater-derived fraction by terrigenous debris.

ANALYTICAL TECHNIQUES AND DATA EVALUATION

Major-Element-Oxide Analyses

Samples are aliquants of ground powders dried at 60°C. Analyses were made on two series of samples. The first, the 75-series, was analyzed by inductively coupled plasma-atomic-emission spectroscopy (ICP-AES) after acid digestion (Lichte and others, 1987). The second series, the 53-series, was analyzed earlier by quantitative DC arc emission spectrography (Golightly and others, 1987). Water (H_2O+ and H_2O-) was measured only on the 53-series (Jackson and others, 1987). All analytical techniques are reported in Table 1 and discussed in detail in Baedecker (1987).

The limit of detection and the precision and accuracy of each analytical technique has been determined by repeated analyses of rock standards by several analytical techniques (Table 1). A strong correlation between CO_2 measured and CO_2 calculated (Fig. 3), by summing the carbon contribution by each CO_2-bearing component (apatite plus dolomite plus calcite) based on their stoichiometry (Table 2) and concentration (Table 3), suggests that the accuracy of each elemental analysis given in Table 1 represents an upper limit. The slightly lower values for the 75-series represents a possible systematic error in the measurements of CaO in these samples (see p. 12-13 below).

Components in each sample (Table 3) were determined from major-element-oxide data based on a constant stoichiometry for each component (Table 2). As each successive calculation compounds errors in the original data, evaluating the major-element data becomes crucial. In the worst case, total CaO is used to calculate the concentration of calcite, but only after adjusting, in order, for the CaO contribution by the detrital fraction, the CaO contribution by apatite, and the CaO contribution by dolomite. Therefore, the uncertainty in the calculation of calcite in a sample is dependent upon the uncertainty in the measurements of CaO, as well as of Al_2O_3 (used to calculate the concentration of the detrital fraction), P_2O_5 (used to calculate the concentration of apatite), and MgO (used to calculate the concentration of dolomite).

The data have been evaluated further by comparing analyses of individual elements made by more than one technique for the other sections examined by Medrano and Piper (1995). In the earlier work (Medrano and Piper, 1995; Piper and Isaacs, 1995), x-y plots of individual elements measured by different techniques showed agreement within 5 percent of the one-to-one line in 75 percent of the cases. Analytical results for P_2O_5, measured by wet chemistry are in excellent agreement with more recent measurements made by XRF (Medrano and Piper, 1995). The ICP-AES P_2O_5 data for the Wheat Creek and Fontenelle Creek sections are higher by approximately 13 percent and 9 percent, respectively, than the XRF data. These deviations suggest a systematic error in either the XRF or ICP-AES data for P_2O_5, an error that the Hot Springs Mine data might also have. Results for the other sections gave far better results. The CO_2 plot (Fig. 3) certainly suggests that the Hot Springs Mine data are better as well, despite the apparent offset of the 75-series data.. The analyses of the other major oxides also are in close agreement (Medrano and Piper, 1995).

Trace-Element Analyses and Treatment

In the 75-series of samples, trace elements were determined by ICP-AES and by inductively coupled plasma mass spectroscopy (ICP-MS), in the case of the rare earth elements (Table 4a). Selenium was measured by hydride-generation atomic absorption. Trace elements in the 53-series of samples (Table 4b) were determined by DC arc emission spectrography. The limits of detection, precision, and accuracy are given in Table 1.

La analyses give a measure of the quality of trace-element data. La in the 75-series of samples was analyzed by ICP-MS and ICP-AES. The plot of the two sets of values (Fig. 4) gives similar results to the x-y plots for the major-element oxides analyzed by ICP-AES and XRF, $\sigma \geq 0.98$ (Piper and Isaacs, 1995), and a similar deviation of ≤ 5 percent from the 1:1 curve, as reported earlier (Medrano and Piper, 1995)

The log_{10} of the measured values is used in the evaluation of the partitioning scheme. Linear plots of the raw data often show increasing scatter at high concentration levels; the data are heteroscedastic. That is, residuals of variance are higher at high concentrations than at low concentrations, rather than showing a normal distribution over the full range of concentrations. Such a distribution violates the assumption of homoscedasticity, or normal distribution of residuals, an assumption made in the calculation of the test of significance. This is illustrated by the plot of U versus apatite and the plot of the log_{10} of measured values (Fig. 5). Of course, an additional reason to plot the log_{10} of the data is that the procedure gives equal weight to samples with low elemental concentrations as it gives to samples with high elemental concentrations.

Miscellaneous Analyses

Total sulfur and total carbon, evolved as oxides during combustion, were measured by infrared absorption (Table 1; Jackson and others, 1987). Carbonate carbon was measured as CO_2 by coulometric titration (Jackson and others, 1987). Fluorine was determined by ion-selective electrode following fusion with $LiBO_2$ and dissolution in HNO_3 (Bodkin, 1977; Cremer and others, 1984). Ranges of detection, precision, and accuracy are given in Table 1.

Propagation of Errors

Reference to the propagation of errors was noted in the case of CaO above. Partitioning of trace elements between host components can introduce similar uncertainties. The uncertainty in the calculation of the detrital fraction of a trace element can be estimated for a worst case. The sources of error are (1) the measurement of the element in the bulk sample, (2) the measurement of Al_2O_3 in the bulk sample, (3) the calculation of the concentration of the detrital fraction based on the concentration of Al_2O_3 in the sample, and (4) the calculation of the concentration of the trace element in the detrital fraction. The error becomes significant for a trace element in samples

which contain only a small percentage of a trace element in this fraction, relative to its concentration in the bulk sample, and when the concentration of a trace element in the bulk sample approaches its limit of detection. Both apply to Ag and As and the former to Ba. The error in the measurement of Al_2O_3 in all samples should be approximately 3 percent, the concentration of Al_2O_3 being well above its limit of detection in almost all samples. The uncertainty in the measurement of As, in the range of concentrations for these samples, is approximately 15 to 20 percent. Also, it is not possible to establish its concentration in the detrital fraction to any better than about 50 percent, or about 15 ppm. These errors are additive. Thus, there is an approximate uncertainty in the calculation of the detrital fraction of As of approximately 65 percent of 30 ppm, or 20 ppm and an uncertainty in the measurement of As in the bulk sample of 6 ppm, on average. Addition of the two gives an error in the calculation of the average marine fraction of As of 30 ppm ± 25 ppm, a good reason not to consider As in detail. The bulk concentration of Ba is quite accurately measured, but not its concentration in the detrital fraction. This uncertainty imposes a large uncertainty on the calculation of the total Ba inventory, an uncertainty that cannot be well defined. Fortunately, the trace elements of greatest concern here have concentrations well above their detection limit in almost all samples, making possible a rigorous identification of their partitioning into the different components.

NORMATIVE CALCULATION OF ROCK COMPONENTS

The Phosphoria Formation is composed of two sediment fractions, a marine fraction derived from seawater and a detrital fraction of terrigenous origin (Piper and Medrano, 1994). Major components (Table 3) are bulk aluminosilicate/quartz debris—the detrital fraction—and dolomite, calcite, opal, or diagenetic quartz (i.e., biogenic silica), apatite, and organic matter—the marine fraction. Bulk major-element-oxide analyses are used to calculate the concentrations of these components in each sample (Table 4), assuming a constant composition for each (Table 2). Studies of modern and ancient sediments have shown that Al_2O_3 is the diagnostic major-element oxide of detrital material, being hosted essentially totally in this fraction of sediment (Isaacs, 1980 and references therein). The concentration of P_2O_5 is diagnostic of apatite, after making a small correction for a P_2O_5 contribution by the detrital fraction. MgO is diagnostic of dolomite, after making a similar adjustment. CaO is diagnostic of calcite, after adjusting for contributions by the detrital fraction, dolomite, and apatite. SiO_2 is diagnostic of biogenic silica, now opal-CT or even quartz, again following an adjustment for a detrital contribution to the bulk content of silica. Lastly, organic carbon gives the concentration of organic matter in each sample. Metal sulfides and (or) oxides may also be present, but their contribution to the bulk, major-element-oxide composition of the sediment is minor.

The concentration of each diagnostic element oxide in its major mineral component can be determined from x-y plots. These plots give the concentration of each component in a sample and provide a check on the assumption of constant composition. In the same way, plots of trace ele-

ments versus Al$_2$O$_3$, or versus the concentration of the detrital fraction itself, allow the trace-element composition of this fraction to be determined, but only in the case of those trace elements that exhibit a strong correlation with the detrital fraction which extrapolates to the origin. In the case of trace elements that do not correlate with the detrital fraction, their concentration in this fraction is determined from minima of the x-y plot, defined by the samples with the lowest trace-element concentration versus the detrital fraction. Excursion of the data from these minima then gives the contribution of trace elements by the marine fraction, on a sample by sample basis.

Partitioning of trace elements between the different components should largely determine the introduction of these elements into the ground water and surface water system via weathering and, in the case of bioreactive trace elements, eventually into the food web. Such partitioning can be estimated by either leaching experiments or by a statistical approach. We have chosen a statistical approach because of a strong loading of trace elements in both relatively insoluble and labile components. The labile components, such as organic matter (Littke and others, 1991), will release their complement of trace elements to solution under weathering conditions more easily, more quickly, than the relatively insoluble components such as apatite, chert, and terrigenous debris.

Detrital Fraction and Component

The detrital fraction is a mix of several minerals—detrital quartz, clay minerals, feldspars, micas, and minor amounts of accessory minerals such as zircon and rutile (Gulbrandsen, 1966). Even so, it can be treated as a single entity. Piper and Medrano, (1994) and Medrano and Piper (1995) established that this component has a rather constant composition at any one site, despite its complex mineral assemblage. It must have remained largely non-reactive during its passage through the ocean and remained largely unchanged during burial and weathering. Its source also remained the same even into the Triassic Period, with the deposition of the overlying Dinwoody Formation (McKelvey and others, 1959; Peterson, 1980). This component, then is a source phase as well as a current host phase for the major-element oxides and a portion of the trace elements.

The Hot Springs Mine samples also show a relatively constant composition for the detrital fraction. The plot of Al$_2$O$_3$ versus CaO show that the CaO:Al$_2$O$_3$ ratio is limited by a strongly defined maximum curve (Fig. 6b), which extrapolates to an Al$_2$O$_3$ concentration of 16.6 percent at a CaO concentration of zero and to 15.5 percent at a CaO concentration of 3.09 percent. The latter

9

values represent the Al_2O_3 and CaO concentrations in WSA (Wedepohl, 1969-1978; Table 5). The extrapolation gives an Al_2O_3 concentration in the detrital fraction that closely approximates its concentration in this fraction of the Phosphoria Formation at other sites (Table 5). The plots of Al_2O_3 versus K_2O and Fe_2O_3 (Figs. 6c and d) exhibit single trends that extrapolate to zero, further suggesting a constant composition for the detrital fraction. Their approach to the composition of WSA (Wedepohl, 1969-1978) indicates that the detrital fraction had a terrigenous source. In the case of iron, the small scatter of the Al_2O_3 versus Fe_2O_3 plot would seem to limit the amount of pyrite that might be present in the formation at this site to less than one percent.

Ba, Co, and Th also correlate with detritus (Fig. 7), i.e., Al_2O_3 x 6.0 (Table 2). They too suggest a composition for the detrital fraction similar to that of WSA (Table 5). Factor analysis (Table 6) offers an alternative approach to ascertain those elements hosted by the detrital fraction. The above trace elements again show a strong coherence with the detrital fraction. That is, factor 1, the factor with a strong detritus loading also shows strong loadings (greater than 0.75) for the above three trace elements as well as for B, Cs, Hf, Rb, Sc, and Ta and slightly weaker loadings (0.60 to 0.75) of Ce, Li, Mn. Somewhat unexpected is the strong loading of Ce on factor 1.

The concentration in the detrital fraction of any other trace element is determined from the detritus versus trace-element minimum , which represents the lowest apparent relation between the detrital fraction and that trace element. Extrapolation of the minima for Ag, As, Cu, Mo, Pb, Se, U, V, and Zn (Fig. 8) closely approach their concentrations in WSA (Table 5). In the cases of Cr, and Ni, the minima give higher concentrations than their WSA values (Table 5), relations seen also at other sites (Piper, 2000). This excess above the minima is interpreted to represent the marine fraction of trace elements. For Cr and Ni, a marine fraction may be present in all samples, pushing the minima for these elements above their WSA value. For these elements in most of the samples, the minima require that the marine contribution is large relative to the detrital contribution. As should be expected, these trace elements exhibit strong loadings on the factors dominated by a marine component, e.g., apatite and organic matter (factors two and three, respectively; Table 6).

The rare earth elements (REE) are plotted after normalizing the data to WSA values on an element-by-element basis (Piper, 1974), the REE pattern. The patterns of samples composed dominantly of the detrital fraction (for example, 188-76, 98-76, and 216-74, Table 3, Figs. 9a-d)

10

closely approach the shale pattern, thus requiring a REE composition for the detrital fraction that is also similar to WSA. This relation is seen as well in the minimum of the detrital fraction versus individual REE plots (Fig. 10). Extrapolation of the apatite versus Ce anomaly curve to zero (Fig. 11a), by definition the anomaly of WSA, further supports a REE concentration for the detrital fraction that is similar to WSA. The anomaly represents the offset of Ce within the REE pattern, relative to the value obtained by interpolating between La and Pr. It is defined as:

$$Ce^* = \log[(3Ce)/(2La + Pr)]. \tag{1}$$

Italics are used to denote values normalized to WSA on an element-by-element basis. This definition gives Ce depletions as negative values, Ce enrichments as positive values, and the same absolute value to a depletion and enrichment of equal offset.

Marine Fraction and Components

Calculation of the marine fraction of trace elements from minima of bulk trace-element versus detritus plots can be expressed for each sample by the following equation:

$$C = A - B \text{ x (terrigenous fraction)}, \tag{2}$$

where A = total trace-element content of a sample, B = trace-element contribution by the terrigenous fraction, and C = marine-derived trace-element contribution. It is not possible to determine the actual concentration of trace elements in each marine component, as most trace elements are distributed between several components. However, factor loadings (Table 6) and (or) linear correlations between the marine fraction of trace-elements and the different major marine components permit an estimate to be made. Also, such loadings lend support to the interpretation that this fraction of trace elements indeed has a marine origin.

Apatite

Apatite is the carbonate fluorapatite francolite (McClellan and Lehr, 1969). The CaO concentration of 55.5% is obtained from the extrapolation of CaO versus Al_2O_3 (Fig. 6b) and from the P_2O_5 versus CaO plot (Fig. 11a). Several samples from the 75-series fall below the minimum in Figure 11a, but electron microprobe analyses of two samples (unpublished data) support the relation shown by the 53-series in this study and by samples from the other sites (Medrano and Piper,

11

1995). Although CaO is present in this and other components and has almost the same concentration in calcite as it has in apatite, the CaO versus P_2O_5 plot (Fig. 11a) demonstrates that the bulk of the CaO must be in apatite. Their ratio of 1.37 given by this plot is similar to that for apatite from other sites (Medrano and Piper, 1995). A minor P_2O_5 concentration in the detrital fraction of 0.16 percent (Table 5), equal to its concentration in WSA (Wedepohl, 1969-78), and of 40.5 percent in apatite are supported by the P_2O_5 versus CaO relation (Fig. 11a). A CO_3^{2-} concentration (see next section) of 2.4 percent (Table 2) is taken from Gulbrandsen (1970). The fluoride content is between 3.3 and 3.5 percent (Fig. 11c), the same as the value of 3.43 percent reported by McClellan and Lehr (1969). The discrepancy between the 53-series and the 75-series data (Fig. 11c) is again resolved by the microprobe data. The microprobe data are similar to the 75-series data. As troubling as this and the CaO discrepancies are, they do not effect the calculation of the content of apatite in the samples nor the partitioning of trace elements into apatite.

Trace elements strongly incorporated into apatite, as determined by their strong loadings on factor 2 (Table 6) include Sr, U (Fig. 5), Y, and the REE, exclusive of Ce. Nonetheless, the relation between apatite and the La concentration in apatite (and the other 3+ valence REE) is quite complex (Fig. 11d). Whereas apatite within the center waste zone may have a relatively constant La content (La $\approx$ 600 ppm; R = 0.76), apatite-enriched samples within the ore zones (and the upper waste zone) have a different distribution and La content that does not exceed roughly 100pm. These relations demonstrate the difficulty of determining a single concentration for these and other trace elements in this and the other marine components. As apatite forms within the surface veneer of sediment (Kolodny, 1981; Burnett and others, 1988), the higher content of La in apatite from the ore zones than from the center waste zone would seem to reflect a pore-water instability within the very surface sediment driven by bottom water conditions (Piper, 2000).

The Ce anomaly exhibits a strongly negative correlation with apatite (Fig. 11b) that seems to limit the variation of the anomaly within the apatite itself. This relation was much stronger at the Enoch Valley Mine than here (Piper, 2000). Also, the anomalies of apatite enriched samples from the ore zones were slightly more negative than apatite from the waste zones at the Enoch Valley Mine, again a relation not seen at the Hot Springs Mine (Fig. 12). Extrapolation of the anomaly to

zero, at zero percent apatite (Fig. 11b), further gives the Ce anomaly for the detrital fraction, which is the value for terrigenous debris (Wedepohl, 1969-78; Piper, 1974).

The difference in the REE composition of apatite from the ore zones and center waste zone (Fig. 11d) extends to the REE patterns. In samples with greater than 25 percent apatite (Fig. 9e-h), the pattern for samples from the ore zones show a slight enrichment of the heavy REE, on average, over the samples from the center waste zone, best shown by the Yb:Sm ratios (Fig, 12). Compare, for example, the patterns in Figure 9f and 9g.

The samples with less than 25 percent apatite show strongly varying patterns (Fig. 9a-d). The samples with the lowest bulk concentrations, normalized values less than 0.5, correspond to the carbonate enriched samples. They too have negative Ce anomalies in most cases, but no consistency in a heavy REE enrichment. The Ce anomalies become less negative as the REE concentrations increase to normalized values of one. These samples, as noted above, are composed dominantly of the detrital fraction. The anomalies then increase as REE concentrations increase (normalized values greater than 1), owing to an increase in apatite in the range of 1 to 25 percent. This trend reflects simple mixing of the components—detritus, apatite, biogenic carbonate minerals, and biogenic silica (opal and/or quartz).

Carbonate Minerals

The plot of MgO and CaO versus CO_2 (Fig. 13) suggests that calcite and dolomite are stoichiometric (Table 2), even though the relations are complicated by CaO and MgO being present in the detrital fraction (Table 2) and CaO being present mostly in the apatite component (Fig. 11a). The correlation between CO_2 measured and CO_2 calculated (Fig. 3), for which dolomite and calcite represent the dominant hosts of CO_2, further supports the interpretation of a stoichiometric composition for both. Both are present at this site, dolomite being dominant in most samples (Table 3). The relation of CaO versus CO_2 (Fig. 13a) at low CO_2 concentrations further supports the interpretation of a CO_3^{2-} concentration in apatite of 2.4 percent. The slight offset of samples to the right of the curve for apatite requires a small amount of carbonate minerals admixed with apatite enriched samples. In samples from the Enoch Valley Mine there was a much clearer separation of the two groups (Piper, 2000).

The lack of correlation between trace elements and the carbonate minerals (Table 6) suggests that the trace element content of these two components is quite low. Nonetheless, the samples with little or no apatite, that have strong Ce anomalies (Fig. 11b), have high concentrations of dolomite plus calcite (Fig. 14); a reflection of the seawater anomaly (Goldberg and others, 1963; de Baar and others, 1985), the negative Ce anomaly of marine calcite (Palmer, 1985), but a relatively low overall concentration of REEs in marine calcite (Table 7). Thus, diagenetic alteration within the sediment pore water of the marine calcite and formation of dolomite do not seem to have altered significantly the REE pattern or concentrations of REE present in the original accumulating carbonate phases.

Organic Matter

The proportionality constant used to convert organic carbon to organic matter of 1.4 (Table 2) has been taken from Powell and others (1975). This value gave excellent closure for the sum of the major components to 100 percent for all sites studied (Medrano and Piper, 1995). Factor analysis (Table 6) shows a strong loading for organic matter and the trace elements Cr, Cu, Mo, Ni, Sb, Se and, less so Ag, As, Cd, V, and Zn onto factor three. Organic matter has only a slightly less strong loading on factor two, as do Cu and Cr, the factor which might be considered the apatite factor. However, the grouping of the above trace elements and sulfur and nitrogen on factor three as well suggests an association predominantly with organic matter. Conversely, the near absence of REE, Y, U, and Sr loadings on factor three, but strongly on factor two, supports their association with apatite, an association reported by others (Wright and others, 1987).

The plot of trace elements versus organic matter can allow for a possible estimate of the actual concentration of a trace element in organic matter, which is not possible to ascertain from factor analyses. The original organic matter has been shown (Piper, 1994, 2000; Piper and Medrano, 1994) to have had a composition similar to that of modern planktonic debris (Table 7). The trace-element concentrations in the organic matter suggested by these plots (Fig. 15) require strong trace-element enrichments in the residual organic matter over their concentrations in the original organic matter. These relations emphasize the contrast between the composition of the original planktonic source material of trace elements and the composition of the current residual organic-matter host. We should emphasize, however, that the plots show co-occurrence, which

may or may not reflect actual incorporation of trace elements into the organic component. Nonetheless, most of these trace elements did indeed have a marine planktonic source (Piper, 2000), which then seemingly required a strong enrichment in the organic component (see page 17).

A similar co-occurrence of trace elements and organic matter was reported by Leventhal (1989), Odermatt and Curiale (1991), and Piper and Isaacs (1995) for the Monterey Formation; by Swanson (1961) for Paleozoic organic-matter-enriched shales; and by Nissenbaum and Swaine (1976) for modern marine sediment. Lewan (1984), Moldowan and others (1986), and Odermatt and Curiale (1991) further examined the fractionation of metals between various phases of organic matter. For example, Lewan (1984) interpreted the V/(Ni+V) ratio in crude oils to reflect the Eh, pH, and sulfide activity of the depositional environment.

Biogenic Silica

Total silica was not measured in the 75-series of samples, precluding a direct calculation of biogenic silica. Biogenic silica can be estimated from the deficit of the analyses by estimating a single relation between Al_2O_3 and H_2O^+ plus H_2O^- in the 53-series (Table 4b) and the Al_2O_3 content of the 75-series, followed by the determination of the residual in the latter group (100% minus all oxides and elements). This estimate can then be compared to the silica values measured for the 53-series of samples, for which both Al_2O_3 and SiO_2 measurements are available Table 4b). The relation between Al_2O_3 and SiO_2 measured and estimated for these two groups of samples is similar (Fig. 6a). Also, the minimum for the 75-series of samples approaches the Al_2O_3:SiO_2 ratio of the detrital fraction measured for other sites (Medrano and Piper, 1995).

The trace-element content of biogenic silica is likely small (Martin and Knauer, 1973), similar to that of $CaCO_3$ (Table 7), although Elderfield and others (1981) measured a La value of 5.8 ppm and Ce anomaly of – 0.2 in a single sample of marine planktonic silica. The dominance of apatite as the host component for the REE and the absence of SiO_2 analyses in the 75-series of samples, unfortunately, precludes estimating the possible importance of silica as a host. At the Enoch Valley Mine site (Piper, 2000), the Rex Chert Member has a La concentration of approximately 15 ppm and a Ce anomaly of –0.71. The near absence of apatite in this member certainly suggests that the biogenic silica itself could host as much as 5 to 10 ppm La and have a negative Ce anomaly.

Miscellaneous

Microprobe analyses show minor amounts of both pyrite and sphalerite, the latter being the dominant sulfide mineral in several samples from this site. Unfortunately, it is not possible to calculate normative abundances of either from the bulk analyses (Table 4). Thus, no attempt is made to ascertain the trace-element composition of pyrite or sphalerite although their trace-element contributions to the total sample inventory should be small (for example, pyrite appears to constitute less than 1 percent of the total sample of all thin sections examined. The presence of factor five, which has strong loadings for Cd, Tl, V, and less so Zn (Table 6a), however, suggests the presence of an as yet undetermined host.

History of Trace-Element Partitioning

Partitioning of trace elements into marine host phases, particularly, into apatite and organic matter, occurs during diagenesis and, possibly, during later alteration of the originally deposited marine phases, in contrast to the partitioning of trace elements in the detrital fraction, which is an inherited feature of provenance. The slopes of the trace-element/organic-matter curves (Fig. 15) are unrelated to the composition of modern marine planktonic organic matter, similar to that observed for other deposits (Calvert and Price, 1983; Piper and Isaacs, 1995). They require that trace elements are enriched by more than 10-fold in the residual organic fraction over their concentrations in modern planktonic debris. Yet, the trace-element/organic-matter relations probably did not change drastically during settling through the water column. Fisher and Wente (1993, p. 671) concluded from a study of particulate organic matter in the modern ocean that Am, Ag, and Sn are:

"* * * retained sufficiently long, even by decomposing cells, to suggest that phytoplankton sinking as aggregates at rates of 100 m per day would effectively transport these metals hundreds of meters out of oceanic surface waters."

It can be concluded then that the current high trace-element content of sedimentary organic matter reflects uptake of trace elements by the residual organic phase during sediment diagenesis, or perhaps merely their retention. This interpretation parallels that advanced to explain the relation between C and S in organic matter of modern sediment (Mossmann and others, 1991). Also, apatite, which precipitates within the upper few centimeters of the sediment (Kolodny, 1981; Burnett

and others, 1988), must, by the very nature of its precipitation, acquire its REE and U signal from sediment pore water. The partitioning of trace elements among the different marine host phases of sediment should then reflect pore-water conditions, that is, diagenetic conditions, exceptions, as noted above, apparently being the carbonate minerals and possibly biogenic silica.

In the case of organic matter, depth profiles of organic carbon in modern sedimentary environments (Douglas and others, 1986; Froelich and others, 1988; Calvert, 1990), which have organic-matter contents similar to those of the Phosphoria Formation, suggest that organic matter is lost during early diagenesis, as HCO_3^-. Sediment-trap studies further reveal the loss of organic matter during early diagenesis (Fischer and others, 1986; Baldwin and others, 1998). Settling particulate matter collected at greater than 3,000 m depth in the ocean can have an organic-matter content approximately five times that of its detrital content, whereas surface sediment (0 to 10 cm) has approximately 50-fold more detritus than organic matter. This relation requires that as much as 95 percent of the organic matter that rains out of the water column is lost at the very surface. Ocean-margin areas have an even larger flux of organic matter to the sea floor owing to (1) a shallower sea floor (Suess, 1980; Sarnthein and others, 1988), (2) a higher primary productivity (Berger and others, 1988), and (3) a positive relation between the relative rain rate of organic matter and primary productivity (Baines and others, 1994). The estimated loss of organic matter from the sea floor of the Phosphoria Sea, that is, the accumulation rate versus the rain rate, is approximately 98 percent (Piper, 2000).

In oxic (Fischer and others, 1986) and mildly O_2-depleted environments (Shaw and others, 1990), a large fraction of associated trace elements can also be lost to the water column. The high content of trace elements in the Phosphoria Formation suggests that this was not the case for this deposit. That is, their concentrations reflect conditions of deposition, whereas the current partitioning of trace elements among host components reflects conditions of diagenesis.

Weathering Susceptibility

Partitioning of trace elements between their current host components should contribute to the behavior of trace elements under conditions of weathering. If the trace elements hosted by the different components, as determined by factor analysis (Table 6), behave similar to the hosting components themselves, then an order can be estimated for the reactivity of the trace elements un-

der the condition of oxic subaerial weathering, as it exists today. This environment, which is far different from the O_2-depleted environment of deposition (Piper, 2000), should largely account for the release of trace elements to surface and ground water. Clayton and King (1987), Clayton and Swetland (1978), and Littke and others (1991) have established an approximate order of weathering of host mineral components in shale formations of similar high organic-matter contents. Their order of stability under conditions of subaerial weathering is roughly as follows:

Sphalerite = pyrite < organic matter < carbonates < apatite < chert < terrigenous debris.

In positioning apatite, we have taken the constancy of its U and F contents (Figs. 5 and 11c) to indicate that it is relatively non-reactive during weathering, but less so than chert and the detrital fraction. The positions of sphalerite and chert are a guess.

Combining the order of component instability with the partitioning of trace elements (Table 6) gives an order of release to ground water approximately as follows:

Zn > Ag > Cr = Cu = Mo = Se > Ni > As >> U ≥ REE > Ba > Co = Ga = Th = Sc.

The behavior of any element once released to ground water, of course, will be influenced by its thermodynamic properties. The thermodynamic properties of many trace elements require that they are more soluble under oxidizing than reducing conditions and should be held in solution once their host phase(s) is dissolved. They will remain in solution until they again enter the terrestrial food chain (Presser and Piper, 1998), accumulate in some O_2-depleted environment (Jacobs and others, 1987), or both.

Cd, V, and Tl are not included in the above sequence, as their dominant host phase has not been identified. If subsequent analysis determines that they are hosted largely by a sulfide phase, then they could be the most reactive of the elements examined here. Measurements of V in surface and subsurface (40-ft depth) samples (McKelvey and others, 1986) gave similar concentrations, which suggests that that will not be the case, at least for V.

The stratigraphic distributions of trace elements might further contribute to their introduction into ground water. Although As, Cu, Se, Tl, Mo, Zn, as well as F tend to be enriched in the ore zones, they also achieve high concentrations in the center waste and Cr is most enriched in the center waste (Fig. 16).

18

Dispersal of Selenium in the Environment

Se represents perhaps the most severe problem element of the trace elements examined here. It is highly enriched in this formation (Table 4); it is present in components that are quite labile under oxic weathering conditions (Table 6); it is highly biologically reactive (Presser, 1994; Presser and others, 1994; USDOI, 1998); and it is now strongly enriched in the food web at every trophic level in southeast Idaho (Table 8), except perhaps the single very highest trophic level. The narrow range in concentration between which it is an essential nutrient and at which it becomes a toxic nuisance (Table 8; Presser and Piper, 1998) makes it a particularly insidious trace element among those elements that can be toxic even at very low concentrations.

Several other areas in the United States have also been examined where teratogenesis in wildlife has been attributed to high Se concentrations in the environment (Skorupa, 1998). For example, it severely impacted the avian population in the San Joaquin Valley of California in the 1980's (Presser and Ohlendorf, 1987). In that area, the concentration of Se in the source rocks has a range of 1.4 to 45 ppm, with a mean of approximately 8.9 ppm (1989; Presser, 1994), or roughly an order of magnitude less than in the Phosphoria Formation.

Certainly, other additional properties of Se and of the associated trace elements will determine their impact on the environment. These include but are not limited to their bulk concentration in streams, speciation in solution, differential uptake by biota, and different levels of toxicity for various biota. Yet, Se's elevated concentrations in surface water, ground water, plants, bird eggs (Fig. 17), fish, and other wildlife from southeast Idaho is now strongly documented (Table 8) and was the apparent cause recently of deaths among livestock (Anonymous, 1999).

Within the aquatic environment, concentrations of Se in 13 of 74 streams from the Blackfoot River watershed (Montgomery Watson, 1999) exceed the freshwater criterion for the protection of organisms of 5 μg/L (Table 8, USEPA, 1992), raising concern also for aquatic resources. This loading expresses itself through Se accumulation in the aquatic ecosystem, especially in areas such as backwaters, side channels, and other low flow, shallow areas, e.g., ponds, wetlands, and pastures.

The Se concentrations in fish reflect the elevated levels of Se in streams. However, its concentration in fish, as reported (Table 8), tend to give a somewhat diminished view of the scope of

the problem, for the following three reasons. One, fish fillets containing 6 µg/g Se (maximum of 7.9 µg/g from East Mill Creek) were reported in wet weight. From two low-Se reference sites (Blackfoot River and South Fork Sage Creek), they had 1.2 to 1.3 µg/g wet weight (Montgomery Watson, 1999). Converting these values to a dry weight basis (dry weight = wet weight x 4; assuming 75% moisture), the standard reporting procedure, translate into a Se concentration of 24 µg/g in fish fillets of biota from East Mill Creek and 4.8 to 5.2 µg/g in fish fillets from the reference sites. Two, even these concentrations will underestimate the concentrations in whole-body fish analyses, again the dominant matrix of selenium (Se) residues in fish as reported in the literature. Muscle contains less Se than whole-body due to the relatively high amounts of Se in spleen, liver, kidney, heart, and other tissues, especially mature ovaries (Adams, 1976; Sato and others, 1980; Lemly, 1982, 1996; Hilton and others, 1982; Hilton and Hodson, 1983; Kleinow and Brooks, 1986; Hermanutz and others, 1992). Consequently, the actual whole-body Se concentrations would be about 40 µg/g in fish from East Mill Creek and 8 to 8.7 µg/g in fish from the Blackfoot River and South Fork Sage Creek, using a conversion factor of 1.667 x muscle concentration = whole body concentration. A conversion factor of 2.355 for rainbow trout (Adams, 1976) would further increase the converted values for trout as reported (Montgomery Watson, 1999). These values give a substantially different reference point when considering the hazard of Se exposure and accumulation in the aquatic ecosystem of the Blackfoot River watershed. Three, older life stages typically are more tolerant of contaminant stresses than are early life stages (Rand and Petrocelli, 1985). That is, adverse effects in early life stages will be underestimated by examining only adults. Thus, Se contamination of the Blackfoot River and its tributaries may very likely adversely affect aquatic resources, especially in early life stages of fish. But even dismissing this third problem, residues were substantially above background concentrations in fish from both laboratory and field investigations. Background Se concentrations in fish are typically 1 to 2 µg/g (Maier and Knight, 1994; Hamilton and others, 2000). More importantly, of course, observed values were above values reported to cause adverse effects in early life stages of fish, including salmonids, of 4 to 5 µg/g (Hamilton and others, 2000). In particular, Se residues of 5.2 µg/g in rainbow trout have been associated with reduced survival (Hunn and others, 1987), and 3.8 to 4.9

20

µg/g in chinook salmon were associated with reduced survival and growth (Hamilton and others, 1986; Hamilton and Wiedmeyer, 1990).

Within the avian population the situation seems no less a concern. Toxicity of Se to birds has been well documented in field studies across the United States (Ohlendorf, 1989; Skorupa, 1998a). Avian embryonic exposure to Se and response to that exposure, both in the form of teratogenesis and embryo viability, can be predicted using Se concentrations in bird eggs. In southeast Idaho, Se concentrations in waters associated with mining activities (Table 8), including several sites of mine pit ponds, are within ranges in which elevated levels in bird eggs are predicted, based on results of the other field studies. Indeed, the few bird eggs examined to date have predicted elevated values. The few preliminary results (Figure 17) show a trend between Se in water and bird eggs seen elsewhere. Even though Se concentrations in water have been shown to be a good predictor of the maximum potential for Se bioaccumulation in avian eggs (Skorupa, 1998b), it is not as reliable a predictor of the average achieved Se in eggs (Skorupa and Ohlendorf, 1991), information needed to fully ascertain the impact from Se exposure, thus making actual measurements of eggs necessary.

The distribution of Se in southeast Idaho clearly demonstrates why environmental studies in this area are focusing on Se, even though other trace elements listed in the weathering sequence might also represent a concern. These include As, Cr, and Cu, as well as Se. Their high concentrations, particularly in the waste zones (Fig. 16); their designation as priority pollutants by the U.S. Environmental Protection Agency, and the concentrations at which they achieve levels of concern in the environment (for Cu, 0.23 to 12 ppb in water and 34 to 270 ppm in sediment; USDOI, 1998); suggest that they too might pose an ecological problem. However, the elevated Se concentration in the environment in southeast Idaho at virtually all trophic levels, i.e., above levels of concern for protection of wildlife (Fig. 17; Table 8), should heighten concern about the impact of Se on wildlife and livestock and would seem to demand that, with very limited funding at hand, attention should continue to focus on this trace element until a complete inventory of Se has been fully documented.

The available data (Table 8) allow only a first step toward quantifying the regional discharge of Se from these rocks and its dispersal in water, vegetation, and wildlife. A mass balance

of Se could possibly allow us to ascertain the long-term impact of weathering of freshly exposed phosphate ore and waste to this ecosystem, in contrast to the impact of weathering of the Phosphoria Formation in unmined areas, and overcome complications introduced by nonequilibrium biologic reactions (Louma and others, 1992). Such an approach requires making an inventory of Se in each of the different environmental compartments. This is particular important in the case of fish and birds, for which we currently have only a meager amount of data that allow for a very rough estimate of Se at these trophic levels, at best. These biota represent perhaps the most sensitive species to elevated Se loading on the environment and certainly are the most studied elsewhere for possible adverse affects among wildlife (Ohlendorf, 1989; Lemly, 1996; Skorupa, 1998a).

CONCLUSIONS

The precision of the major-element-oxide and trace-element analyses of this study allows identification of (1) the major host components of trace elements—detrital material, organic matter, apatite, biogenic silica, dolomite, calcite, and possibly trace-metal sulfides. The interelement relations between the major oxides and several trace elements (for example, Al_2O_3 versus Th) approach those of the world shale average. These relations indicate that the detrital fraction is the sole host for several elements and that the fraction had a terrigenous source. The strength of these relations allows us to determine the detrital contribution of other trace elements (As, Ag, Cd, Cr, Cu, Mo, Ni, Sb, Se, Tl, U, V, Zn, and REEs) from the content of the detrital fraction in each sample alone, even though this latter group does not correlate with the detrital fraction. This latter group of trace elements is hosted largely by apatite and possibly organic matter.

Under conditions of subaerial weathering, the current hosts of trace elements will contribute to the behavior of trace elements within the oxic environment of surface and ground waters. Th, as noted, is hosted by the detrital fraction. Ba and As are hosted in large part by the detrital fraction, but significant portions of As show strong affinities for organic phases, as do Ag, Cd, Cu, Cr, Mo, Ni, Sb, Se, V, and Zn. The REE and U are hosted mostly by the apatite phase. Tl is associated with an as yet unidentified factor, which also as strong loadings of Cd and V. It is tempting to attribute this factor to sulfides, as preliminary microprobe analyses have show the presence of pyrite and sphalerite.

The order of stability for the dominant host phases under ground and surface water conditions as they exist today is roughly the following:

metal sulfides < organic matter < carbonates < apatite < chert < detrital debris.

Elements hosted predominantly by the more labile components—metal sulfides and organic matter—can be expected to be more readily released to the hydrosphere than those hosted by apatite. Those hosted by detritus, for example, Th, should be the least labile, or slowest released to water. This gives an order of release of trace elements to surface and ground water as follows:

$$Zn > Cr = Cu = Mo = Ag > Se > As > Ni > Cd > V \gg U \geq REE > Ba > Co > Ga = Th = Sc.$$

The thermodynamics of each will influence its behavior within surface and ground water and its availability to wildlife, once host components are oxidized.

The distribution of trace elements show that many have their highest concentration in samples from the lower ore zone (As, Cd, Cu, Mo, Se, U, V, and Zn). However, As, Cu, Se, Tl, and several of the others, a rather unpleasant group, also have elevated concentrations in the waste zones; and Cr has its highest concentrations in the center waste zone. These distributions may further contribute to the release of trace elements into ground and surface water long after mining has ceased, owing to exposure to weathering of waste rock used in the past in back filling of mined areas and as cross-valley fill.

Of this group of trace elements, Se is currently having the most adverse impact on the environment because of its high concentration in this formation, its release to the hydrosphere through weathering, its elevated concentration at virtually every trophic level of the food web, and its highly toxic nature at a seemingly quite low concentration. Planned disposal in the future of waste rock strongly enriched in Se and other possible toxic elements might lessen the environmental problems Se and additional trace elements will otherwise pose in the future.

ACKNOWLEDGMENTS

REFERENCES

Adams, W.J. 1976, The toxicity and residues dynamics of selenium in fish and aquatic invertebrates. PhD dissertation, East Lansing, Michigan State University.

Anonymous, 1999, Toxicologist and vet say dead sheep likely died from Se: The Caribou Sun, v. 11/11, p. 1.

Baedecker, P.A. (ed.), 1987, Methods for geochemical analysis: U.S. Geological Survey Bulletin 1770.

Baines, S.B., Pace, M.L., and Karl, D.M., 1994, Why does the relationship between sinking flux and planktonic primary productivity differ between lakes and oceans?: Limnology and Oceanography, v. 39, p. 213-226.

Baldwin, R.J., Glatts, R.C., and Smith, K.L., Jr., 1998, Particulate matter fluxes to the benthic boundary layer at a long time-series station in the abyssal NE Pacific--composition and fluxes: Deep-Sea Research, v. 45, p. 643-665.

Berger, W.H., Fischer, K., Lai, C., and Wu, G., 1988, Ocean carbon flux—global maps of primary production and export production, in Agegian, C.R., ed., Biogeochemical cycling and fluxes between the deep euphotic zone and other oceanic realms: NOAA Under Sea Research Program, Report 88-1, p. 131-176.

Bodkin, J.B., 1977, Determination of fluorine in silicates by use of an ion-selective electrode following fusion with lithium metaborate: The Analyst, v. 102, p.409-413.

Bond, M.M., 1999, Characterization and control of selenium releases from mining in the Idaho phosphate region: University of Idaho, Moscow, MS thesis, 97p.

Boyle, E.A., 1981, Cadmium, zinc, copper, and barium in foraminifera tests: Earth and Planetary Science Letters, v. 53, p 11-35.

Boyle, E.A., Sclater, F.R., and Edmond, J.M., 1976, On the marine geochemistry of cadmium: Nature, v. 263, p. 42-44.

Boyle, E.A., Sclater, F.R., and Edmond, J.M., 1977, The distribution of dissolved copper in the Pacific: Earth and Planetary Science Letters, v. 37, no. 1, p. 38-54.

Bruland, K.W., 1983, Trace elements in sea-water: in Riley, J.P., and Chester, R. eds., Chemical oceanography, v. 8, p. 158-220.

Brumsack, H.J., 1986, The inorganic geochemistry of Cretaceous black shales (DSDP Leg 41) in comparison to modern upwelling sediments from the Gulf of California, *in* Summerhayes, C.P., and Shackleton, N.J., eds., North Atlantic paleoceanography: Geological Society of London Special Publication 21, p. 447-462.

Brumsack, H.J., 1986, The inorganic geochemistry of Cretaceous black shales (DSDP Leg 41) in comparison to modern upwelling sediments from the Gulf of California, *in* Summerhayes, C.P., and Shackleton, N.J., eds., North Atlantic paleoceanography: Geological Society of London Special Publication 21, p. 447-462.

Burnett, W.C., Baker, K.B., Chin, P.A., McCabe, William, and Ditchburn, Robert, 1988, Uranium-series and AMS ^{14}C studies of modern phosphate pellets from Peru shelf muds: Marine Geology, v. 80, p. 215-230.

California Code of Regulation (CCR), 1979 and as amended; title 22, Social Security Division 4, Minimum standards for management of hazardous and extremely hazardous wastes, Environmental Health, Chapter 30, Article 66001-66699, s-161, 1121-0649.

Calvert, S.E., 1990, Geochemistry and origin of the Holocene sapropel in the Black Sea, *in* Ittekkot, Venugopalan, Kempe, Stephan, Michaelis, Walter, and Spitzy, Alejandro, eds., Facets of modern biogeochemistry: Berlin, Springer-Verlag, p. 326-352.

Calvert, S.E., and Price, N.B., 1983, Geochemistry of Namibian shelf sediments, *in* Suess, Erwin, and Thiede, Jörn, eds., Coastal upwelling, its sediment records: New York, Plenum, p. 337-375.

Clayton, J.L., King, J.D., 1987, Effects of weathering on biological marker and aromatic hydrocarbon composition of organic matter in Phosphoria shale outcrop: Geochimica et Cosmochimica Acta, v. 51, p. 2153-2157.

Clayton, J.L., and Swetland, P.J., 1978, Subaerial weathering of sedimentary organic matter: Geochimica et Cosmochimica Acta, v. 42, p. 305-312.

Collier, R.W., 1984, Particulate and dissolved vanadium in the North Pacific Ocean: Nature, v. 309, p. 441-444.

Collier, R.W., 1985, Molybdenum in the northeast Pacific Ocean: Limnology and Oceanography, v. 30, p. 1351-1354.

Connor, J.J., and Shacklette, H.T., 1975, Background geochemistry of some rocks, soils, plants, and vegetables in the conterminous United States: U.S. Geological Survey Professional Paper 574-F, 168p.

Cremer, M.J., Klock, P.R., Neil, S.T., and Riviello, J.M., 1984, Chemical methods for analysis of rocks and minerals: U.S. Geological Survey Open-File Report 84-565, 148p.

de Baar, H.J.W., Bacon, M.P., Brewer, P.G., and Bruland, K.W., 1985, Rare earth elements in the Pacific and Atlantic Oceans: Geochimica et Cosmochimica Acta, v. 4, p. 1943-1959.

Douglas, G.S., Mills, G.L., and Quinn, J.G., 1986, Organic copper and chromium complexes in the interstitial waters of Narragansett Bay sediments: Marine Chemistry, v. 19, p. 161-174.

Elderfield, H., Hawkesworth, C.J., Greaves, M.J. and Calvert, S.E., 1981, Rare earth element geochemistry of oceanic ferromanganese nodules and associated sediments: Geochimica et Cosmochimica Acta, v. 45, p. 513-528.

Fischer, Kathleen, Dymond, Jack, Lyle, Mitchell, Soutar, Andrew, and Rau, Susan, 1986, The benthic cycle of copper—evidence from sediment trap experiments in the eastern tropical North Pacific Ocean: Geochimica et Cosmochimica Acta, v. 50, p. 1535-1543.

Fisher, N.S., and Wente, M., 1993, The release of trace elements by dying marine phytoplankton: Deep-Sea Research, v. 40, p. 671-694.

Froelich, P.N., Arthur, M.A., Burnett, W.C., Deakin, M., Hensley, V., Jahnke, Richard, Kaul, L., Kim, Kee Hyun, Roe, K., Soutar, Andrew, and Vathakanon, C., 1988, Early diagenesis of organic matter Peru continental margin sediments—phosphorite precipitation: Marine Geology, v. 80, p. 309-343.

Goldberg, E.D., Koide, Minoru, Schmitt, R.A., and Smith, R.M., 1963, Rare earth distributions in the marine environment: Journal of Geophysical Research, v. 68, p. 4209-4217.

Golightly, D.W., Dorrzapf, A.F., Mays, R.E., and Fries, T.L., 1987, Analysis of geologic materials by direct-current arc emission spectrography and spectrometry, in Baedecker, P.A., ed., Methods for geochemical analyses: U. S. Geological Survey Bulletin 1770, p. A1-A13.

Grauch, R.I., Meeker, G.O., Desborough, G.A., Tysdal, R.G., Herring, J.R., and Moyle, P.R., 1999, Selenium residence in the Phosphoria Formation: Geological Society of America Annual Meeting Abstracts and Programs, v. 31, no. 7, p. A35.

Gromet, P.L., Dymek, R.F., Haskin, L.A., and Korotev, R.L., 1984, The "North American shale composite"—its compilation, major and trace element characteristics: Geochimica et Cosmochimica Acta, v. 48, p 2469-2482.

Gulbrandsen, R.A., 1966, Composition of phosphorites of the Phosphoria Formation: Geochimica et Cosmochimica Acta, v. 30, p. 769-778.

Gulbrandsen, R.A., 1970, Relation of carbon dioxide content of apatite of the Phosphoria Formation to regional facies: U.S. Geological Survey Professional Paper 700-B, p. B9-B13.

Gulbrandsen, R.A., 1979, Preliminary analytical data on the Meade Peak Member of the Phosphoria Formation at Hot Springs underground mine, Trail Canyon trench, and Conda underground mine, southeast Idaho, U.S. Geological Survey Open-File Report 79-369, 35p.

Hamilton, S.J., Palmisano, A.N, Wedemeyer, G.A. and Yasutake, W.T., 1986. Impacts of selenium on early life stages and smoltification of fall chinook salmon: Transactions of the North American Wildlife and Natural Resources Conference, v. 51, p. 343-356.

Hamilton, S.J., and Wiedmeyer, R.H, 1990. Concentrations of boron, molybdenum, and selenium in chinook salmon: Transactions of the American Fisheries Society, v. 119, p. 500-510.

Hamilton, S.J., Muth, R.T., Waddell, B. and May, T.W., 2000, Hazard assessment of selenium and other trace elements in wild larval razorback sucker from the Green River, Utah: Ecotoxicology and Environmental Safety, v. 45, p. 132-147.

Haskin, M.A., and Haskin, L.A., 1966, Rare earths in European shales—a redetermination: Science, v. 154, p. 507-509.

Hermanutz, R.O., Allen, K.N., Roush, T.H. and Hedtke, S.F., 1992, Effects of elevated selenium concentrations on bluegills (*Lepomis macrochirus*) in outdoor experimental streams: Environmental Toxicology and Chemistry, v.11, p. 217-224.

Herring, J.R., Desborough, G.A., Wilson, S.A., Tysdal, R.T., Grauch, R.I., and Gunter, M.E., 1999, Chemical composition of weathered and unweathered strata of the Meade Peak Phosphatic Shale Member of the Permian Phosphoria Formation—measured sections A and B, central part of Rasmussen Ridge, Caribou county, Idaho: U.S. Geological Survey Open-File Report 99-147A, 24p.

Hilton, J.W., Hodson, P.V. and Slinger, S.J., 1982, Absorption, distribution, half-life and possible routes of elimination of dietary selenium in juvenile rainbow trout (*Salmo gairdneri*): Comparative Biochemistry and Physiology, v. 71C, p. 49-55.

Hilton, J.W., and Hodson, P.V., 1983, Effect of increased dietary carbohydrate on selenium metabolism and toxicity in rainbow trout (*Salmo gairdneri*): Journal of Nutrition, v. 113, p. 1241-1248.

Hunn, J.P., Hamilton, S.J. and Buckler, D.R. , 1987, Toxicity of sodium selenite to rainbow trout fry: Water Research, v. 21, p. 233-238.

Isaacs, C.M., 1980, Diagenesis in the Monterey Formation examined laterally along the coast near Santa Barbara, California: Stanford University, California, Ph.D. thesis, 329 p., [U.S. Geological Survey Open-File Report 80-606].

Jackson, L.L, Brown, F.W., and Neil, S.T., 1987, Major and minor elements requiring individual determination, classical whole rock analysis, and rapid rock analysis, *in* Baedecker, P.A., ed., Methods of geochemical analysis: U.S. Geological Survey Bulletin 1770, p. G1-G23.

Jacobs, Lucinda, Emerson, S.R., and Huested, S.S., 1987, Trace metal chemistry in the Cariaco Trench: Deep-Sea Research, v. 34, no. 5-6A, p. 965-981.

Kleinow, K.M., and Brooks, A.S., 1986, Selenium compounds in the fathead minnow (*Pimephales promelas*) I. Uptake, distribution, and elimination of orally administered selenate, selenite and l-selenomethionine: Comparative Biochemistry and Physiology, v. 83C, p. 61-69.

Kolodny, Yehoshua. 1981, Phosphorites, *in* Emiliani, Chesare, ed., The oceanic lithosphere, v.7 of The Sea—ideas and observations on progress in the study of the seas: New York, Wiley-Interscience, p. 981-1023.

Lemly, A.D., 1982, Response of juvenile centrarchids to sublethal concentrations of waterborne selenium. I. Uptake, tissue distribution, and retention: Aquatic Toxicology, v. 2, p. 235-252.

Lemly, A.D., 1996, Selenium in aquatic organisms, *in* Beyer, W.N., Heinz, G.H., and Redmon-Norwood, A.W., eds, Environmental contaminants in wildlife-interpreting tissue concentrations: Boca Raton, CRC Press, Lewis Publishing, p. 427-445.

Leventhal, J.S., 1989, Geochemistry of minor and trace elements of 22 core samples from the Monterey Formation and related rocks in the Santa Maria Basin, California: U.S. Geological Survey Bulletin 1581-B, p. B1-B11.

Levy, M., and Christie-Blick, N., 1989, Pre-Mesozoic palinspastic reconstruction of the Eastern Great Basin (western United States): Science, v. 245, p. 1454-1462.

Lewan, M.D., 1984, Factors controlling the proportionality of vanadium to nickel in crude oils: Geochimica et Cosmochimica Acta, v. 48, no. 11, p. 2231-2238.

Lichte, F.E., Golightly, D., and Lamothe, P.J., 1987, Inductively coupled plasma-atomic emission spectrometry, in Baedecker, P.A., ed., Methods of geochemical analysis: U.S. Geological Survey Bulletin 1770, p. B1-B10.

Littke, R., Klussmann, U., Krooss, B., and Leythaeuser, D., 1991, Quantification of loss of calcite, pyrite, and organic matter due to weathering of Toarcian black shales and effects on kerogen and bitumen characteristics: Geochimica et Cosmochimica Acta, v. 55, p. 3369-3378.

Luoma, S.N., Johns, C., Fisher, N.S., Steinberg, N.I., Oremland, R.S., and Reinfeld, J.R., 1992, Determination of selenium bioavailability to a benthic bivalve from particulate and solute pathways: Environmental Science and Technology, v. 26, p. 485-497.

Maier, K.J., and Knight, A.W., 1994, Ecotoxicology of selenium in freshwater systems: Reviews in Environmental Contamination and Toxicology, v. 134, p. 31-48.

Mansfield, G.R.,1916, A reconnaissance for phosphate in the Salt River Range, Wyoming: U.S. Geological Survey Bulletin, v. 620, p. 331-350.

Martin, J.H., and Knauer, G.A., 1973, The elemental composition of plankton: Geochimica et Cosmochimica Acta, v. 37, no. 7, p. 1639-1653.

Maughan, E.K., 1976, Organic carbon and selected element distributions in the phosphatic shale members of the Permian Phosphoria Formation, eastern Idaho and parts of adjacent States: U.S. Geological Survey Open-File Report, 76-577, 92p.

McClellan, G.H., and Lehr, J.R., 1969, Crystal-chemical investigation of natural apatites: The American Mineralogist, v. 54, p 1374-1391.

McKelvey, V.E., Strobell, J.D., Jr., and Slaughter, A.L., 1986, The vanadiferous zone of the Phosphoria Formation in western Wyoming and southeastern Idaho: U.S. Geological Survey Professional Paper 1465, 27p.

McKelvey, V.E., Williams, J.S., Sheldon, R.P., Cressman, E.R., Cheney, T.M., and Swanson, R.W., 1959, The Phosphoria, Park City, and Shedhorn Formations in the western phosphate field: U.S. Geological Survey Professional Paper 313-A, 47p.

Medrano, M.D., and Piper, D.Z., 1995, Partition of minor elements and major-element oxides between rock components and calculation of the marine-derived fraction of the minor elements in rocks of the Phosphoria Formation, Idaho and Wyoming, U.S. Geological Survey Open-File Report 95-270, 79pp.

Moldowan, J.M., Sundararaman, Padmanabhan, and Schoell, Martin, 1986, Sensitivity of bio-marker properties to depositional environments and/or source input in the lower Toarcian of SW Germany: Organic Geochemistry, v. 10, p. 915-926.

Montgomery-Watson, December 1999, Final 1998 investigative report, southeast Idaho phosphate resource area selenium project: Steamboat Springs, Idaho Mining Association Selenium Sub-committee, Chapters 1-7, Appendices A-F.

Mossmann, J.-R., Aplin, A.C., Curtis, C.D., and Coleman, M.L., 1991, Geochemistry of inor-ganic and organic sulfur in organic-rich sediments from the Peru Margin: Geochimica et Cos-mochimica Acta, v. 55, p. 3581-3595.

Murata, K.J., Friedman, I., and Gulbrandsen, R.A., 1972, Geochemistry of carbonate rocks in the Phosphoria and related formations of the western phosphate field: U.S. Geological Survey Professional Paper 800D, p. D103-D110.

Murchey, B.L., and Jones, D.L., 1992, A mid-Permian chert event—widespread deposition of biogenic siliceous sediments in coastal, island arc, and oceanic basins: Palaeogeography, Palaeoclimatology, Palaeoecology, v. 96, p. 161-174.

Nissenbaum, A., and Swaine, D.J., 1976, Organic matter-metal interactions in recent sedi-ments—the role of humic substances: Geochimica et Cosmochimica Acta, v. 40, p. 809-816.

Odermatt, J.R., and Curiale, J.A., 1991, Organically bound metals and biomarkers in the Monterey Formation of the Santa Maria Basin, California: Chemical Geology, v. 91, no. 2, p. 99-113.

Olendorf, H.M., 1989, Bioaccumulation and effects of selenium in wildlife, in Jacobs, L.W., ed., Selenium in agriculture and the environment: Madison, American Society of Agronomy, Soil Science Society of America, p. 133-177.

Palmer, M.A., 1985, Rare earth elements in foraminifera tests: Earth and Planetary Science Letters, v. 73, no. 2-4, p. 285-298.

Peterson, J.A., 1980, Depositional history and petroleum geology of the Permian Phosphoria, Park City, and Shedhorn Formations, Wyoming and Southeastern Idaho: U.S. Geological Survey Open-File Report 80-667, p. 18-20.

Piper, D.Z., 1974, Rare earth elements in the sedimentary cycle—a summary: Chemical Geology, v. 14, p. 285-304.

Piper, D.Z., 1994, Seawater as a source of minor elements in black shales, phosphorites, and other sedimentary deposits: Chemical Geology, v. 114, p. 95-114.

Piper, D.Z., 1999, Trace elements and major-element oxides in the Phosphoria Formation at Enoch Valley, Idaho-Permian sources and current reactivities: U.S. Geological Survey Open-File Report 99-163, 66p.

Piper, D.Z., 2000, The Phosphoria Formation in SE Idaho: Geochemistry of deposition in Permian time and of subaerial weathering at the present time: Economic Geology, 64p. (Submitted).

Piper, D.Z., and Isaacs, C.M., 1995, Geochemistry of minor elements in the Monterey Formation, California—seawater chemistry of deposition: U.S. Geological Survey Professional Paper 1566, 41p.

Piper, D.Z., and Medrano, M.D., 1994, Geochemistry of the Phosphoria Formation at Montpelier Canyon, Idaho—environment of deposition: U.S. Geological Survey Bulletin 2023-B, p. B1-B28.

Powell, T.G., Cook, P.J., and McKirdy, D.M., 1975, Organic geochemistry of phosphorites—relevance to petroleum genesis: American Association of Petroleum Geologists Bulletin 59, p 618-632.

Presser, T.S., 1994, The Kesterson effect: Environmental Management, v. 18, p. 437-454.

Presser, T.S. and Ohlendorf, H.M., 1987, Biogeochemical cycling of selenium in the San Joaquin Valley, California: Environmental Management, v. 11, pp. 805-821.

Presser, T.S., Swain, W.C.,, Tidball, R.R., and Severson, R.C., 1990, Geologic sources, mobilization, and transport of selenium from the California Coast Ranges to the western San Joaquin Valley: A reconnaissance study: U.S. Geological Survey Water Resources Investigation Report 90-4070, p. 66.

Presser, T.S., and Piper, D.Z., 1998, Mass balance approach to selenium cycling through the San Joaquin Valley from source to river to bay, in Frankenberger, W.T., Jr., and Engberg, R.A., eds., Environmental chemistry of selenium: New York, Marcel Decker, Inc., p. 153-182.

Puls, R. 1994, Mineral levels in animal health-diagnostic data: Clearbrook, BC, Sherpa International, 356p.

Rand, G.M., and Petrocelli, S.R., (editors.), 1985, Fundamental of aquatic toxicology: methods and applications: Washington, DC. , Hemisphere, 666 p.

Sarnthein, M., Winn, K., Duplessy, J-C., and Fontugne, M.R., 1988, Global variations of surface ocean productivity in low and mid latitudes—influence on CO_2 reservoirs on the deep ocean and atmosphere during the last 21,000 years: Paleoceanography, v. 3, p. 361-399.

Sato, T., Ose, Y. and Sakai, T. 1980, Toxicological effect of selenium in fish: Environmental Pollution, v. 21, p. 217-224.

Shacklette, H.T. and Boerngen, 1984, Element concentration is soils and other surficial material of the conterminous U.S.: U.S. Geological Survey Professional Paper 1270, 105p.

Shaw, T.J., Gieskes, J.M., and Jahnke, R.A., 1990, Early diagenesis in differing depositional environments—the response of transition metals in pore water: Geochimica et Cosmochimica Acta, v. 54, no. 5, p. 1233-1246.

32

Seiler, R.L., Skorupa, J.P., and Peltz, L.A., 1999, Areas susceptible to irrigation-induced selenium contamination of water and biota in the western United States: U.S. Geological Survey Circular 1180, 36p.

Sheldon, R.P., 1957, Physical stratigraphy of the Phosphoria Formation in northwestern Wyoming: U.S. Geological Survey Bulletin 1042-E, p. 105-185.

Sheldon, R.P., 1964, Paleolatitudinal and paleogeographic distribution of phosphorite: U.S. Geological Survey Professional Paper 501-C, p. C106-C113.

Skorupa, J.P., 1998a, Selenium poisoning of fish and wildlife in nature—lessons from twelve real-world examples, in Frankenberger, W.T., Jr., and Engberg, R.A., eds., Environmental chemistry of selenium: New York, Marcel Decker, Inc., p. 315-354.

Skorupa, J.P., 1998b, Risk assessment for the biota database of the National Irrigation Water Quality Program: Washington D.C., U.S. Department of the Interior, 151p.

Skorupa, J.P., and Ohlendorf, H.M., 1991, Contaminants in drainage water and avain risk threshold, in Dinnar, A., and Zilberman, D., eds., The economics and management of water and drainage in agriculture: Boston, Kluwer Academic Press , p. 345-368.

Suess, E., 1980, Particulate organic carbon flux in the oceans—surface productivity and oxygen utilization: Nature, v. 288, p. 260-263.

Swanson, V.E., 1961, Geology and geochemistry of uranium in marine black shales—a review: U.S. Geological Survey Professional Paper 356-C, p. 67-112.

Talcott, P.A., November 4, 1999, Selenium comments: Washington State University Memorandum to Mr. Bob Geddes, Solutia Inc., Idaho, 18p.

TRC Environmental Corporation, 1999, Maybe Canyon (south) site investigation, Caribou National Forest, Caribou County, ID.: Englewood CO., Appendices A-W, 122p.

Turekian, K.K., and Wedepohl, K.H., 1961, Distribution of the elements in some major units of the Earth's crust: Geological Society of America Bulletin, v. 72, no. 2, p. 175-191.

U.S. Bureau of Reclamation, 1986, Final environmental impact statement, Kesterson program: v. 2, Sacramento, U.S. Bureau of Reclamation, Mid-Pacific Region, Chapters 1-7, Appendix 1.

U.S. Department of Interior, 1998, Guidelines for interpretation of the biological effects of selected constituents in biota, water, and sediment: National Irrigation Water Quality Program,

Information Report no. 3, U.S. Bureau of Reclamation, U.S. Fish and Wildlife Service, U.S. Geological Survey, and U.S. Bureau of Indian Affairs, in the U.S. Department of the Interior, Washington, D.C., 198 p.

U.S. Department of Interior, Bureau of Land Management, 1999, Draft of environmental impact statement-FMC Dry Valley Mine, south extension, Caribou County, Idaho: Pocatello, ID., USDOI, 6 chapters, Appendices A-E.

U.S. Environmental Protection Agency, 1980, Hazardous waste management system: Federal Register 45:33,063-33, 285p.

U.S. Environmental Protection Agency, 1992a, Rulemaking; water quality standards; establishment of numeric criteria for priority toxic pollutants; States' compliance-final rule: Federal Register v. 57, no. 246, p. 60848-60923.

U.S. Environmental Protection Agency, 1992b, Water quality criteria: Washington DC, USEPA. 450p.

U.S. Forest Service-U.S. Bureau of Land Management, 1999, Elevated selenium associated with phosphate mining in southeast Idaho: USFS/USBLM Joint Briefing Paper, August, 1999, 10p.

Wardlaw, B.R. and Collinson, J.W., 1984, Conodont paleoecology of Permian Phosphoria Formation and related rocks of Wyoming and adjacent areas, in Clark, D.L., ed., Conodont biofacies and provincialism: Geological Society of America, Special Paper 196, p. 263-281.

Wedepohl, K.H. (editor), 1969-1978, Handbook of geochemistry: Berlin, Springer-Verlag, 4 volumes.

Wright, Judith, Schrader, Hans, and Holser, W.T., 1987, Paleoredox variations in ancient oceans recorded by rare earth elements in fossil apatite: Geochimica et Cosmochimica Acta, v. 51, no. 3, p. 631-644.

Yochelson, E.L., 1968, Biostratigraphy of the Phosphoria, Park City, and Shedhorn Formations: U.S. Geological Survey Professional Paper 313-D, p. 571-660.

Table 1. Summary of detection limits, accuracy, and precision for elements analyzed by the different analytical techniques, as determined by repeated analysis of rock standards. All procedures are discussed in detail in Baedecker (1987).

Analytical Technique	Detection Limit	Accuracy	Precision
ICP-AES	Limits of detection, in weight percent, in parentheses: Al_2O_3 (0.09), CaO (0.07), Fe_2O_3 (0.07), K_2O (0.1), MgO (0.08), Na_2O (0.1), P_2O_5 (0.02), and TiO_2 (0.02). Limit of detection in parts per million in parentheses: Ag (2), As (10), Au (8), Ba (1), Be (1), Bi (10), Cd (2), Ce (4), Co (1), Cr (1), Cu (1), Eu (2), Ga (4), Ho (4), La (2), Li (2), Mn (10), Mo (2), Nb (4), Nd (4), Ni (2), Pb (4), Sc (2), Sn (10), Sr (2), Ta (40), Th (4), U (100), V (2), Y (2), Yb (1), and Zn (2)	Standards analyzed varied 0.5 to 10 % from the proposed value	±2 to 10 percent for concentrations greater than 10 times the lower limit of detection
XRF	Limits of detection and concentration range SiO_2 0.10% to 99.0% Al_2O_3 0.10% to 28.0% Fe_2O_3 0.04% to 28.0% MgO 0.10% to 60.0% CaO 0.02% to 60.0% Na_2O 0.15% to 30.0% K_2O 0.02% to 30.0% TiO_2 0.02% to 10.0% P_2O_5 0.05% to 50.0% MnO 0.01% to 15.0% LOI 0.01% to 100.0%	Standards analyzed varied between 0.5 and 3 % of the proposed value	Precision is better than ±5 percent and, depending on the element, as low as ±0.2 percent
ICP-MS	Limits of detection in parts per million: La (0.002), Ce (0.002), Pr (0.002), Nd (0.009), Sm (0.006), Eu (0.003), Gd (0.011), Tb (0.002), Dy (0.007), Ho (0.002), Er (0.007), Tm (0.002), Yb (0.006), Lu (0.002).	Accuracy similar to ICP-AES and instrumental neutron activation analysis (INAA)	The average RSD for the REE is 2.5%. They range from 1.7% to 5.1%.
Delayed neutron activation analysis	Th (1), U (0.1)		Precision 5 to 10% above about 5 ppm.
DC arc emission spectroscopy	Ag (0.1), As (1), B (3), Ba (1), Co (1), Cr (1), Cu (1), Mo (1), Ni (1), Rb (3), Sc (1), Se (5), Sr (1), V (1), Y (1), Zn (10)	Accuracy can be up to 20% of accepted values, based on analyses of standard rock samples.	Relative errors in the range of 5 to 15%, for elements 10 fold above detection limit.
Combustion/ coulometry (total carbon, nitrogen, H_2O^+, H_2O^-)	Limit of detection and concentration range C 0.05% to 30% N 0.05% to 10% H_2O 0.1% to 10%	Standard: MAG-1, $\overline{X}$ = 2.28%, n = 12, s = 0.009%, proposed value: 2.15±0.40% 0.1 to 4 %	RSD is ≤ 5% for samples with > 0.01% C or an absolute standard deviation of 0.05% C, whichever is greater.
Combustion	Limit of detection and concentration range S 0.05% to 30%	Standard: SDO-1, $\overline{X}$ = 5.44%, n = 10, proposed value: 5.35±0.44%	RSD for standard is 0.2%
Coulometric titration (carbonate carbon)	Limit of detection and concentration range CO_2 0.01% to 50.0%	Standard: GSP-1, $\overline{X}$ = 0.10±0.003%, n = 12, proposed value: 0.11%	RSD is < 5% for concentration range of 0.01% to 36%.
Hydride-generation atomic absorption	Limit of detection Se 0.1ppm. Tl 0.1ppm. Sb 0.2ppm		RSD is 2.0% for solution concentration of 50 ppb.
Ion-selective electrode	Limit of detection and concentration range F 100ppm to 2.7%	Standard: GSP-1, $\overline{X}$ = 3240 ppm, n = 23, proposed value: 3630 ppm	RSD for standard is 11%.

Table 1. Summary of detection limits, accuracy, and precision for elements analyzed by the different analytical techniques, as determined by repeated analysis of rock standards. All procedures are discussed in detail in Baedecker (1987).

Analytical Technique	Detection Limit	Accuracy	Precision
ICP-AES	Limits of detection, in weight percent, in parentheses: Al_2O_3 (0.09), CaO (0.07), Fe_2O_3 (0.07), K_2O (0.1), MgO (0.08), Na_2O (0.1), P_2O_5 (0.02), and TiO_2 (0.02). Limit of detection in parts per million in parentheses: Ag (2), As (10), Au (8), Ba (1), Be (1), Bi (10), Cd (2), Ce (4), Co (1), Cr (1), Cu (1), Eu (2), Ga (4), Ho (4), La (2), Li (2), Mn (10), Mo (2), Nb (4), Nd (4), Ni (2), Pb (4), Sc (2), Sn (10), Sr (2), Ta (40), Th (4), U (100), V (2), Y (2), Yb (1), and Zn (2)	Standards analyzed varied 0.5 to 10 % from the proposed value	±2 to 10 percent for concentrations greater than 10 times the lower limit of detection
XRF	Limits of detection and concentration range SiO_2 0.10% to 99.0% Al_2O_3 0.10% to 28.0% Fe_2O_3 0.04% to 28.0% MgO 0.10% to 60.0% CaO 0.02% to 60.0% Na_2O 0.15% to 30.0% K_2O 0.02% to 30.0% TiO_2 0.02% to 10.0% P_2O_5 0.05% to 50.0% MnO 0.01% to 15.0% LOI 0.01% to 100.0%	Standards analyzed varied between 0.5 and 3 % of the proposed value	Precision is better than ±5 percent and, depending on the element, as low as ±0.2 percent
ICP-MS	Limits of detection in parts per million: La (0.002), Ce (0.002), Pr (0.002), Nd (0.009), Sm (0.006), Eu (0.003), Gd (0.011), Tb (0.002), Dy (0.007), Ho (0.002), Er (0.007), Tm (0.002), Yb (0.006), Lu (0.002).	Accuracy similar to ICP-AES and instrumental neutron activation analysis (INAA)	The average RSD for the REE is 2.5%. They range from 1.7% to 5.1%.
Delayed neutron activation analysis	Th (1), U (0.1)		Precision 5 to 10% above about 5 ppm.
DC arc emission spectroscopy	Ag (0.1), As (1), B (3), Ba (1), Co (1), Cr (1), Cu (1), Mo (1), Ni (1), Rb (3), Sc (1), Se (5), Sr (1), V (1), Y (1), Zn (10)	Accuracy can be up to 20% of accepted values, based on analyses of standard rock samples.	Relative errors in the range of 5 to 15%, for elements 10 fold above detection limit.
Combustion/ coulometry (total carbon, nitrogen, H_2O^+, H_2O^-)	Limit of detection and concentration range C 0.05% to 30% N 0.05% to 10% H_2O 0.1% to 10%	Standard: MAG-1, $\overline{X}$ = 2.28%, n = 12, s = 0.009%, proposed value: 2.15±0.40% 0.1 to 4 %	RSD is ≤ 5% for samples with > 0.01% C or an absolute standard deviation of 0.05% C, whichever is greater.
Combustion	Limit of detection and concentration range S 0.05% to 30%	Standard: SDO-1, $\overline{X}$ = 5.44%, n = 10, proposed value: 5.35±0.44%	RSD for standard is 0.2%
Coulometric titration (carbonate carbon)	Limit of detection and concentration range CO_2 0.01% to 50.0%	Standard: GSP-1, $\overline{X}$ = 0.10±0.003%, n = 12, proposed value: 0.11%	RSD is < 5% for concentration range of 0.01% to 36%.
Hydride-generation atomic absorption	Limit of detection Se 0.1ppm. Tl 0.1ppm. Sb 0.2ppm		RSD is 2.0% for solution concentration of 50 ppb.
Ion-selective electrode	Limit of detection and concentration range F 100ppm to 2.7%	Standard: GSP-1, $\overline{X}$ = 3240 ppm, n = 23, proposed value: 3630 ppm	RSD for standard is 11%.

Table 2. Formulas used to calculate the normative components and total CO_2, based on measured concentrations of major-element oxides (Table 4). See table 5 for the trace-element concentrations of the detrital component. The amount of H_2O in organic matter was selected to give a carbon concentration of 71.6% and is not intended to imply a concentration of hydrogen or oxygen in the organic component as shown.

Component	Formula	Stoichiometry
Detritus	$6.0 \times Al_2O_3$	$Ca_{.46}Mg_{.3}Na_{.93}K_{1.45}Fe_{.7}Al_{3.35}Si_{10} \cdot 5.7(H_2O)$
Biogenic silica	$SiO_2 - 3.5 \times Al_2O_3$	SiO_2
Apatite	$(P_2O_5 - 0.01 \times Al_2O_3) / 0.4$	$Ca_5(PO_4)_{2.85}(CO_3)_{.02}F$
Dolomite	$(MgO - 0.07 \times Al_2O_3) / 0.22$	$MgCa(CO_3)_2$
Calcite	$(CaO - 0.072 \times Al_2O_3 - 1.41 \times MgO - 1.42 \times P_2O_5) / 0.56$	$CaCO_3$
Organic matter	Organic Carbon x 1.4	$C_4(H_2O)$
ΣCO_2	0.48 x Dolomite + 0.016 x Apatite + 0.44 x Calcite	CO_2

Table 3. Major components (in percent) of samples from Hot Springs Mine, based on element-oxide compositions. Lithology is taken from Gulbrandsen (1979). Identification of major units is based on lithology of all 304 samples collected by Gulbrandsen and approximate thicknesses as compared to those at the Enoch Valley Mine (Piper, 2000).

Sample #	Cumulative Thickness (cm)	Lithology	Detritus	Apatite	Dolomite	Calcite	Organic Mattter	Biogenic SiO$_2$
586-77------			14.4	1.1	54.8	8.0	0.5	21.2
192-76------	5236	Phosphorite	22.2	68.9	2.4	0.1	3.2	3.3
189-76------	5214	Mudstone	47.4	5.6	5.6	5.6	4.3	31.5
188-76------	5149	Mudstone	59.6	0.2	8.1	2.6	3.7	25.9
581-77------	5080	Mudstone	55.2	6.8	5.9	3.6	3.5	25.0
576-77------	5079	Phosphorite	2.9	100.1	0.6	0.0	4.1	0.0
573-77------	4998	Mudstone	50.6	4.0	6.8	4.4	4.1	30.1
570-77------	4945	Phosphorite	29.1	46.9	2.9	5.0	5.1	11.0
567-77------	4895	Phosphorite	6.3	89.9	1.1	0.5	4.0	0.0
559-77------	4794	Phosphorite	31.8	52.2	3.1	2.1	6.0	4.9
557-77------	4770	Phosphorite	1.8	98.4	0.4	0.0	6.8	0.0
552-77------	4716	Phosphorite	3.0	90.5	0.7	1.1	7.8	0.0
548-77------	4676	Phosphorite	15.8	72.9	1.7	1.3	8.4	0.0
542-77------	4634	Phosphorite	2.9	52.6	2.6	19.9	2.9	19.1
535-77------	4573	Phosphorite (top of upper ore zone)	3.1	89.4	0.7	0.9	11.3	0.0
176-76------	4547	Phosphorite	7.1	79.2	1.5	0.0	13.6	0.0
530-77------	4464	Phosphorite	10.3	71.8	1.6	1.2	16.9	0.0
525-77------	4360	Phosphorite (bottom of upper ore zone)	11.7	70.1	2.4	0.7	17.2	0.0
521-77------	4276	Mudstone	37.8	23.6	4.6	2.5	18.7	12.8
168-76------	4221	Mudstone	48.1	17.2	3.6	1.8	11.1	18.2
167-76------	4179	Dolomite	28.5	0.1	46.2	7.2	1.9	16.2
515-77------	4073	Phosphorite	23.5	42.7	3.2	3.3	14.6	12.8
164-76------	4025	Mudstone	51.1	11.2	4.5	3.7	10.9	18.5
163-76------	3975	Mudstone	42.9	22.7	3.3	3.9	10.1	17.0
161-76------	3872	Phosphorite	27.4	50.7	1.7	2.0	5.8	12.4
157-76------	3660	Phosphorite	10.0	72.9	2.5	1.6	8.9	4.2
154-76------	3512	Mudstone	45.6	8.2	3.1	4.8	13.7	24.7
148-76------	3342	Phosphorite	6.7	91.6	0.2	0.0	5.0	0.0
145-76------	3243	Dolomite	28.9	0.1	45.4	3.5	4.0	18.2
141-76------	3084	Phosphorite	4.6	86.5	0.1	0.4	4.9	3.5
138-76------	3000		8.5	71.3	1.2	0.7	18.3	0.0
137-76------	2965	Mudstone	62.2	3.1	2.7	2.8	7.4	21.8
136-76------	2925	Phosphorite	32.5	44.2	3.5	4.3	15.8	0.0
135-76------	2870	Mudstone	53.2	19.3	5.2	3.9	13.5	4.9
133-76------	2782	limestone	8.7	0.5	10.0	40.9	0.7	39.4
125-76------	2658	Mudstone	65.2	6.0	5.9	0.6	12.4	9.9
120-76------	2528	Mudstone	65.6	9.8	0.9	0.9	6.5	16.4
117-76------	2457	Mudstone	49.3	0.0	13.9	5.0	1.8	30.0
113-76------	2384	Mudstone	45.3	16.4	5.4	5.0	5.4	22.6
110-76------	2353	Mudstone	65.7	19.4	3.5	0.3	10.2	1.0
105-76------	2293	Phosphorite	33.1	36.6	3.2	6.6	10.9	9.6

Table 3. Cont.

Sample #	Cumulative Thickness (cm)	Lithology	Detritus	Apatite	Dolomite	Calcite	Organic Matter	Biogenic SiO_2
101-76------	2211	limestone	37.0	13.9	6.0	17.6	12.7	12.8
99-76-------	2181	Phosphorite	39.1	37.8	3.7	3.5	12.7	3.2
98-76-------	2100		99.3	0.9	0.0	0.0	6.4	0.0
90-76-------	2038	Mudstone	73.6	13.1	6.5	0.9	11.1	0.0
89-76-------	2028	Mudstone	124.5	-0.3	1.9	0.0	3.8	0.0
83-76-------	1951	Mudstone	38.4	39.2	2.9	2.2	14.5	2.9
79-76-------	1903	Phosphorite	17.4	45.5	3.9	10.4	14.9	8.0
77-76-------	1867	Phosphorite	16.1	40.0	4.9	13.7	14.1	11.2
74-76-------	1836	Phosphorite (top of lower ore zone)	19.8	37.5	4.6	11.8	15.7	10.5
70-76-------	1792	Phosphorite	12.2	75.2	1.3	0.3	15.9	0.0
56-76-------	1670	Phosphorite	13.0	58.8	3.3	1.3	18.5	5.1
54-76-------	1665	Phosphorite	18.2	58.8	3.9	1.4	14.9	2.8
50-76-------	1588	Dolomite	10.1	6.3	65.8	5.9	2.1	9.9
44-76-------	1460	Mudstone	30.0	16.3	15.2	1.5	6.2	30.9
39-76-------	1402	Mudstone	40.7	34.7	8.2	0.4	7.6	8.4
36-76-------	1322	Dolomite (false cap)	19.9	0.2	65.3	3.8	3.2	7.6
28-76-------	1165	Dolomite	5.5	5.8	65.1	4.7	2.4	16.5
16-76-------	962	Phosphorite	14.4	62.7	2.3	0.7	16.2	3.7
13-76-------	911	Phosphorite	24.6	53.2	2.8	0.8	9.4	9.3
250-74------	802	Phosphorite	12.0	70.7	1.9	0.3	11.3	3.8
248-74------	770	Phosphorite	24.1	48.3	3.0	1.7	11.5	11.4
243-74------	687	Phosphorite	22.6	56.5	4.8	0.7	8.4	7.1
239-74------	632	Phosphorite	14.3	57.1	4.1	1.2	11.5	11.9
232-74------	530	Phosphorite	23.0	53.7	4.0	1.5	8.2	9.7
231-74------	524	Phosphorite	32.6	48.5	6.1	0.6	8.3	3.9
226-74------	448	Phosphorite	13.7	57.7	6.4	1.9	7.8	12.5
225-74------	441	Phosphorite	17.6	59.3	7.4	0.9	7.4	7.3
222-74------	384	Dolomite	5.5	11.6	44.5	17.4	1.1	20.0
220-74------	308	Phosphorite	6.1	92.2	0.8	0.0	8.5	0.0
219-74------	246	Phosphorite (bottom of lower ore zone)	6.6	89.4	0.4	0.0	7.9	0.0
216-74------	146	Mudstone	52.1	0.3	10.4	0.0	13.2	24.1
212-74------	92	Dolomite	25.6	0.1	55.3	1.5	2.8	14.7
209-74------	37	Dolomite	26.7	0.0	53.7	0.9	0.6	18.1
207-74------	8	Phosphorite (fish scale)	11.8	88.8	0.9	0.0	1.5	0.0

Table 4a*. Major elements and oxides, in percent, and minor elemets, in parts per million, in the 75-series of samples. Thicknesses, in meters, are cumulative. Blanks indicate no analysis. Numbers in () give detection limits in cases for which concentrations were less than the detection limit. Such values are then listed as mid-value to zero.

Sample	Thickness	SiO_2+	AL_2O_3	Fe_2O_3	MgO	CaO	Na_2O	K_2O	TiO_2	P_2O_5	MnO	$H_2O\#$	F
586-77----		21.0	2.4	0.86	12.2	25.6	0.3	0.51	0.06	0.5	0.040	1.2	0.1
192-76----	52.36	18.3	3.7	1.19	0.8	35.8	0.8	0.76	0.09	28.0	0.006	1.9	2.5
189-76----	52.14	53.1	7.9	2.69	1.8	11.2	1.3	1.55	0.30	2.3	0.022	4.1	0.3
188-76----	51.49	57.2	10.0	3.12	2.5	6.6	1.3	2.05	0.36	0.2	0.033	5.1	0.1
581-77----	50.80	52.6	9.2	3.00	2.0	10.2	1.3	1.96	0.32	2.8	0.026	4.7	0.4
576-77----	50.79	0.0	0.5	0.16	0.2	49.3	0.5	0.11	0.02	40.6	0.002	0.3	3.4
573-77----	49.98	55.0	8.4	2.39	2.1	9.8	1.4	1.69	0.30	1.7	0.027	4.3	0.3
570-77----	49.45	26.1	4.9	1.53	1.0	30.1	0.8	1.06	0.10	19.0	0.014	2.5	1.6
567-77----	48.95	4.3	1.1	0.89	0.3	45.9	0.5	0.22	0.02	36.4	0.005	0.5	2.9
559-77----	47.94	25.0	5.3	1.62	1.1	29.9	0.7	1.19	0.11	21.2	0.011	2.7	1.9
557-77----	47.70	0.0	0.3	0.14	0.1	48.8	0.4	0.06	0.02	39.9	0.003	0.2	2.8
552-77----	47.16	2.7	0.5	0.29	0.2	46.6	0.3	0.12	0.02	36.7	0.005	0.3	2.5
548-77----	46.76	11.9	2.6	0.87	0.6	38.6	0.5	0.59	0.08	29.6	0.006	1.4	2.3
542-77----	46.34	7.3	0.5	0.13	0.6	47.0	0.3	0.10	0.02	21.3	0.018	0.3	1.5
535-77----	45.73	2.0	0.5	0.17	0.2	45.9	0.2	0.12	0.02	36.2	0.004	0.3	2.3
176-76----	45.47	8.5	1.2	0.46	0.4	39.9	0.3	0.27	0.04	32.1	0.003	0.6	2.4
530-77----	44.64	9.2	1.7	0.64	0.5	37.8	0.3	0.40	0.06	29.1	0.004	0.9	2.2
525-77----	43.60	9.8	2.0	0.71	0.7	36.8	0.3	0.47	0.06	28.4	0.005	1.0	2.1
521-77----	42.76	36.0	6.3	2.17	1.5	16.7	0.9	1.51	0.22	9.6	0.012	3.2	1.1
168-76----	42.21	45.4	8.0	2.46	1.4	12.7	1.2	1.98	0.23	7.1	0.012	4.1	0.8
167-76----	41.79	23.8	4.8	1.40	10.5	22.0	0.9	1.08	0.14	0.1	0.050	2.4	0.1
515-77----	40.73	27.5	3.9	1.62	1.0	26.2	0.6	0.96	0.10	17.3	0.008	2.0	1.8
164-76----	40.25	45.4	8.5	2.80	1.6	12.0	1.2	2.18	0.24	4.6	0.020	4.4	0.6
163-76----	39.75	39.6	7.2	2.26	1.2	17.4	1.1	1.77	0.19	9.3	0.017	3.7	1.1
161-76----	38.72	29.0	4.6	1.63	0.7	28.5	1.0	1.12	0.06	20.6	0.010	2.4	1.8
157-76----	36.60	12.8	1.7	0.56	0.7	39.0	0.5	0.40	0.02	29.6	0.007	0.9	2.7
154-76----	35.12	48.6	7.6	2.23	1.2	11.0	1.3	1.88	0.24	3.4	0.018	3.9	0.4
148-76----	33.42	5.2	1.1	0.51	0.1	45.5	0.5	0.31	0.02	37.1	0.002	0.6	3.0
145-76----	32.43	30.5	4.8	1.37	10.3	18.0	1.2	1.11	0.15	0.1	0.041	2.5	0.0
141-76----	30.84	9.5	0.8	0.79	0.1	43.8	0.4	0.22	0.02	35.1	0.004	0.4	2.5
138-76----	30.00	10.2	1.4	0.90	0.4	36.9	0.4	0.35	0.03	28.9	0.002	0.7	2.3
137-76----	29.65	54.2	10.4	3.37	1.3	6.7	1.8	2.37	0.36	1.4	0.025	5.3	0.2
136-76----	29.25	19.7	5.4	1.97	1.2	28.3	0.7	1.28	0.10	17.9	0.009	2.8	1.8
135-76----	28.70	33.6	8.9	3.25	1.8	16.5	0.9	2.14	0.26	7.9	0.016	4.6	1.1
133-76----	27.82	10.5	1.4	0.44	2.3	44.4	0.3	0.35	0.04	0.2	0.015	0.7	0.0
125-76----	26.58	47.8	10.9	3.22	2.1	7.0	1.2	2.69	0.34	2.6	0.020	5.6	0.4
120-76----	25.28	52.6	11.0	3.36	1.0	7.7	1.5	2.66	0.33	4.1	0.019	5.6	0.5
117-76----	24.57	52.0	8.2	2.60	3.6	10.4	1.9	1.87	0.18	0.1	0.038	4.2	0.0
113-76----	23.84	44.4	7.6	2.37	1.7	16.0	1.2	1.86	0.21	6.7	0.023	3.9	0.6
110-76----	23.53	39.9	11.0	3.40	1.6	12.7	0.7	2.66	0.30	8.0	0.017	5.6	1.0
105-76----	22.93	25.7	5.5	2.00	1.1	26.7	0.7	1.39	0.14	14.9	0.009	2.8	1.5
101-76----	22.11	22.1	6.2	2.03	1.8	27.3	0.4	1.55	0.17	5.7	0.010	3.2	0.6
99-76----	21.81	25.4	6.5	2.04	1.3	24.5	0.8	1.64	0.16	15.4	0.010	3.4	1.4

Table 4a. Cont.

Sample	Total S	CO_2	Org. C	N	Ag (2)	As	Ba	Cd (2)	Cr	Cu	Ga (4)	Li (2)	Mo (2)
586-77----	0.7	34.3	0.3		1	6.1	47	1	46	17	8	9	3
192-76----	1.6	2.4	2.3	0.24	1	12.3	462	12	402	50	17	13	11
189-76----	2.3	8.0	3.1		1	16.0	204	6	496	39	16	24	21
188-76----	2.5	6.4	2.6		1	25.7	229	3	79	23	19	25	13
581-77----	2.4	6.6	2.5		1	21.9	238	5	414	40	17	27	10
576-77----	1.0	2.0	2.9	0.18	1	3.1	238	92	372	29	2	6	18
573-77----	2.0	7.7	2.9		1	26.3	212	8	420	30	18	24	14
570-77----	2.0	5.8	3.6	0.42	1	23.2	170	134	515	52	19	20	46
567-77----	1.5	2.6	2.8	0.32	1	17.3	95	93	228	55	7	7	36
559-77----	2.2	2.8	4.3	0.38	6	36.1	173	94	877	95	21	23	69
557-77----	1.2	1.9	4.9	0.27	1	6.5	63	135	367	32	2	5	36
552-77----	1.4	3.0	5.6	0.32	1	10.6	61	169	566	75	2	5	59
548-77----	1.7	3.3	6.0	0.38	3	27.7	111	72	815	63	8	15	59
542-77----	0.5	18.5	2.1	0.30	1	4.6	31	18	170	19	7	1	17
535-77----	1.4	2.6	8.1	0.39	1	15.8	62	131	637	54	7	4	79
176-76----	2.1	2.1	9.7	0.44	1	31.8	72	281	936	86	2	8	187
530-77----	2.4	2.8	12.0	0.52	2	28.8	83	324	1080	96	7	10	208
525-77----	2.4	3.0	12.3	0.65	4	28.0	90	171	1310	91	12	10	88
521-77----	3.6	3.9	13.3	0.99	8	57.5	201	374	1660	140	24	25	271
168-76----	2.9	3.8	7.9	0.83	3	47.1	265	37	854	65	25	17	37
167-76----	1.1	30.5	1.3	0.32	1	26.0	111	2	150	18	14	4	4
515-77----	2.6	4.0	10.4	0.50	4	30.2	150	13	1520	122	14	21	31
164-76----	2.9	5.8	7.8	0.74	4	35.8	238	10	1070	93	25	25	21
163-76----	2.6	5.4	7.2	0.64	4	26.4	231	50	1060	96	20	22	66
161-76----	2.3	2.1	4.2	0.42	1	34.6	185	4	637	37	20	10	20
157-76----	1.4	3.5	6.4	0.37	1	14.3	147	7	759	69	8	7	4
154-76----	2.8	5.7	9.8	1.06	6	17.8	252	28	1360	89	21	26	49
148-76----	1.3	1.2	3.6	0.32	1	12.1	152	6	298	38	11	4	6
145-76----	1.4	25.7	2.8	0.42	1	6.7	103	1	139	13	10	2	1
141-76----	1.3	1.7	3.5	0.26	1	16.0	122	4	198	20	2	3	1
138-76----	2.5	1.9	13.1		1	23.9	104	45	1640	145	2	14	30
137-76----	3.3	4.0	5.3	0.70	3	25.5	313	10	855	46	20	21	40
136-76----	3.2	4.6	11.3	0.65	5	21.0	201	11	2110	128	20	41	41
135-76----	3.7	5.8	9.6	0.87	4	27.3	252	9	1860	113	25	55	41
133-76----	0.3	38.6	0.5		1	2.1	29	1	40	16	13	2	1
125-76----	3.6	3.9	8.9		8	17.2	322	65	1510	98	27	42	127
120-76----	3.1	2.0	4.6	0.97	1	23.6	344	9	690	65	27	28	62
117-76----	2.0	11.5	1.3		1	23.2	215	1	315	22	18	6	13
113-76----	2.3	7.3	3.8	0.62	2	23.9	234	3	591	56	16	18	13
110-76----	3.4	2.6	7.3	1.00	3	28.2	291	6	1440	95	19	51	35
105-76----	2.7	7.0	7.8	0.69	1	20.4	199	5	780	85	16	26	32
101-76----	2.7	17.3	9.1	0.89	4	23.6	170	9	2120	125	23	40	78
99-76----	2.8	5.6	9.1	0.89	2	20.6	248	34	1180	86	19	25	67

Table 4a. Cont.

Sample	Ni	Pb	Sb (.6)	Sc (2)	Se	Sr	Th	Tl (.2)	U	V	Y	Zn	La
586-77----	26	11	0.3	2	5.5	238	2.0	0.1	4.1	30	14	96	17.5
192-76----	109	19	0.9	6	26.8	1010	7.0	2.4	88.3	61	513	599	307.0
189-76----	138	14	1.3	7	39.7	162	8.1	0.9	19.7	84	87	320	60.4
188-76----	63	15	1.7	9	26.1	105	9.0	1.5	3.8	105	26	123	31.9
581-77----	88	17	1.3	9	28.8	198	9.4	1.5	14.3	111	95	246	76.3
576-77----	58	18	0.3	1	6.7	1420	1.3	1.4	202.0	656	220	1820	145.0
573-77----	96	14	2.5	7	38.5	150	9.3	2.0	9.0	200	52	248	36.0
570-77----	138	16	2.9	1	50.2	756	5.1	4.7	74.3	450	117	2010	67.3
567-77----	414	16	1.6	1	82.7	1240	5.3	10.4	186.0	604	90	3690	49.7
559-77----	192	20	7.1	1	129.0	656	4.7	6.4	74.0	1190	130	1610	66.6
557-77----	119	21	1.9	1	27.2	1150	0.8	2.4	328.0	644	168	2640	80.1
552-77----	156	20	3.9	1	37.6	936	1.4	4.9	243.0	1370	150	3750	72.6
548-77----	146	17	3.7	4	78.4	881	3.0	4.7	88.2	1180	210	1300	102.0
542-77----	26	14	0.6	1	13.6	642	0.9	1.3	88.0	395	77	398	34.9
535-77----	119	13	7.0	1	30.2	945	1.0	2.1	130.0	1800	120	2430	58.1
176-76----	259	15	19.0	1	73.5	934	2.0	6.8	191.0	3180	120	6600	68.4
530-77----	303	14	15.2	2	83.4	1040	1.9	5.9	124.0	3600	126	4530	62.0
525-77----	223	16	10.4	3	76.8	1050	2.5	2.6	80.2	1500	161	2150	78.2
521-77----	356	18	16.7	7	120.0	503	5.6	5.5	52.1	1680	118	4240	64.3
168-76----	170	17	7.3	8	81.6	366	7.1	1.2	32.9	263	117	923	73.1
167-76----	27	12	1.6	4	30.4	233	4.5	0.2	2.4	90	14	59	14.8
515-77----	280	16	3.6	6	61.6	930	4.4	1.0	50.9	197	291	1210	133.0
164-76----	199	15	4.9	9	81.8	374	7.6	1.1	19.4	150	127	758	79.8
163-76----	213	19	5.0	8	83.3	591	7.2	1.5	38.0	185	170	1210	99.4
161-76----	80	19	3.1	1	39.5	1010	10.5	1.5	59.5	93	680	218	395.0
157-76----	146	16	2.0	7	33.0	1310	6.3	2.2	61.9	99	749	460	441.0
154-76----	237	16	4.0	8	70.1	240	7.8	0.7	17.9	356	110	786	64.1
148-76----	96	19	1.0	1	29.7	1350	7.3	4.1	113.0	90	675	335	438.0
145-76----	22	10	0.6	4	10.2	192	5.0	0.5	1.9	66	15	25	17.4
141-76----	33	16	1.2	3	17.9	1370	4.3	1.6	60.9	43	257	246	206.0
138-76----	434	26	4.4	7	97.1	1170	5.9	2.3	179.0	176	1380	1260	1120.0
137-76----	183	17	5.3	9	136.0	180	9.5	1.0	7.1	157	60	424	56.5
136-76----	362	15	5.9	6	119.0	1160	5.5	0.5	35.3	196	423	1210	409.0
135-76----	343	18	6.2	12	155.0	524	6.9	0.4	29.4	210	164	1170	142.0
133-76----	13	11	0.7	1	12.9	452	1.1	0.1	1.1	16	9	51	9.4
125-76----	432	20	5.2	13	211.0	207	10.3	1.6	41.2	710	155	1790	113.0
120-76----	201	18	5.1	12	77.8	342	10.7	0.5	15.4	151	131	839	98.8
117-76----	41	18	2.7	7	30.2	213	7.5	0.3	3.2	93	12	86	21.3
113-76----	126	15	4.8	7	53.3	526	7.0	0.5	10.0	86	51	453	44.7
110-76----	283	17	6.9	12	118.0	498	7.3	0.4	17.7	187	131	1090	109.0
105-76----	219	10	3.9	8	62.1	1490	5.2	0.5	21.5	115	227	866	177.0
101-76----	330	15	6.2	9	119.0	770	4.6	0.3	26.4	194	163	1320	120.0
99-76----	252	14	4.0	8	70.6	1280	5.7	0.4	47.7	214	226	1030	155.0

Table 4a. Cont.

Sample	Ce	Pr	Nd	Sm	Eu	Gd	Tb	Dy	Ho	Er	Tm	Yb	Lu
586-77----	12.6	2.3	8.8	1.5	0.32	1.6	0.2	1.5	0.31	1.0	0.1	0.9	0.12
192-76----	73.6	35.0	142.0	21.8	5.10	31.6	4.2	31.0	7.72	25.3	3.3	20.2	3.21
189-76----	60.8	12.4	50.2	9.1	1.94	10.1	1.4	9.4	1.99	6.2	0.8	5.1	0.76
188-76----	52.9	6.7	23.5	4.5	0.86	4.4	0.6	4.3	0.88	2.9	0.4	3.0	0.45
581-77----	69.5	13.4	52.9	9.6	1.96	10.8	1.5	10.2	2.19	6.6	0.9	5.5	0.88
576-77----	26.3	14.8	58.2	8.9	1.95	13.2	1.6	12.2	3.05	10.2	1.3	8.4	1.34
573-77----	53.9	8.4	33.6	6.5	1.31	6.8	1.0	6.3	1.33	3.9	0.6	3.4	0.49
570-77----	39.1	9.5	37.7	6.5	1.35	7.9	1.1	7.4	1.73	5.7	0.8	4.9	0.79
567-77----	17.6	5.7	22.6	3.8	0.87	5.1	0.7	4.9	1.21	3.9	0.6	3.6	0.60
559-77----	34.7	9.5	38.7	6.8	1.52	9.0	1.2	8.5	2.02	6.4	0.9	5.9	0.93
557-77----	14.5	8.8	36.3	5.9	1.38	8.2	1.1	8.1	2.10	7.0	1.0	6.4	1.06
552-77----	13.4	7.7	31.9	5.2	1.19	7.7	1.0	7.3	1.86	6.3	0.9	5.6	0.93
548-77----	28.1	12.4	50.9	8.3	1.91	12.0	1.6	12.1	2.99	10.1	1.4	9.4	1.54
542-77----	13.6	5.2	20.9	3.7	0.81	4.9	0.7	4.7	1.12	3.7	0.5	3.3	0.52
535-77----	11.3	6.8	28.0	4.4	0.97	6.4	0.8	6.2	1.56	5.1	0.7	4.6	0.78
176-76----	16.0	8.3	34.5	5.4	1.32	7.7	1.0	7.5	1.81	5.8	0.8	4.9	0.77
530-77----	16.3	7.7	31.7	5.4	1.15	7.0	0.9	6.8	1.67	5.4	0.7	4.8	0.78
525-77----	18.8	9.5	38.6	6.4	1.44	8.7	1.2	8.5	2.12	7.0	0.9	6.0	0.97
521-77----	40.4	10.0	40.5	7.3	1.56	8.5	1.1	7.7	1.72	5.6	0.8	5.1	0.81
168-76----	57.1	11.8	47.1	8.3	1.84	10.3	1.4	9.6	2.19	7.1	1.0	6.1	1.00
167-76----	27.2	3.6	14.6	2.8	0.54	2.8	0.4	2.6	0.51	1.6	0.2	1.4	0.20
515-77----	37.1	17.6	74.1	12.6	2.89	17.0	2.3	16.4	3.99	13.3	1.8	11.6	1.90
164-76----	58.8	13.2	52.3	9.1	2.02	11.3	1.6	11.0	2.49	8.0	1.1	6.7	1.04
163-76----	53.9	14.6	58.2	10.0	2.13	12.9	1.7	12.5	2.87	9.4	1.3	8.0	1.24
161-76----	112.0	65.9	272.0	47.4	10.40	60.6	7.8	53.8	11.80	35.4	4.5	26.1	3.90
157-76----	91.1	63.1	261.0	43.9	10.00	58.8	7.5	53.5	12.20	37.5	4.9	28.6	4.28
154-76----	57.2	11.4	45.7	8.3	1.79	10.0	1.4	9.8	2.19	7.1	1.0	6.5	1.00
148-76----	91.4	71.4	291.0	49.6	10.80	61.8	7.7	51.7	11.00	32.5	4.0	21.8	3.25
145-76----	30.9	4.0	15.1	3.0	0.57	2.9	0.4	2.5	0.49	1.7	0.2	1.7	0.21
141-76----	58.3	39.3	159.0	27.3	5.82	30.3	3.7	23.6	4.80	13.7	1.6	9.3	1.34
138-76----	129.0	111.0	440.0	65.9	14.30	85.4	10.4	71.8	16.30	49.2	6.1	34.4	5.03
137-76----	62.6	11.6	44.8	8.0	1.61	8.7	1.1	7.4	1.47	4.5	0.6	3.7	0.54
136-76----	69.7	51.3	203.0	30.6	6.55	38.0	4.6	31.8	7.06	20.9	2.6	14.8	2.25
135-76----	55.6	22.2	87.3	14.4	2.92	16.8	2.1	14.0	2.99	9.0	1.1	6.8	1.03
133-76----	6.8	1.7	6.6	1.1	0.25	1.1	0.2	1.0	0.20	0.6		0.5	0.06
125-76----	75.6	22.2	89.2	16.6	3.49	18.4	2.5	15.8	3.35	10.2	1.4	8.6	1.30
120-76----	70.0	16.9	66.4	11.8	2.36	12.9	1.8	12.0	2.60	8.0	1.0	6.4	0.98
117-76----	38.4	4.6	17.1	3.2	0.54	2.7	0.3	2.3	0.50	1.7	0.3	2.0	0.34
113-76----	53.6	10.9	42.8	8.2	1.73	8.4	1.2	7.7	1.53	4.3	0.6	3.6	0.54
110-76----	55.7	21.4	85.0	14.6	3.05	16.0	2.0	12.9	2.68	7.7	1.0	5.8	0.81
105-76----	53.1	29.6	118.0	19.5	4.08	22.1	2.8	18.4	3.98	11.7	1.5	8.8	1.28
101-76----	39.2	18.3	72.5	11.7	2.63	14.5	1.8	12.7	2.76	8.3	1.1	6.4	0.96
99-76----	50.9	22.0	88.2	14.2	3.15	18.0	2.3	16.0	3.67	11.3	1.4	8.9	1.37

Table 4a. Cont.

Sample	Thickness	SiO₂+	AL₂O₃	Fe₂O₃	MgO	CaO	Na₂O	K₂O	TiO₂	P₂O₅	MnO	H₂O#	F
98-76----	21.00	51.0	16.6	6.16	0.8	1.4	1.5	3.28	0.13	0.5	0.022	8.5	0.2
90-76----	20.38	38.7	12.3	3.15	2.3	11.3	0.5	3.02	0.22	5.4	0.019	6.3	0.6
89-76----	20.28	52.8	20.8	2.70	1.9	1.6	0.1	3.23	0.14	0.1	0.026	10.7	0.7
83-76----	19.51	27.3	6.4	1.97	1.1	23.6	0.8	1.63	0.11	15.9	0.010	3.3	1.5
79-76----	19.03	13.2	2.9	0.93	1.1	34.7	0.4	0.81	0.06	18.4	0.004	1.5	1.4
77-76----	18.67	12.5	2.7	0.86	1.3	35.5	0.3	0.76	0.06	16.2	0.005	1.4	1.2
74-76----	18.36	15.3	3.3	1.10	1.3	32.5	0.4	0.92	0.07	15.2	0.006	1.7	1.3
70-76----	17.92	7.4	2.0	0.77	0.4	38.6	0.5	0.57	0.02	30.5	0.002	1.1	2.1
56-76----	16.70	16.9	2.2	0.83	0.9	32.0	0.3	0.64	0.07	23.8	0.005	1.1	1.8
54-76----	16.65	16.6	3.0	1.04	1.1	32.5	0.4	0.89	0.09	23.8	0.006	1.6	2.0
50-76----	15.88	10.1	1.7	0.41	14.5	29.2	0.4	0.47	0.05	2.6	0.019	0.9	0.2
44-76----	14.60	47.2	5.0	1.56	3.7	15.0	0.5	1.53	0.14	6.6	0.013	2.6	0.8
39-76----	14.02	33.1	6.8	2.02	2.3	21.3	0.7	2.05	0.17	14.1	0.012	3.5	1.4
36-76----	13.22	16.9	3.3	0.93	14.5	24.2	0.5	1.11	0.10	0.1	0.024	1.7	0.0
28-76----	11.65	15.0	0.9	0.24	14.3	27.6	0.2	0.28	0.02	2.4	0.019	0.5	0.2
16-76----	9.62	16.5	2.4	0.89	0.7	33.2	0.4	0.71	0.07	25.4	0.006	1.2	1.9
13-76----	9.11	25.8	4.1	1.39	0.9	28.8	0.7	1.22	0.12	21.6	0.008	2.1	1.7
250-74----	8.02	17.4	2.0	0.73	0.6	36.5	0.3	0.61	0.06	28.6	0.004	1.0	0.0
248-74----	7.70	28.2	4.0	1.22	1.0	27.4	0.5	1.25	0.10	19.6	0.007	2.1	1.5
243-74----	6.87	22.6	3.8	1.09	1.3	30.9	0.4	1.24	0.07	22.9	0.006	1.9	2.0
239-74----	6.32	23.7	2.4	0.67	1.1	31.3	0.3	0.76	0.06	23.1	0.005	1.2	1.8
232-74----	5.30	25.0	3.8	0.97	1.1	30.1	0.4	1.20	0.08	21.8	0.005	2.0	1.9
231-74----	5.24	24.8	5.4	1.33	1.7	27.6	0.6	1.75	0.09	19.7	0.007	2.8	1.6
226-74----	4.48	23.6	2.3	0.57	1.6	33.0	0.2	0.70	0.05	23.4	0.004	1.2	1.8
225-74----	4.41	20.0	2.9	0.79	1.8	33.3	0.3	0.90	0.06	24.1	0.005	1.5	2.0
222-74----	3.84	5.0	0.9	0.41	9.8	36.8	0.1	0.23	0.02	4.7	0.010	0.5	0.3
220-74----	3.08	3.5	1.0	0.27	0.2	44.5	0.4	0.30	0.03	37.3	0.001	0.5	2.9
219-74----	2.46	6.7	1.1	0.43	0.2	43.1	0.5	0.34	0.04	36.2	0.001	0.6	2.8
216-74----	1.46	52.4	8.7	3.16	2.9	4.4	0.6	2.70	0.32	0.2	0.016	4.5	1.8
212-74----	0.92	28.0	4.3	1.04	12.4	19.0	0.4	1.18	0.13	0.1	0.018	2.2	0.6
209-74----	0.37	30.2	4.5	1.10	12.1	17.9	0.2	1.28	0.10	0.1	0.020	2.3	0.6
207-74----	0.08	6.2	2.0	1.44	0.3	44.2	0.5	0.61	0.05	36.0	0.004	1.0	3.3

Table 4b*. Major elements and oxides, in percent, and minor elements, in parts per million, in the 53-series of samples. Thicknesses are cumulative, in meters. Blanks indicate no analysis.

Sample	Thickness	SiO₂	Al₂O₃	Fe₂O₃	MgO	CaO	Na₂O	K₂O	TiO₂	P₂O₅	MnO	H₂O⁻	H⁺
584-77----	52.41	61.3	10.20	3.10	1.8	7.5	1.4	2.10	0.69	2.20	0.039	0.23	0.31
187-76----	51.34	61.0	8.80	2.40	1.9	7.5	1.4	1.60	0.62	0.37	0.057	0.16	0.25
575-77----	50.39	6.3	1.40	0.54	0.2	48.4	0.5	0.18	0.09	34.30	0.006	0.10	0.17
568-77----	49.40	25.8	4.40	1.50	1.9	34.2	1.0	0.66	0.31	0.09	0.111	0.01	0.11
562-77----	48.47	6.5	0.76	0.24	0.5	46.9	0.3	0.07	0.06	29.30	0.022	0.08	0.18
553-77----	47.37	5.7	0.96	0.34	0.8	45.8	0.2	0.17	0.08	26.60	0.022	0.12	0.23
539-77----	46.31	3.5	0.46	0.01	0.9	50.6	0.2	0.01	0.03	18.20	0.021	0.09	0.07
533-77----	45.40	4.4	1.20	0.28	0.3	45.0	0.2	0.14	0.08	31.20	0.006	0.25	0.47

Table 4a. Cont.

Sample	Total S	CO$_2$	Org. C	N	Ag (2)	As	Ba	Cd (2)	Cr	Cu	Ga (4)	Li (2)	Mo (2)
98-76----	5.2	0.2	4.6		4	90.4	157	3	653	110	2	14	36
90-76----	3.4	4.9	8.0	1.83	2	44.6	216	2	1320	66	22	26	15
89-76----	2.4	0.2	2.7	2.23	1	57.9	186	2	197	24	11	34	7
83-76----	2.9	3.1	10.4	0.85	3	51.0	203	7	704	107	17	21	29
79-76----	2.1	11.9	10.7	0.76	3	20.4	98	8	992	136	16	16	56
77-76----	2.0	15.1	10.1	0.72	2	21.0	87	7	666	124	11	14	48
74-76----	2.3	13.4	11.2	0.70	3	55.2	99	6	1030	166	17	20	52
70-76----	2.3	2.3	11.4	0.65	2	21.8	104	11	1730	168	9	13	37
56-76----	2.5	3.6	13.2	0.24	4	15.5	129	263	877	82	19	12	76
54-76----	2.4	3.9	10.6	0.62	3	18.7	162	222	873	115	16	17	153
50-76----	0.5	37.5	1.5		1	9.8	49	1	47	20	9	2	3
44-76----	1.9	9.2	4.4		1	26.8	185	3	297	38	19	16	13
39-76----	2.2	5.1	5.4		4	33.2	225	29	660	48	27	25	27
36-76----	1.0	33.3	2.3		1	14.9	47	3	26	18	4	2	5
28-76----	0.4	36.3	1.7		1	4.4	24	1	68	20	8	2	3
16-76----	2.7	2.3	11.6	0.47	1	17.6	112	193	602	55	8	9	115
13-76----	2.4	2.4	6.7	0.39	1	26.4	153	220	498	62	18	10	121
250-74----	1.8	2.2	8.1	0.38	1	16.0	93	187	600	68	12	9	149
248-74----	2.3	2.6	8.2	0.41	5	28.8	138	234	728	78	14	15	138
243-74----	1.7	4.1	6.0	0.31	5	26.7	117	84	835	79	16	17	87
239-74----	1.7	3.6	8.2	0.47	3	16.7	84	67	756	66	9	14	45
232-74----	1.7	4.0	5.8	0.53	3	20.5	120	69	689	62	13	19	62
231-74----	1.9	4.8	5.9	0.54	4	28.3	149	67	616	82	20	26	48
226-74----	1.3	4.7	5.6	0.51	3	15.2	75	52	629	58	17	14	43
225-74----	1.5	5.5	5.3	0.30	3	15.4	83	41	700	63	19	18	29
222-74----	0.5	40.0	0.8		1	7.1	22	1	66	15	6	5	5
220-74----	1.3	1.5	6.0	0.43	1	4.9	50	100	405	58	6	8	32
219-74----	1.0	1.5	5.6	0.39	1	15.2	59	102	672	61	5	10	19
216-74----	3.8	5.1	9.4	0.70	4	39.4	262	230	959	119	19	56	694
212-74----	1.0	27.6	2.0	0.20	1	10.7	121	2	113	14	15	13	5
209-74----	0.9	28.4	0.4	0.18	1	11.5	103	8	138	15	10	14	4
207-74----	1.7	1.6	1.1	0.13	1	23.6	60	38	903	33	9	18	27

Table 4b. Cont.

Sample	Total S	sulfide	CO$_2$	Org. C	N	Ag	As	B	Ba	Co	Cr	Cs	Cu
584-77----	2.34	2.16	3.2	3.1	0.24	0.1	13.0	200	300	7.2	741	5.4	40
187-76----	2.18	1.57	6.5	2.5	0.20	0.1	15.0	150	220	6.4	225	3.4	17
575-77----	1.01	0.14	1.8	2.3	0.09	2.1	10.0	12	340	0.7	602	0.7	21
568-77----	1.24	0.71	27.3	1.2	0.07	4.0	19.0	39	130	3.5	229	1.6	22
562-77----	0.64	0.06	7.1	3.1	0.09	1.0	3.5	7	140	0.5	236	0.3	20
553-77----	0.95	0.07	9.6	4.1	0.16	3.0	8.6	8	150	0.7	484	0.4	29
539-77----	0.29	0.04	22.0	1.3	0.04	0.8	4.7	5	94	0.2	122	0.2	5.6
533-77----	1.64	0.26	2.2	9.8	0.31	2.8	13.0	11	170	0.8	687	0.5	46

Table 4a. Cont.

Sample	Ni	Pb	Sb (.6)	Sc (2)	Se	Sr	Th	Tl (.2)	U	V	Y	Zn	La
98-76----	181	48	12.4	3	236.0	79	27.3	2.4	2.5	152	10	848	17.8
90-76----	212	18	6.4	10	137.0	394	13.1	1.2	21.8	174	116	736	104.0
89-76----	57	43	8.2	4	95.1	64	11.0	1.2	1.1	157	3	214	5.2
83-76----	264	13	8.1	5	166.0	895	5.1	0.5	28.9	171	160	1230	142.0
79-76----	261	13	7.5	3	98.0	1090	3.0	0.5	34.4	186	186	1210	134.0
77-76----	247	13	4.8	1	97.0	979	2.4	0.5	31.9	168	206	1120	135.0
74-76----	312	13	6.9	5	102.0	883	3.1	0.6	30.6	178	259	1430	177.0
70-76----	310	18	6.4	5	109.0	1370	4.3	1.7	49.4	295	748	1280	501.0
56-76----	246	19	4.9	6	67.6	783	5.6	2.9	117.0	1670	362	2040	215.0
54-76----	282	17	4.6	4	78.4	767	2.8	3.9	67.3	1720	209	2550	111.0
50-76----	31	10	0.3	1	16.7	276	1.5	0.1	4.9	66	39	88	27.8
44-76----	106	9	3.5	6	36.7	308	4.2	0.5	20.8	135	126	393	90.7
39-76----	130	10	7.2	8	49.7	439	4.9	0.8	26.6	165	149	988	106.0
36-76----	40	7	1.7	3	13.7	178	2.3	0.3	3.8	91	13	106	12
28-76----	29	11	0.3	1	9.2	249	0.9	0.4	4.8	74	25	76	18.7
16-76----	294	15	3.4	2	58.4	727	2.6	5.1	106.0	2370	90	4000	53.2
13-76----	278	16	5.2	4	79.2	589	4.0	8.9	107.0	1500	105	4810	73
250-74----	251	14	2.1	2	41.3	701	4.4	3.2	101.0	1820	84	3100	50
248-74----	301	17	5.7	1	88.6	502	3.6	4.6	109.0	1250	125	3180	92.1
243-74----	249	16	5.1	4	68.5	519	3.3	1.9	85.4	1020	140	1630	101
239-74----	225	14	3.4	2	49.0	514	2.1	1.1	68.9	856	149	1120	98.1
232-74----	228	16	4.4	2	48.3	481	2.9	1.0	44.3	230	167	1310	106
231-74----	286	15	6.7	3	71.0	471	4.3	1.2	60.8	210	258	1440	191
226-74----	189	14	3.1	1	110.0	475	1.7	1.8	47.9	239	132	1130	86.7
225-74----	176	13	3.1	4	43.0	484	2.2	2.5	41.8	209	179	1470	123
222-74----	26	11	0.3	1	11.4	308	1.0	1.0	5.9	63	33	86	24.6
220-74----	143	15	1.5	1	31.6	668	1.4	1.7	84.4	1260	136	1480	88.8
219-74----	86	17	3.3	1	72.9	737	1.9	7.1	133.0	2380	125	1070	79.6
216-74----	730	16	13.7	6	226.0	65	8.5	40.2	8.3	2600	24	7370	21.6
212-74----	29	9	1.4	3	16.8	84	4.1	2.2	1.9	194	15	38	14.5
209-74----	30	8	1.9	3	18.3	73	4.6	5.0	2.3	134	14	77	15
207-74----	94	22	5.3	6	58.6	801	6.9	17.1	121.0	259	734	355	458

Table 4b. Cont.

Sample	Hf	Mo	Ni	Rb	Sb	Sc	Se	Sr	Ta	Th	U	V	Y
584-77----	9.9	22	160	80	2.1	9.7	41.0	140	1.1	10.1	21.7	82	97
187-76----	8.8	3	54	62	1.8	8.4	19.9	120	1.0	8.5	5.2	66	30
575-77----	1.5	10	71	20	1.7	2.7	15.3	1100	0.1	1.8	128.0	210	270
568-77----	3.8	26	68	31	3.3	3.3	44.3	260	0.5	4.3	4.7	140	21
562-77----	1.1	12	56	20	0.9	1.5	14.1	740	0.1	0.6	161.0	340	120
553-77----	0.9	29	90	6	2.5	2.4	41.5	830	0.1	0.9	120.0	520	120
539-77----	0.3	7	22	10	1.3	0.6	9.5	720	0.2	0.2	67.1	190	91
533-77----	0.7	130	280	20	12.5	1.7	48.8	920	0.2	0.7	203.0	1000	140

Table4a. Cont.

Sample	Ce	Pr	Nd	Sm	Eu	Gd	Tb	Dy	Ho	Er	Tm	Yb	Lu
98-76----	30.9	4.6	18.6	3.4	0.66	2.8	0.3	1.7	0.31	0.8		0.7	0.06
90-76----	93.5	19.1	71.3	12.3	2.36	13.3	1.7	11.6	2.37	7.1	0.9	5.8	0.82
89-76----	7.2	1.0	3.4	0.6	0.08	0.5	0.1	0.4	0.08	0.3		0.3	0.05
83-76----	48.3	20.1	80.9	13.1	2.78	15.7	2.0	13.5	3.01	9.3	1.2	7.2	1.06
79-76----	28.0	16.8	68.7	11.0	2.36	14.1	1.8	12.9	3.06	9.8	1.3	8.2	1.26
77-76----	28.3	16.9	68.7	10.7	2.40	13.9	1.8	12.8	3.06	9.8	1.3	8.0	1.23
74-76----	36.3	23.9	95.5	14.9	3.31	19.2	2.4	17.1	4.00	12.7	1.7	10.3	1.59
70-76----	73.8	63.8	256.0	40.0	9.05	53.0	6.7	47.0	10.80	33.1	4.2	25.2	3.82
56-76----	48.4	27.6	111.0	17.8	4.06	23.9	3.1	22.4	5.28	17.4	2.4	15.3	2.55
54-76----	34.4	17.9	73.0	12.5	2.98	16.4	2.2	15.1	3.55	11.2	1.6	10.2	1.63
50-76----	11.8	4.3	16.7	3.0	0.61	3.6	0.4	3.1	0.68	2.1	0.3	1.7	0.24
44-76----	35.7	12.5	50.0	8.4	1.82	10.3	1.3	9.0	2.05	6.2	0.9	5.4	0.84
39-76----	42.3	13.7	54.6	8.9	1.91	11.1	1.4	10.0	2.28	7.2	1.0	6.4	1.01
36-76----	13.4	2.4	9.7	1.8	0.35	1.9	0.2	1.6	0.32	1.0	0.2	1.0	0.13
28-76----	7.0	2.5	9.8	1.6	0.34	2.1	0.2	1.8	0.39	1.2	0.2	1.1	0.16
16-76----	21.4	7.6	30.4	5.2	1.12	6.8	0.9	6.4	1.49	4.6	0.6	4.0	0.64
13-76----	37.6	10.0	39.1	6.6	1.40	7.9	1.0	7.1	1.62	5.1	0.7	4.4	0.70
250-74----	16.3	6.5	26.1	4.3	0.98	5.5	0.7	5.0	1.20	3.8	0.5	3.2	0.50
248-74----	35.4	12.2	48.8	8.3	1.79	10.3	1.4	9.3	2.13	6.8	0.9	5.7	0.91
243-74----	33.5	13.2	53.5	8.9	2.04	11.4	1.5	10.4	2.40	7.8	1.0	6.3	0.94
239-74----	25.3	11.4	46.4	6.9	1.59	9.1	1.2	8.2	1.95	6.3	0.8	5.3	0.84
232-74----	31.3	13.0	52.8	8.5	1.87	10.8	1.4	9.9	2.29	7.5	1.0	6.4	1.01
231-74----	52.3	22.0	87.7	13.8	3.01	18.5	2.4	17.1	4.10	13.4	1.8	11.7	1.86
226-74----	21.8	9.8	39.9	6.1	1.35	7.9	1.0	7.4	1.70	5.6	0.8	4.8	0.73
225-74----	31.3	13.6	56.0	8.5	1.82	10.9	1.4	9.8	2.37	7.8	1.0	6.6	1.02
222-74----	9.6	3.1	12.6	2.1	0.43	2.5	0.3	2.1	0.50	1.6	0.2	1.3	0.19
220-74----	18.3	8.8	36.2	5.4	1.21	7.2	0.9	6.7	1.61	5.5	0.8	4.8	0.78
219-74----	17.2	8.5	35.2	5.4	1.21	7.0	0.9	6.4	1.55	5.2	0.7	4.4	0.68
216-74----	40.7	5.7	23.2	4.5	0.87	4.2	0.6	3.9	0.76	2.4	0.3	2.3	0.33
212-74----	25.5	3.4	13.3	2.6	0.48	2.4	0.3	2.3	0.49	1.6	0.2	1.6	0.23
209-74----	23.3	3.1	11.8	2.3	0.41	2.1	0.3	2.1	0.43	1.4	0.2	1.6	0.22
207-74----	106.0	65.2	272.0	47.3	10.20	56.1	6.7	45.6	9.76	29.7	3.7	21.9	3.31

Tablke 4b. Cont.

Sample	Zn	La	Ce
584-77----	561	62	73
187-76----	93	31	46
575-77----	700	133	37
568-77----	518	15	22
562-77----	607	41	14
553-77----	1210	39	13
539-77----	295	27	8
533-77----	4470	50	16

Table 4b. Cont.

Sample	Thickness	SiO$_2$	Al$_2$O$_3$	Fe$_2$O$_3$	MgO	CaO	Na$_2$O	K$_2$O	TiO$_2$	P$_2$O$_5$	MnO	H$_2$O$^-$	H$^+$
529-77----	44.42	19.5	3.90	1.50	0.9	31.5	0.5	0.79	0.25	18.20	0.017	0.23	0.61
523-77----	43.35	2.7	0.57	0.09	1.5	50.2	0.1	0.09	0.02	2.60	0.019	0.01	0.09
168-76----	42.36	46.6	7.90	2.60	1.5	13.0	1.2	1.90	0.50	6.80	0.022	0.13	0.52
518-77----	41.57	38.3	7.30	2.80	1.1	18.0	0.9	1.70	0.44	10.20	0.034	0.19	0.56
164-76----	40.40	47.0	8.30	3.00	1.9	12.1	1.4	2.20	0.55	4.80	0.062	0.14	0.49
162-76----	39.40	35.9	5.90	2.10	1.6	21.6	1.0	1.30	0.41	8.00	0.059	0.12	0.43
160-76----	38.41	37.3	4.90	1.50	2.0	24.2	1.3	0.99	0.36	13.60	0.059	0.23	0.27
158-76----	37.40	53.0	8.70	2.80	1.7	10.8	1.5	2.00	0.57	5.40	0.063	0.21	0.36
156-76----	36.31	52.6	7.90	2.30	1.1	11.0	1.4	1.80	0.55	5.90	0.049	0.24	0.44
154-76----	35.27	49.9	7.70	2.30	1.3	11.1	1.4	1.80	0.54	3.10	0.049	0.27	0.56
152-76----	34.23	59.6	9.30	2.80	1.2	6.3	1.6	2.20	0.68	0.93	0.052	0.25	0.48
147-76----	33.35	34.8	4.50	1.40	9.9	18.6	1.2	0.83	0.34	0.10	0.102	0.20	0.15
145-76----	32.43	33.5	4.70	1.60	9.8	18.5	1.2	0.96	0.37	0.08	0.096	0.16	0.19
143-76----	31.42	56.9	7.70	2.80	3.6	7.4	1.7	1.80	0.64	0.20	0.058	0.35	0.36
508-77----	30.40	16.0	3.10	1.50	0.7	30.0	0.4	0.69	0.17	20.90	0.012	0.51	0.72
503-77----	29.58	57.5	9.30	3.30	1.6	6.4	1.9	2.00	0.64	0.89	0.056	0.28	0.44
501-77----	28.51	39.5	9.10	3.30	3.3	18.3	0.8	2.30	0.43	5.90	0.037	0.28	0.37
130-76----	27.43	27.7	4.90	1.50	10.8	21.8	0.3	1.10	0.22	0.95	0.057	0.18	0.24
124-76----	26.46	58.3	10.00	3.10	2.7	4.2	1.7	2.40	0.68	0.17	0.061	0.25	0.47
120-76----	25.43	56.1	10.50	3.50	1.1	7.4	1.6	2.40	0.67	0.09	0.052	0.34	0.46
116-76----	24.45	61.3	8.90	3.20	2.9	5.8	2.0	2.00	0.69	0.10	0.065	0.30	0.28
107-76----	23.38	32.1	5.30	2.60	1.2	26.9	0.9	1.20	0.35	0.89	0.057	0.24	0.30
102-76----	22.49	39.6	9.00	2.70	2.0	14.2	0.6	2.20	0.43	2.90	0.036	0.36	0.69
95-76----	21.49	24.9	6.50	2.00	1.4	24.4	0.5	1.60	0.30	10.20	0.028	0.43	0.70
88-76----	20.42	26.9	5.60	1.50	9.0	20.0	0.6	1.40	0.26	2.90	0.081	0.18	0.42
81-76----	19.44	32.2	8.00	3.00	2.1	17.4	1.0	2.30	0.40	8.50	0.028	0.38	0.70
73-76----	18.40	15.0	3.40	1.40	0.9	34.1	0.5	0.89	0.16	21.50	0.010	0.35	0.66
63-76----	17.41	18.7	2.80	1.40	1.3	29.4	0.4	0.86	0.24	17.80	0.013	0.40	0.74
52-76----	16.50	15.0	1.90	0.57	2.6	40.6	0.4	0.56	0.11	1.20	0.037	0.05	0.17
48-76----	15.41	38.3	6.80	2.30	3.4	18.9	0.6	2.10	0.34	9.70	0.032	0.31	0.37
42-76----	14.37	37.8	6.60	2.20	3.0	19.2	0.7	2.00	0.35	10.70	0.043	0.28	0.40
37-76----	13.36	23.3	3.40	1.00	12.9	22.1	0.4	1.10	0.19	0.06	0.050	0.11	0.21
32-76----	12.28	36.7	5.40	1.40	6.4	19.4	0.5	1.70	0.27	6.10	0.026	0.22	0.30
27-76----	11.45	37.8	5.40	1.70	1.9	22.1	0.6	1.70	0.32	13.90	0.025	0.23	0.36
22-76----	10.36	11.7	1.80	0.70	0.6	35.9	0.4	0.47	0.14	25.40	0.009	0.27	0.61
5-76----	9.50	23.2	3.30	1.30	1.0	28.3	0.5	0.93	0.26	20.40	0.013	0.29	0.55
251-74----	8.46	22.4	3.10	0.97	1.7	36.0	0.8	0.71	0.23	0.76	0.057	0.05	0.11
247-74----	7.50	28.6	2.90	1.20	1.2	28.7	0.4	0.91	0.20	19.00	0.012	0.24	0.42
240-74----	6.45	25.7	3.30	1.10	1.7	29.9	0.4	0.99	0.20	20.40	0.015	0.31	0.37
233-74----	5.37	31.6	2.60	0.79	1.2	29.3	0.3	0.79	0.15	18.80	0.012	0.25	0.31
225-74----	4.41	19.2	2.30	0.78	2.0	36.6	0.2	0.71	0.13	22.90	0.010	0.28	0.32
221-74----	3.34	4.1	0.76	0.18	18.2	30.8	0.1	0.15	0.05	1.50	0.034	0.06	0.07
219-74----	2.46	4.4	1.10	0.42	0.2	46.4	0.4	0.30	0.06	33.60	0.001	0.47	0.45
215-74----	1.37	56.4	9.30	3.50	2.6	5.1	0.8	2.90	0.69	0.86	0.032	0.52	0.29
209-74----	0.37	32.9	3.90	1.30	11.8	19.6	0.3	1.30	0.32	0.07	0.041	0.21	0.11

Table 4b. Cont.

Sample	Total S	sulfide	CO_2	Org. C	N	Ag	As	B	Ba	Co	Cr	Cs	Cu
529-77----	2.50	0.78	5.2	11.5	0.56	10.0	23.0	120	220	3.2	1080	1.8	63
523-77----	0.27	0.01	39.9	1.9	0.06	0.8	3.1	5	41	0.2	189	0.2	9.9
168-76----	2.60	1.87	4.2	7.8	0.67	7.3	25.0	120	300	5.2	846	2.2	60
518-77----	2.91	2.05	4.0	8.7	0.69	17.0	16.0	160	280	5.1	1320	2.3	61
164-76----	2.77	1.72	6.0	7.5	0.59	15.0	27.0	140	340	6.7	1140	3.0	62
162-76----	2.26	1.18	9.6	7.3	0.46	12.0	1.1	120	290	4.4	1210	2.3	62
160-76----	1.71	0.82	4.7	4.5	0.33	1.7	11.0	31	240	3.4	203	0.9	27
158-76----	2.48	1.65	4.3	4.0	0.53	4.7	14.0	120	380	5.9	749	2.4	41
156-76----	2.06	1.07	3.4	6.7	0.53	10.0	14.0	160	360	5.3	1340	2.8	51
154-76----	2.33	1.15	6.0	9.3	0.60	15.0	10.0	140	400	5.4	1380	2.9	49
152-76----	2.34	1.29	3.1	6.6	0.60	7.9	9.1	130	430	6.7	1020	3.1	40
147-76----	1.27	0.71	25.1	1.8	0.19	0.6	9.5	14	130	2.7	110	0.6	10
145-76----	1.16	0.78	25.1	2.6	0.23	0.1	7.5	11	130	3.1	73	0.6	12
143-76----	2.52	1.44	8.0	4.4	0.50	0.9	13.0	46	300	5.9	159	1.5	24
508-77----	2.42	0.87	2.9	14.2	0.62	14.0	9.4	94	330	2.5	2330	2.6	49
503-77----	2.81	2.16	5.0	5.8	0.59	5.6	12.0	67	350	7.4	489	2.6	32
501-77----	2.30	1.95	10.7	1.7	0.65	3.6	14.0	120	270	6.2	806	3.8	39
130-76----	1.08	1.04	27.7	1.5	0.42	0.9	6.8	16	120	3.1	313	1.2	28
124-76----	2.29	1.76	5.7	5.7	0.71	4.8	13.0	90	300	7.7	364	2.7	44
120-76----	2.39	2.21	2.3	4.5	0.71	4.3	11.0	170	380	6.8	1250	4.1	72
116-76----	1.97	1.77	6.9	1.8	0.44	0.8	17.0	48	250	6.3	272	1.5	28
107-76----	1.92	1.75	20.5	4.1	0.38	4.4	13.0	48	170	4.0	506	1.4	48
102-76----	2.27	1.70	9.5	8.7	0.96	7.5	25.0	180	250	5.8	2590	6.6	89
95-76----	2.64	1.18	8.8	4.8	0.82	11.0	15.0	140	280	4.3	1780	4.5	63
88-76----	1.49	0.86	23.0	4.6	0.69	3.0	18.0	19	140	3.2	910	1.3	42
81-76----	3.43	1.68	5.8	10.6	0.81	15.0	32.0	190	270	6.4	3570	5.6	120
73-76----	2.37	0.69	3.9	12.3	0.59	6.9	16.0	89	270	2.6	1830	2.1	89
63-76----	2.68	0.96	4.1	13.5	0.64	22.0	20.0	72	260	2.7	1420	2.2	85
52-76----	0.82	0.26	33.2	2.8	0.15	2.8	5.8	8	24	1.1	183	0.5	14
48-76----	2.36	1.23	7.7	4.1	0.42	4.6	24.0	130	300	4.4	828	3.0	51
42-76----	2.58	1.25	6.2	5.1	0.43	4.1	34.0	110	300	4.8	797	3.3	57
37-76----	1.38	0.54	31.0	2.9	0.26	1.3	19.0	5	73	2.6	172	0.6	19
32-76----	1.89	0.93	15.0	3.2	0.33	2.3	28.0	57	190	3.6	369	2.0	24
27-76----	2.14	0.91	4.1	6.1	0.35	10.0	38.0	92	230	3.8	717	2.4	55
22-76----	1.91	0.27	2.6	12.0	0.43	7.5	18.0	37	160	1.5	598	1.2	37
5-76----	2.12	0.01	2.8	9.6	0.36	6.0	14.0	62	210	2.9	681	2.1	40
251-74----	0.86	0.45	29.0	1.8	0.08	0.6	13.0	11	89	2.3	98	0.7	14
247-74----	1.45	0.68	3.5	7.4	0.30	8.5	6.0	60	160	2.5	1010	1.8	54
240-74----	1.42	0.25	4.2	6.2	0.26	11.0	6.4	76	180	2.5	804	2.0	38
233-74----	1.16	0.08	4.0	4.9	0.19	5.4	5.6	59	140	2.5	1010	1.8	38
225-74----	1.20	0.29	5.3	4.5	0.20	6.0	6.1	45	130	1.4	587	1.0	45
221-74----	0.35	0.14	41.5	1.0	0.02	1.3	5.3	5	27	0.7	94	0.5	7.3
219-74----	0.87	0.01	1.5	6.6	0.26	3.0	6.4	10	60	0.1	538	1.3	42
215-74----	3.33	1.51	4.2	4.7	0.18	7.1	26.0	150	310	8.8	696	7.0	78
209-74----	0.92	0.62	26.8	0.8	0.03	0.5	17.0	70	100	3.0	97	2.3	15

Table 4b. Cont.

Sample	Hf	Mo	Ni	Rb	Sb	Sc	Se	Sr	Ta	Th	U	V	Y
529-77----	2.5	200	420	32	12.3	4.5	120.0	760	0.4	3.3	86.5	1300	200
523-77----	0.2	10	33	9	0.5	0.9	6.3	800	0.2	0.2	8.1	170	59
168-76----	6.3	42	230	59	7.4	8.5	73.6	340	0.8	7.1	33.3	210	130
518-77----	5.3	57	320	57	6.5	10.0	77.2	510	0.7	6.3	34.4	160	300
164-76----	5.9	34	370	56	5.0	9.1	80.1	340	0.9	7.1	17.5	190	160
162-76----	5.4	52	330	48	3.9	7.5	67.4	520	0.6	5.7	21.1	150	220
160-76----	6.3	15	110	31	2.1	5.7	19.4	620	0.6	6.1	18.2	90	260
158-76----	8.5	19	170	66	3.1	8.4	41.9	280	0.9	8.0	15.0	120	180
156-76----	9.4	65	380	55	3.7	8.9	63.1	300	1.0	8.1	22.4	·230	210
154-76----	8.8	67	380	55	4.7	8.1	70.3	210	0.9	6.8	14.6	250	150
152-76----	9.9	37	280	68	3.4	8.2	54.3	110	1.1	9.0	10.6	200	93
147-76----	6.6	25	35	30	2.3	4.3	10.9	180	0.6	4.9	2.2	85	17
145-76----	6.0	3	37	33	2.4	4.3	7.3	160	0.6	4.9	2.1	76	19
143-76----	10.2	5	65	59	3.2	6.7	16.0	80	1.1	9.3	3.4	110	31
508-77----	2.1	100	940	31	4.9	9.6	109.0	870	0.3	4.8	150.0	160	1600
503-77----	8.0	22	130	76	5.4	9.1	157.0	140	1.2	9.7	6.2	130	63
501-77----	2.7	11	130	86	4.5	10.6	78.9	350	0.7	6.0	16.3	90	99
130-76----	1.3	5	72	42	2.4	4.7	30.0	140	0.4	3.1	5.3	60	42
124-76----	7.5	13	96	73	4.9	8.5	93.3	84	1.1	9.6	3.2	240	23
120-76----	7.6	64	300	88	5.5	11.9	66.0	300	1.1	9.5	15.6	150	120
116-76----	8.9	8	56	60	3.6	7.7	37.7	120	0.9	8.9	2.3	110	21
107-76----	3.6	26	120	40	4.6	6.2	62.0	640	0.6	4.4	4.0	79	47
102-76----	2.7	25	320	94	6.9	11.2	140.0	520	0.7	6.1	13.8	130	95
95-76----	1.7	89	640	62	6.4	8.1	104.0	880	0.5	3.6	29.2	130	170
88-76----	1.6	6	130	42	3.6	7.3	94.3	530	0.5	3.5	10.6	130	68
81-76----	2.8	44	650	77	10.4	11.0	229.0	590	0.6	5.4	33.9	170	200
73-76----	1.4	45	550	33	5.2	8.2	107.0	1100	0.3	3.1	31.1	150	880
63-76----	2.3	180	850	27	9.7	9.8	152.0	680	0.3	2.9	173.0	1300	870
52-76----	1.3	16	68	18	2.1	2.5	41.7	270	0.2	1.6	5.1	170	79
48-76----	2.1	18	140	61	5.7	8.9	78.7	460	0.5	4.6	21.7	140	160
42-76----	2.7	20	160	66	6.1	9.2	57.0	470	0.6	4.8	25.6	150	170
37-76----	1.6	8	57	27	2.9	3.7	19.0	160	0.3	2.8	4.2	94	15
32-76----	2.2	8	79	48	4.4	6.9	37.8	280	0.5	4.3	14.8	84	110
27-76----	2.8	21	160	54	7.2	8.5	76.0	440	0.5	4.5	32.4	140	180
22-76----	1.4	98	390	16	4.3	2.7	57.7	730	0.2	1.2	117.0	1300	150
5-76----	2.7	74	330	34	4.2	4.0	69.9	640	0.4	2.8	87.2	1000	110
251-74----	3.1	7	43	21	1.5	3.2	40.3	180	0.3	3.4	2.6	130	35
247-74----	2.0	72	290	28	5.3	4.6	66.8	510	0.3	2.3	73.5	480	150
240-74----	1.8	55	240	39	6.1	4.4	82.0	500	0.3	2.5	51.1	610	160
233-74----	2.0	47	320	27	5.2	4.6	67.8	500	0.3	2.2	72.8	170	190
225-74----	1.4	33	160	14	6.0	2.7	56.6	510	0.2	1.2	99.7	150	200
221-74----	0.4	13	40	9	1.2	1.3	19.0	120	0.2	0.6	4.8	150	31
219-74----	0.7	17	93	14	3.1	1.6	68.2	710	0.2	0.5	155.0	950	180
215-74----	8.6	440	700	86	11.4	8.2	196.0	88	0.9	9.1	19.7	1300	53
209-74----	4.8	7	43	30	2.1	3.5	19.1	88	0.4	3.9	2.0	120	10

Table 4b. Cont.

Sample	Total S	sulfide	CO_2	Org. C	N	Ag	As	B	Ba	Co	Cr	Cs	Cu
529-77----	2.50	0.78	5.2	11.5	0.56	10.0	23.0	120	220	3.2	1080	1.8	63
523-77----	0.27	0.01	39.9	1.9	0.06	0.8	3.1	5	41	0.2	189	0.2	9.9
168-76----	2.60	1.87	4.2	7.8	0.67	7.3	25.0	120	300	5.2	846	2.2	60
518-77----	2.91	2.05	4.0	8.7	0.69	17.0	16.0	160	280	5.1	1320	2.3	61
164-76----	2.77	1.72	6.0	7.5	0.59	15.0	27.0	140	340	6.7	1140	3.0	62
162-76----	2.26	1.18	9.6	7.3	0.46	12.0	1.1	120	290	4.4	1210	2.3	62
160-76----	1.71	0.82	4.7	4.5	0.33	1.7	11.0	31	240	3.4	203	0.9	27
158-76----	2.48	1.65	4.3	4.0	0.53	4.7	14.0	120	380	5.9	749	2.4	41
156-76----	2.06	1.07	3.4	6.7	0.53	10.0	14.0	160	360	5.3	1340	2.8	51
154-76----	2.33	1.15	6.0	9.3	0.60	15.0	10.0	140	400	5.4	1380	2.9	49
152-76----	2.34	1.29	3.1	6.6	0.60	7.9	9.1	130	430	6.7	1020	3.1	40
147-76----	1.27	0.71	25.1	1.8	0.19	0.6	9.5	14	130	2.7	110	0.6	10
145-76----	1.16	0.78	25.1	2.6	0.23	0.1	7.5	11	130	3.1	73	0.6	12
143-76----	2.52	1.44	8.0	4.4	0.50	0.9	13.0	46	300	5.9	159	1.5	24
508-77----	2.42	0.87	2.9	14.2	0.62	14.0	9.4	94	330	2.5	2330	2.6	49
503-77----	2.81	2.16	5.0	5.8	0.59	5.6	12.0	67	350	7.4	489	2.6	32
501-77----	2.30	1.95	10.7	1.7	0.65	3.6	14.0	120	270	6.2	806	3.8	39
130-76----	1.08	1.04	27.7	1.5	0.42	0.9	6.8	16	120	3.1	313	1.2	28
124-76----	2.29	1.76	5.7	5.7	0.71	4.8	13.0	90	300	7.7	364	2.7	44
120-76----	2.39	2.21	2.3	4.5	0.71	4.3	11.0	170	380	6.8	1250	4.1	72
116-76----	1.97	1.77	6.9	1.8	0.44	0.8	17.0	48	250	6.3	272	1.5	28
107-76----	1.92	1.75	20.5	4.1	0.38	4.4	13.0	48	170	4.0	506	1.4	48
102-76----	2.27	1.70	9.5	8.7	0.96	7.5	25.0	180	250	5.8	2590	6.6	89
95-76----	2.64	1.18	8.8	4.8	0.82	11.0	15.0	140	280	4.3	1780	4.5	63
88-76----	1.49	0.86	23.0	4.6	0.69	3.0	18.0	19	140	3.2	910	1.3	42
81-76----	3.43	1.68	5.8	10.6	0.81	15.0	32.0	190	270	6.4	3570	5.6	120
73-76----	2.37	0.69	3.9	12.3	0.59	6.9	16.0	89	270	2.6	1830	2.1	89
63-76----	2.68	0.96	4.1	13.5	0.64	22.0	20.0	72	260	2.7	1420	2.2	85
52-76----	0.82	0.26	33.2	2.8	0.15	2.8	5.8	8	24	1.1	183	0.5	14
48-76----	2.36	1.23	7.7	4.1	0.42	4.6	24.0	130	300	4.4	828	3.0	51
42-76----	2.58	1.25	6.2	5.1	0.43	4.1	34.0	110	300	4.8	797	3.3	57
37-76----	1.38	0.54	31.0	2.9	0.26	1.3	19.0	5	73	2.6	172	0.6	19
32-76----	1.89	0.93	15.0	3.2	0.33	2.3	28.0	57	190	3.6	369	2.0	24
27-76----	2.14	0.91	4.1	6.1	0.35	10.0	38.0	92	230	3.8	717	2.4	55
22-76----	1.91	0.27	2.6	12.0	0.43	7.5	18.0	37	160	1.5	598	1.2	37
5-76----	2.12	0.01	2.8	9.6	0.36	6.0	14.0	62	210	2.9	681	2.1	40
251-74----	0.86	0.45	29.0	1.8	0.08	0.6	13.0	11	89	2.3	98	0.7	14
247-74----	1.45	0.68	3.5	7.4	0.30	8.5	6.0	60	160	2.5	1010	1.8	54
240-74----	1.42	0.25	4.2	6.2	0.26	11.0	6.4	76	180	2.5	804	2.0	38
233-74----	1.16	0.08	4.0	4.9	0.19	5.4	5.6	59	140	2.5	1010	1.8	38
225-74----	1.20	0.29	5.3	4.5	0.20	6.0	6.1	45	130	1.4	587	1.0	45
221-74----	0.35	0.14	41.5	1.0	0.02	1.3	5.3	5	27	0.7	94	0.5	7.3
219-74----	0.87	0.01	1.5	6.6	0.26	3.0	6.4	10	60	0.1	538	1.3	42
215-74----	3.33	1.51	4.2	4.7	0.18	7.1	26.0	150	310	8.8	696	7.0	78
209-74----	0.92	0.62	26.8	0.8	0.03	0.5	17.0	70	100	3.0	97	2.3	15

Table 4b. Cont.

Sample	Hf	Mo	Ni	Rb	Sb	Sc	Se	Sr	Ta	Th	U	V	Y
529-77----	2.5	200	420	32	12.3	4.5	120.0	760	0.4	3.3	86.5	1300	200
523-77----	0.2	10	33	9	0.5	0.9	6.3	800	0.2	0.2	8.1	170	59
168-76----	6.3	42	230	59	7.4	8.5	73.6	340	0.8	7.1	33.3	210	130
518-77----	5.3	57	320	57	6.5	10.0	77.2	510	0.7	6.3	34.4	160	300
164-76----	5.9	34	370	56	5.0	9.1	80.1	340	0.9	7.1	17.5	190	160
162-76----	5.4	52	330	48	3.9	7.5	67.4	520	0.6	5.7	21.1	150	220
160-76----	6.3	15	110	31	2.1	5.7	19.4	620	0.6	6.1	18.2	90	260
158-76----	8.5	19	170	66	3.1	8.4	41.9	280	0.9	8.0	15.0	120	180
156-76----	9.4	65	380	55	3.7	8.9	63.1	300	1.0	8.1	22.4	230	210
154-76----	8.8	67	380	55	4.7	8.1	70.3	210	0.9	6.8	14.6	250	150
152-76----	9.9	37	280	68	3.4	8.2	54.3	110	1.1	9.0	10.6	200	93
147-76----	6.6	25	35	30	2.3	4.3	10.9	180	0.6	4.9	2.2	85	17
145-76----	6.0	3	37	33	2.4	4.3	7.3	160	0.6	4.9	2.1	76	19
143-76----	10.2	5	65	59	3.2	6.7	16.0	80	1.1	9.3	3.4	110	31
508-77----	2.1	100	940	31	4.9	9.6	109.0	870	0.3	4.8	150.0	160	1600
503-77----	8.0	22	130	76	5.4	9.1	157.0	140	1.2	9.7	6.2	130	63
501-77----	2.7	11	130	86	4.5	10.6	78.9	350	0.7	6.0	16.3	90	99
130-76----	1.3	5	72	42	2.4	4.7	30.0	140	0.4	3.1	5.3	60	42
124-76----	7.5	13	96	73	4.9	8.5	93.3	84	1.1	9.6	3.2	240	23
120-76----	7.6	64	300	88	5.5	11.9	66.0	300	1.1	9.5	15.6	150	120
116-76----	8.9	8	56	60	3.6	7.7	37.7	120	0.9	8.9	2.3	110	21
107-76----	3.6	26	120	40	4.6	6.2	62.0	640	0.6	4.4	4.0	79	47
102-76----	2.7	25	320	94	6.9	11.2	140.0	520	0.7	6.1	13.8	130	95
95-76----	1.7	89	640	62	6.4	8.1	104.0	880	0.5	3.6	29.2	130	170
88-76----	1.6	6	130	42	3.6	7.3	94.3	530	0.5	3.5	10.6	130	68
81-76----	2.8	44	650	77	10.4	11.0	229.0	590	0.6	5.4	33.9	170	200
73-76----	1.4	45	550	33	5.2	8.2	107.0	1100	0.3	3.1	31.1	150	880
63-76----	2.3	180	850	27	9.7	9.8	152.0	680	0.3	2.9	173.0	1300	870
52-76----	1.3	16	68	18	2.1	2.5	41.7	270	0.2	1.6	5.1	170	79
48-76----	2.1	18	140	61	5.7	8.9	78.7	460	0.5	4.6	21.7	140	160
42-76----	2.7	20	160	66	6.1	9.2	57.0	470	0.6	4.8	25.6	150	170
37-76----	1.6	8	57	27	2.9	3.7	19.0	160	0.3	2.8	4.2	94	15
32-76----	2.2	8	79	48	4.4	6.9	37.8	280	0.5	4.3	14.8	84	110
27-76----	2.8	21	160	54	7.2	8.5	76.0	440	0.5	4.5	32.4	140	180
22-76----	1.4	98	390	16	4.3	2.7	57.7	730	0.2	1.2	117.0	1300	150
5-76----	2.7	74	330	34	4.2	4.0	69.9	640	0.4	2.8	87.2	1000	110
251-74----	3.1	7	43	21	1.5	3.2	40.3	180	0.3	3.4	2.6	130	35
247-74----	2.0	72	290	28	5.3	4.6	66.8	510	0.3	2.3	73.5	480	150
240-74----	1.8	55	240	39	6.1	4.4	82.0	500	0.3	2.5	51.1	610	160
233-74----	2.0	47	320	27	5.2	4.6	67.8	500	0.3	2.2	72.8	170	190
225-74----	1.4	33	160	14	6.0	2.7	56.6	510	0.2	1.2	99.7	150	200
221-74----	0.4	13	40	9	1.2	1.3	19.0	120	0.2	0.6	4.8	150	31
219-74----	0.7	17	93	14	3.1	1.6	68.2	710	0.2	0.5	155.0	950	180
215-74----	8.6	440	700	86	11.4	8.2	196.0	88	0.9	9.1	19.7	1300	53
209-74----	4.8	7	43	30	2.1	3.5	19.1	88	0.4	3.9	2.0	120	10

Table 4b. Cont.

Sample	Zn	La	Ce
529-77----	2100	69	35
523-77----	77	15	4
168-76----	822	73	55
518-77----	940	139	54
164-76----	684	77	53
162-76----	575	96	45
160-76----	207	133	163
158-76----	345	101	62
156-76----	739	91	64
154-76----	696	57	51
152-76----	530	47	60
147-76----	43	16	27
145-76----	29	17	30
143-76----	54	29	51
508-77----	1870	621	94
503-77----	230	55	67
501-77----	478	89	46
130-76----	207	39	25
124-76----	124	24	44
120-76----	712	93	64
116-76----	58	22	43
107-76----	250	30	32
102-76----	976	84	47
95-76----	1060	90	36
88-76----	234	49	31
81-76----	1890	195	62
73-76----	1410	321	64
63-76----	3180	322	60
52-76----	110	30	14
48-76----	386	112	40
42-76----	323	125	48
37-76----	135	13	13
32-76----	172	95	47
27-76----	589	133	44
22-76----	3550	74	19
5-76----	1970	53	30
251-74----	60	20	29
247-74----	1490	95	34
240-74----	723	88	32
233-74----	1520	93	32
225-74----	3540	68	23
221-74----	133	14	7
219-74----	831	65	24
215-74----	4370	33	54
209-74----	88	15	23

* Major oxides and trace elements in Table 4a were measured by ICP-AES, except for the REE, which were measured by ICP-MS. Major elements in Table 4b were measured by XRF, trace elements by DC arc emission spectroscopy. Other techniques employed to measure the other elements (e.g., F) and oxides (e.g., H_2O^- and CO_2) are listed in Table 1.

+ SiO_2 was estimated from the deficit of all other oxides and elements versus 100%.

H_2O was estimated from the relation between Al_2O_3 in these samples and H_2O and Al_2O_3 as measured at the Enoch Valley Mine, ID (Piper, 1999).

Table 5. Major-oxide (in percent) and trace-element (in parts per million) composition of terrigenous, detrital fraction. Blanks in column 5 indicate that the concentration of an element was determine by a means other than the use of a minimum curve. Blanks elsewhere indicate that no value was listed, or that it could not be determined.

	World Shale Average[1]	North American Shale Composite[2]	Phosphoria Fm. (Medrano and Piper, 1995)	Value from minimum line (this study)	Value used in calculations (this study)
Major-oxides					
SiO_2	58.4	64.8	58.3		58.3
Al_2O_3	15.1	16.9	16.7		16.6
Fe_2O_3	6.84	6.29	6.2		5.4
MgO	2.49	2.85	1.2		1.2
CaO	3.09	3.58	2.5		2.5
Na_2O	1.3	1.13			
K_2O	3.19	3.94	4.2		4.0
TiO_2	0.77	0.79	0.48		0.48
P_2O_5	0.16	0.14	0.17		0.17
CO_2	2.63[3]				
Minor elements					
Ag	0.05-0.90		0.48		0.48[1]
As	13	28.4	32	10	10
Ba	546	636	429		520
Cd	0.8		0.8		0.5
Co	19	25.7	20		20
Cr	83	124.5	83	140	140
Cu	35		35	34	34
Li	76				76
Mn	600	600		168	170
Mo	0.7-2.0			2.0	2
Ni	42	58	59	70	105
Pb	21.6		10	22	22
Sb					
Sc	13	14.9	15		15
Se	1.0			1	1
Sr	24-359	142	70	120	70
Th	12	12.3	7		12
Tl				0.1	0.1
U	2.5		2.5	2.5	2.5
V	98-2600		180	120	120
Zn	100		60	100	100
Rare Earth Elements					
Y	27	27		36	36
La	41	32	43	38	41
Ce	83	70	93	75	83
Pr	10.1	7.9	10.6	9.5	10.1
Nd	38	31	41	35	38
Sm	7.5	5.7	7.6	6.8	7.5
Eu	1.61	1.24	1.65	1.38	1.61
Gd	6.35	5.21	6.9	6.4	6.35
Tb	1.23	0.85	1.13	0.85	1.03
Dy	5.5		5.5	5.6	5.5
Ho	1.34	1.04	1.38	1.23	1.34
Er	3.75	3.4	4.5	3.94	3.75
Tm	0.63	0.5	0.70	0.58	0.63
Yb	3.53	3.1	4.1	3.58	3.53
Lu	0.61			0.59	0.61

[1] World Shale Average (major-element oxides, Turekian and Wedepohl, 1961; minor elements, Wedepohl, 1969-1978; rare-earth elements, Piper, 1974)

[2] North American Shale Composite (major and minor elements on a volatile free basis: Gromet and others, 1984; rare-earth elements, Haskin and Haskin, 1966)

[3] CO_2, Wedepohl, 1969-1978

Table 6. Varimax orthogonal transformation solution, principal component factor extraction method, using Statview II software. Log$_{10}$ of measured values was used, rather than raw data. Values greater than 0.50 are in bold. Table 6a gives the values for the 75-series samples, 6b the 53-series samples. The two are given separately because of the format of Statview II, it cannot handle blanks in a table.

6a	#1	#2	#3	#4	#5
Detritus	**0.89**	-0.18	0.29	-0.17	-0.14
Apatite	-0.47	**0.67**	0.36	0.16	0.14
Dolomite	0.11	-0.39	-0.19	-0.76	-0.15
Calcite	-0.04	-0.08	0.01	-0.71	-0.53
Org. Mat	0.00	0.40	**0.81**	0.11	0.07
Bio. SiO$_2$	0.30	-0.23	-0.19	-0.75	-0.11
Nitrogen	0.19	0.30	**0.63**	-0.01	0.09
Fluorine	-0.24	**0.56**	0.34	0.26	0.40
Sulfur	**0.63**	0.23	**0.66**	0.19	0.09
MnO	**0.61**	-0.49	-0.18	-0.40	-0.26
Y	-0.14	**0.95**	0.24	0.07	0.12
La	-0.01	**0.96**	0.19	0.13	0.03
Ce	**0.67**	**0.71**	0.06	-0.01	0.05
Pr	0.18	**0.96**	0.16	0.12	0.00
Nd	0.16	**0.96**	0.16	0.12	0.00
Sm	0.21	**0.95**	0.14	0.11	0.01
Eu	0.15	**0.96**	0.16	0.09	0.02
Gd	0.11	**0.97**	0.17	0.09	0.04
Tb	0.11	**0.97**	0.17	0.06	0.06
Dy	0.09	**0.98**	0.17	0.06	0.07
Ho	0.03	**0.97**	0.19	0.05	0.10
Er	0.02	**0.97**	0.19	0.05	0.12
Tm	0.00	**0.91**	0.18	0.14	-0.02
Yb	0.02	**0.96**	0.20	0.03	0.16
Lu	0.00	**0.94**	0.22	0.01	0.19
As	**0.58**	0.05	**0.60**	0.18	0.01
Ag	0.22	0.11	**0.73**	-0.17	-0.07
Ba	**0.80**	0.26	0.26	0.01	0.13
Cd	-0.32	0.18	**0.55**	0.12	**0.68**
Cr	0.22	**0.51**	**0.75**	0.14	0.12
Cu	0.07	0.42	**0.85**	0.12	-0.01
Ga	**0.53**	0.07	0.31	-0.61	-0.05
La	-0.05	**0.95**	0.24	0.15	0.02
Li	**0.62**	0.18	**0.57**	-0.06	0.12
Mn	**0.61**	-0.49	-0.18	-0.40	-0.26
Mo	-0.02	0.14	**0.83**	0.02	0.43
Ni	0.14	0.38	**0.84**	0.10	0.21
Pb	0.29	0.10	0.26	**0.74**	0.08
Sb	0.30	0.07	**0.82**	0.18	0.08
Sc	**0.78**	0.20	0.21	-0.17	-0.14
Se	0.37	0.17	**0.83**	0.21	0.02
Sr	-0.53	**0.71**	0.21	0.15	-0.07
Th	**0.94**	0.13	0.11	0.17	-0.01
Tl	-0.02	0.11	0.19	0.33	**0.84**
U	-0.44	**0.62**	0.34	0.22	0.43
V	-0.32	-0.03	**0.59**	0.16	**0.65**
Zn	-0.22	0.27	**0.77**	0.22	0.41

6b	#1	#2	#3	#4	#5
Detritus	**0.97**	-0.15	-0.02	-0.06	0.13
Apatite	-0.27	**0.85**	0.19	0.16	0.04
Dolomite	0.02	-0.64	-0.25	-0.23	0.46
Calcite	-0.17	-0.26	-0.08	-0.83	-0.13
Org. Mat	0.35	**0.60**	**0.53**	0.15	-0.03
Bio. SiO$_2$	**0.76**	-0.32	-0.20	0.06	-0.11
Nitrogen	0.71	0.37	0.26	-0.11	0.16
Fluorine	-0.24	**0.86**	0.19	0.21	0.01
Sulfur	**0.88**	0.21	0.26	0.12	0.14
MnO	0.48	-0.57	-0.28	-0.47	-0.02
Y	0.08	**0.94**	0.20	0.04	-0.03
La	0.34	**0.88**	0.10	0.09	0.15
Ce	**0.88**	0.33	-0.10	0.13	-0.01
Ag	0.26	0.49	**0.67**	-0.05	0.08
As	0.47	-0.06	0.14	0.24	**0.64**
B	**0.86**	0.25	0.21	0.08	0.04
Ba	**0.81**	0.37	0.03	0.16	-0.12
Co	**0.94**	-0.17	0.05	-0.07	0.13
Cr	0.46	**0.68**	0.47	-0.04	0.11
Cs	**0.85**	0.14	0.23	0.13	0.19
Cu	**0.60**	0.50	**0.52**	0.06	0.17
Hf	**0.90**	-0.24	-0.11	0.10	-0.25
Mo	0.20	0.37	**0.80**	0.16	-0.18
Ni	0.48	**0.55**	**0.63**	0.07	0.02
Rb	**0.93**	-0.04	-0.01	-0.02	0.14
Sb	**0.52**	0.25	**0.63**	0.18	0.32
Sc	**0.95**	0.14	0.04	-0.07	0.19
Se	0.51	0.35	**0.64**	0.04	0.25
Sr	-0.38	**0.82**	0.19	-0.10	0.08
Ta	**0.87**	-0.30	-0.03	-0.10	-0.01
Th	**0.97**	-0.15	-0.08	0.00	0.03
U	-0.26	**0.79**	0.34	0.34	-0.08
V	-0.26	0.21	**0.70**	0.50	-0.19
Zn	0.04	**0.62**	**0.66**	0.25	-0.02

Table 7. Concentration of trace elements in marine plankton (in parts per million) and in seawater (parts per billion) at approximately 2000-m depth in the Pacific Ocean (Martin and Knauer, 1973; Boyle and others, 1976, 1977; Boyle, 1981; Elderfield and others, 1981; Bruland, 1983; Collier, 1984, 1985; de Baar and others, 1985; Palmer, 1985; Brumsack, 1986).

Element	Organic matter content	Seawater content	Biogenic Silica	Biogenic Calcite
Cd-----	12	0.10		0.022
Co-----	<1	0.0012		
Cr-----	2.0	0.22		
Cu----	11	0.18	7	0.7
Mo----	2	10.60		
Ni-----	7.5	0.59		
Se-----	3.0	0.13		
U-----	1(?)	3.00		
V-----	3.0	1.80		-
Zn-----	110	0.52	7	55
La-----	<1	0.0052	5.8	0.13
Ce-----		0.0018	8.2	0.09
Nd-----		0.0043	6.7	0.11

Table 8. Selenium in source rocks, soil, water, sediment, vegetation, and biota in southeast Idaho. Concern levels, levels at which selenium in water extract and solids constitute a hazardous waste, and water quality standards are also given. Sample designations are taken from reports cited, with only minor changes.

	Environmental Components	Se Content (mean/range)	References[#]
Source Rock (μg/g)	Phosphoria Formation		
	Enoch Valley mine	51/1-410	1, 2
	Hot Springs mine	70/6-240	3
	Bloomington Canyon (vanadiferous zone)	560/21-1200	4
	Lakeridge core (western Wyoming)	48/0.5-380	3
Soil (μg/g)	Background (U.S.)	0.26	5
	Regional[†] ambient (upstream of mine activity)	3/0.6-16	6
	Regional waste-rock dumps	30/2-200	6
	Regional waste-rock dump at seeps	120/0.7-300	6
	Maybe Creek watershed		
	Ambient (upland of Maybe Creek)	1.16/0.3-3.7	7[†]
	Floodplain	5.9/0.4-28	7
	In-stream	73 /5.7-279	7
	Dry Valley	1-27.3	8
Sediment (dry wt., μg/g)	Background (U.S.)	0.2-2	9
	Ambient (upland of Maybe Creek)[∞]	1.6	7
	Regional ambient (upstream of mining activity)	1.3/0.9-1.9	6
	Regional streams	1.5/0.2-9	6
	Regional stock ponds	30/1.2-70	6
	Regional waste rock dumps at seeps	80/7-200	6
	Maybe Creek watershed	12-829	7
Vegetation (dry wt., μg/g)	Background (U.S.)	0.06/.013-0.42	10
	Regional (ambient, upland grasses)	0.16/<0.1-8	6
	Regional (upland waste-rock dumps)	15/0.19-80	6
	Regional (riparian waste-rock dump seep)	20/0.18-50	6
	Maybe Creek watershed		
	Ambient (upland of Maybe Creek)	2/<1-6.8	7
	Floodplain	23.5/<1-185	7
	In-stream, ponds, top of cross-valley fill	36.6/2.5-168	7
Biota (dry wt., except where otherwise noted, μg/g)	Fish		
	Salmonids skin-on-fillets (wet wt.)		
	Ambient (South Fork, Sage Creek)	1.3	6
	Blackfoot River	1.2	6
	East Mill Creek	6/3.3-7.9	6
	Muscle		
	Maybe Creek (above mine activity)	0.5-8.5	8
	Maybe and Dry Valley Creeks	2.0-15.8	8
	Liver/kidney tissue		
	Maybe Creek (above mine activity)	5-20	8
	Maybe and Dry Valley Creeks	2.5-60	8
	Birds		
	Eggs (normal)	<5	9
	Coot eggs		
	Conda mine tailings reservoir	13.3/10-16	3
	Smoky Canyon mine tailings reservoir	45.8/29-59	3
	Solutia mine south pond	76.5/73-80	3
	Sheep		
	Diet (adequate/toxic)	0.4-1/>5	11
	Stomach (defunct, 71 sheep at Wooley Valley)	85/44-132[‡]	12
	Liver (defunct; wet wt.)	8.7-10.7	12
	Liver (adequate/toxic; wet wt.)	0.25-1.5/>15	11
	Horses		
	Defunct (6 horses at South Maybe Canyon)	..[‡]	7, 8
	Defunct (2 horses at Conda mine site)	..[‡]	13
	Diet (adequate)	0.3-2	11
	Diet (chronic toxic)	16-80	11
	Diet (acute toxic)	>100	11

Table 8. (cont.)

	Environmental Components	Se Content (mean/range)	References
Biota (cont.)	Small mammals (Maybe Creek watershed)		
	Ambient	1.6-2.9	7
	Adjacent to creek	2-39.8	7
	Aquatic invertebrates (Maybe Creek watershed)		
	Ambient	4.6	7
	In creek	212/110-390	7
	Terrestrial invertebrates (Maybe Creek watershed)		
	Ambient	13.3-45.6	7
	Adjacent to creek	342/191-705	7
Water (µg/l)	Surface water		
	Background (U.S.)	0.1-0.4	9
	Ambient (Maybe and Dry Valley Creeks)	<1-3	7
	Streams		
	Blackfoot River	<5	8
	Regional streams	7/1-300	6
	Woodall Slough	2.3-2.7	3
	Maybe Creek	410-820	8
	Eastside Sage Valley Creek	3.5	3
	Dump seeps		
	Regional waste rock	600/7-2000	6
	Smoky Canyon mine	680	14
	Maybe Creek cross valley fill	716-1394	3
	Ponds		
	Regional stock ponds	60/<1-120	6
	Regional tailings ponds	11/<1-30	6
	Lower Slug Creek spring pond	2.8+	3
	Grace pond	2.5	3
	Dry Valley roadside pond	56	3
	Dry Valley Creek beaver pond	2.5	3
	Little Blackfoot River beaver pond	3.6	3
	South Enoch Valley beaver pond	4.5	3
	Angus Creek settling ponds	4.2-4.4	3
	Maybe Creek settling pond	897	3
	Dry Valley settling ponds	17-31	8
	Solutia Mine west pond	68	3
	Solutia Mine south pond	68.5	3
	Conda Mine pit pond	227	3
	Wetlands, pastures, and spring seeps		
	Conda mine, ephemeral wetland	199	3
	Wooley Valley mine, ephemeral wetland	4.1-772	3
	Upper Sage Valley wetlands	5.0	3
	Champ mine seep	6.0	3
	Champ mine pasture	4.1	3
	Maybe Creek pasture	803	3
	Sage Valley wet pasture	3.1	3
	Dry Valley springs and seeps	2-18	8
	Reservoirs		
	Henry mine	9.7	3
	Smoky Canyon mine	15.3/6-17.9	3
	Upper Angus Creek	22.4	3
	Conda mine (lower tailings)	8.7	3
	Watersheds		
	Angus Creek (Spring, 1999)	2.9/2.1-5.3	3
	Maybe Creek	751/66-1500	7
	Dry Valley	<5-144	6, 8
	Ground water		
	Ambient (upgradient of Maybe Creek)	<1-3	7
	Regional	5/<1-33	6
	Maybe Creek watershed	486/36-1200	7
	Dry Valley (bed rock and backfill)	<5-8	8
	Dry Valley (shallow alluvium)	<5	8

Table 8. (cont.)

Environmental Components		Se Content (mean/range)	References
Water Quality Standard (μg/l)	Water, for protection of aquatic wildlife	5	18
	Drinking water	50	18
Hazardous Waste	Solid (wet wt., μg/g)	100	15
	Water extract (μg/l)	1000	16
Concern Levels (for protection of wildlife)*	Sediment (dry wt., μg/g)	1.0-4.0	9
	Aquatic vegetation & invertebrates (dry wt., μg/g)	2.0-3.0	9
	Fish (whole body, dry wt., μg/g)	2.0-4.0	9
	Avian eggs (dry wt., μg/g)	3.0-6.0	9, 17
	Water (μg/l)	1-2	9, 17

References. 1. Piper, 1999; 2. Herring and others, 1999; 3. This Report; 4. McKelvey and others, 1986; 5. Shacklette and Boerngen, 1984; 6. Montgomery-Watson, 1999; 7. TRC, 1999; 8. USBLM, 1999; 9. USDOI, 1998; 10. Connor and Shacklette, 1975; 11. Puls, 1994; 12. Talcott, 1999; 13. USFS/USBLM, 1999; 14. Bond, 1999; 15. USBR, 1986; CCR, 1979; 16. USEPA, 1980; 17. Skorupa and Ohlendorf, 1991; 18. USEPA, 1992a, 1992b.

♦ The "Region" covers an area that encompasses the mines noted in the table plus the following mines and leases: North Maybe, Mountain Fuel, Ballard, Henry, Gay, Georgetown Canyon, Lanes Creek, Rasmussen Ridge, Dairy Syncline, Manning Creek, Diamond Creek west of the Blackfoot Reservation.

✢ Reference number 7 includes information for South Maybe Canyon Mine. North Maybe Mine is included in regional study (Ref. 6). Maybe Creek watershed is impacted by South Maybe Canyon Mine and adjacent cross-valley fill waste rock dump.

∞ Here and elsewhere in the table we have substituted ambient in the case of local values, where the cited references have used the term background.

‡ Diagnoses and toxicology reports confirmed horses and sheep were suffering from Se toxicosis (horses in 1996 at South Maybe Canyon and in 1997 at Conda Mine and sheep in September, 1999 at Wooley Valley). The sheep were found dead; the horses were "eventually destroyed". The chemical analyses of blood and tissue, in the case of the horses, are not known to have been released.

+ A single listing in this report (Ref. 3) represents a single reported value rather than the mean of several values.

* Toxicity levels, although not listed, are represented by the upper limit of the concern levels.
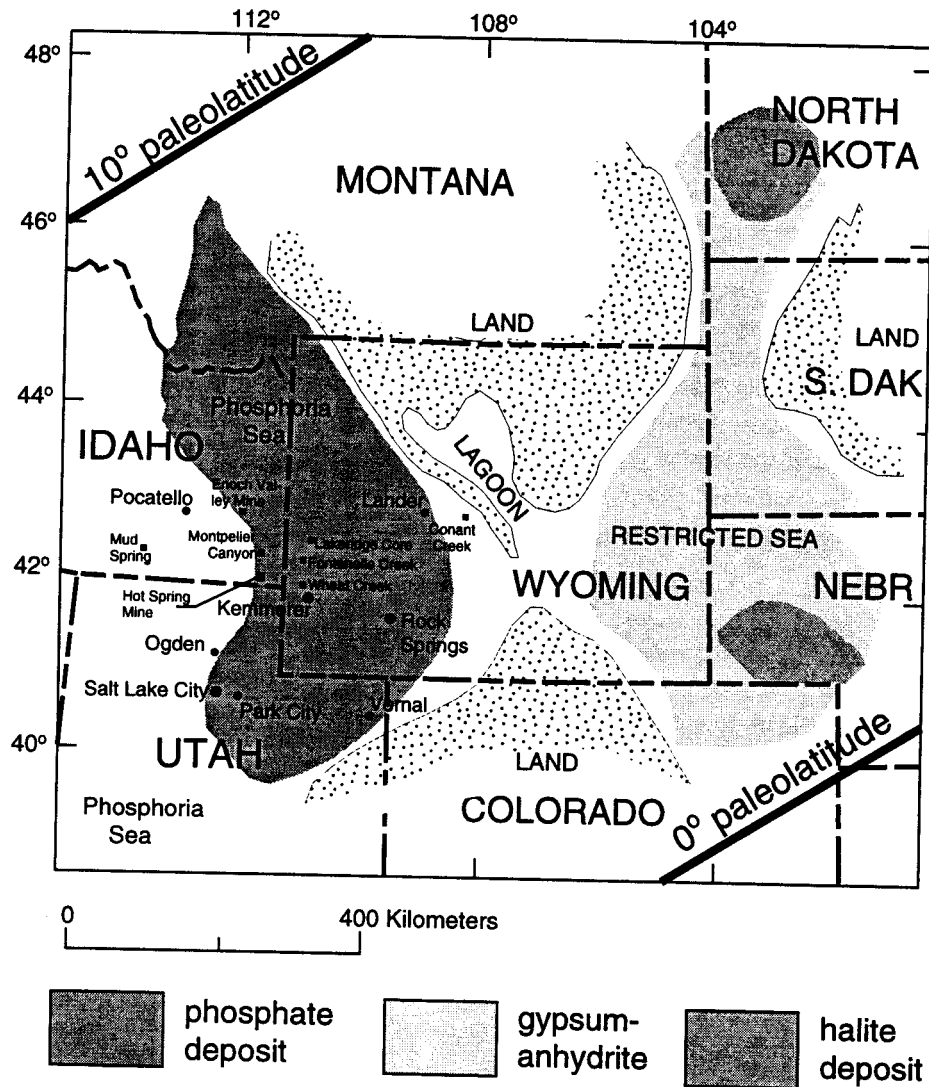
Figure 1. Location map of the northwest United States showing extent of the Phosphoria Formation, location of evaporite deposits to the east, and paleolatitudes during Permian time. In the land areas of Montana and central Wyoming, deposits include red beds. The Hot Springs Mine and location of other sections analyzed earlier are shown by closed squares (Medrano and Piper, 1995, Piper 2000). Figure is adapted from Sheldon (1964).

Hot Springs Mine

Explanation

Mudstone		Calcareous mudstone	
Phosphatic mudstone		Cherty Mudstone	
Chert		Phosphatic chert	
Calcareous chert		Argillaceous chert	
Carbonate		Phosphatic carbonate	
Cherty carbonate		Argillaceous carbonate	
Phosphate rock		Cherty phosphate rock	
Calcareous phosphate rock		Argillaceous phosphate rock	
Sandstone		Calcareous sandstone	
Quartzite		Cherty sandstone	
"Interbedded" carbonate and chert			

thickness
├─┼─┼─┤
200 CM

5236 — 189-76

upper waste zone

576-77
570-77

upper ore zone

552-77

535-77

521-77

515-77
164-76

157-76

3550 — 154-76 1755

148-76

145-76

waste zone

center

133-76

105-76

99-76

83-76

l. waste

0 —

56-76

16-76

250-74

lower ore zone

232-74

226-74

220-74

212-74

207-74

Figure 2. Stratigraphic column of the Meade Peak Member of the Phosphoria Formation at the Hot Springs Mine. Thicknesses (0 to 5236) are in centimeters; sample numbers give level at which samples (53- and 75-series) were collected. Each sample represents about a 10 to 25 cm interval. Position of ore and waste zones are approximated, based on other sections. However, the upper ore zone seems to be more well developed here than at other sites. No distinction has been made between calcite and dolomite, although the carbonate is predominantly dolomite (Table 3). Lithologies are based on report by Gulbrandsen (1979) and on chemical analyses given in Table 4 and in Gulbrandsen (1979).
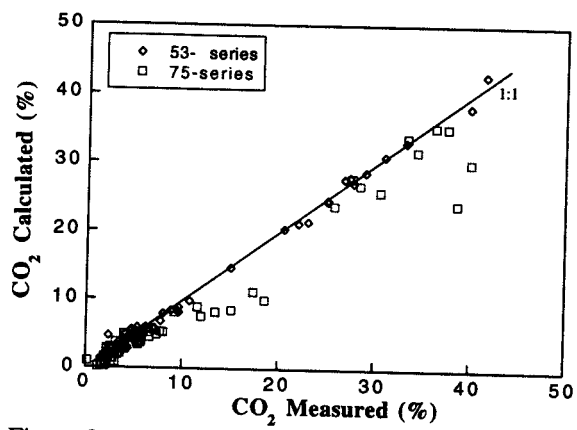
Figure 3. Relation between CO_2 measured and CO_2 calculated, which is based on the stiochiometry and concentration of each carbonate-bearing component (Tables 2 and 3).
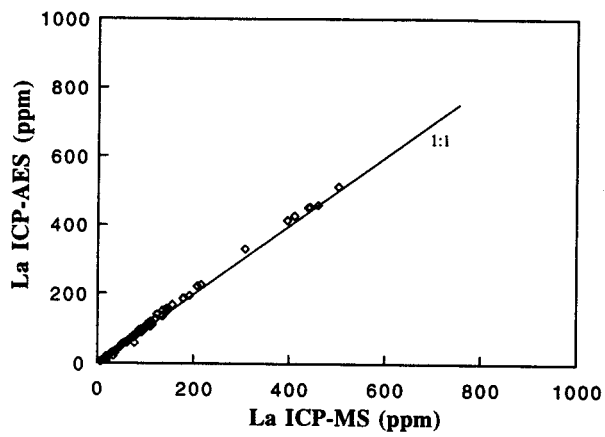
Figure 4. Relation between La measured by ICP-AES and ICP-MS.
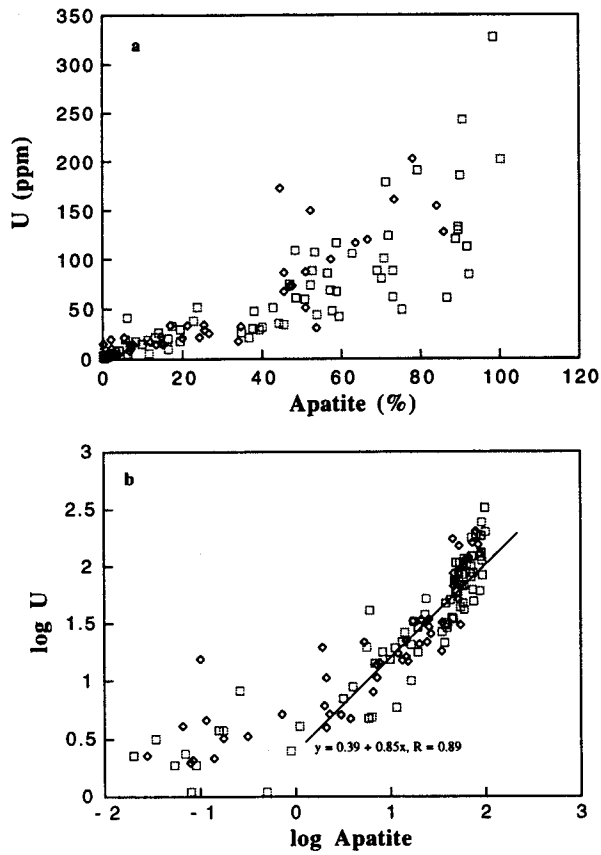
Figure 5. Relation between U and apatite. Measured values are plotted in (a) and Log_{10} of values are plotted in (b).
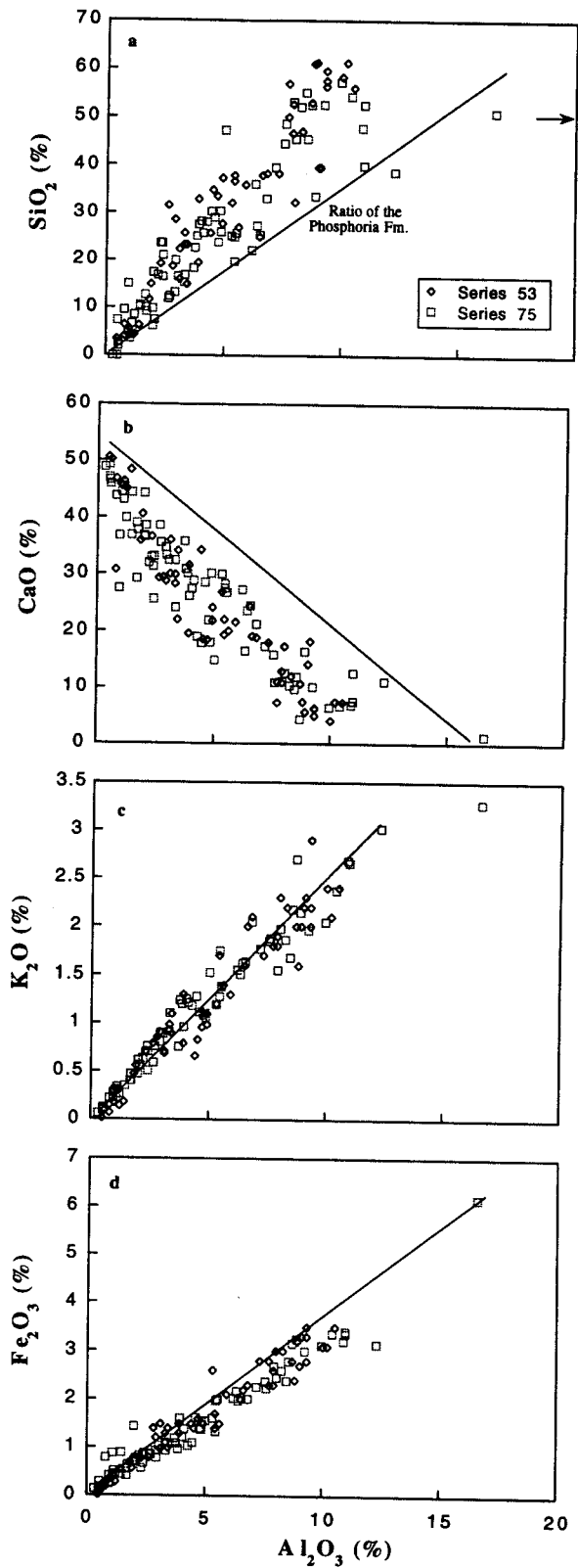
Figure 6. Relation between Al_2O_3 and SiO_2 (a), CaO (b), K_2O (c), and Fe_2O_3 (d). Solid curves represent best estimate of relations based on analyses at other sites, given here for comparison with the Hot Springs Mine data.
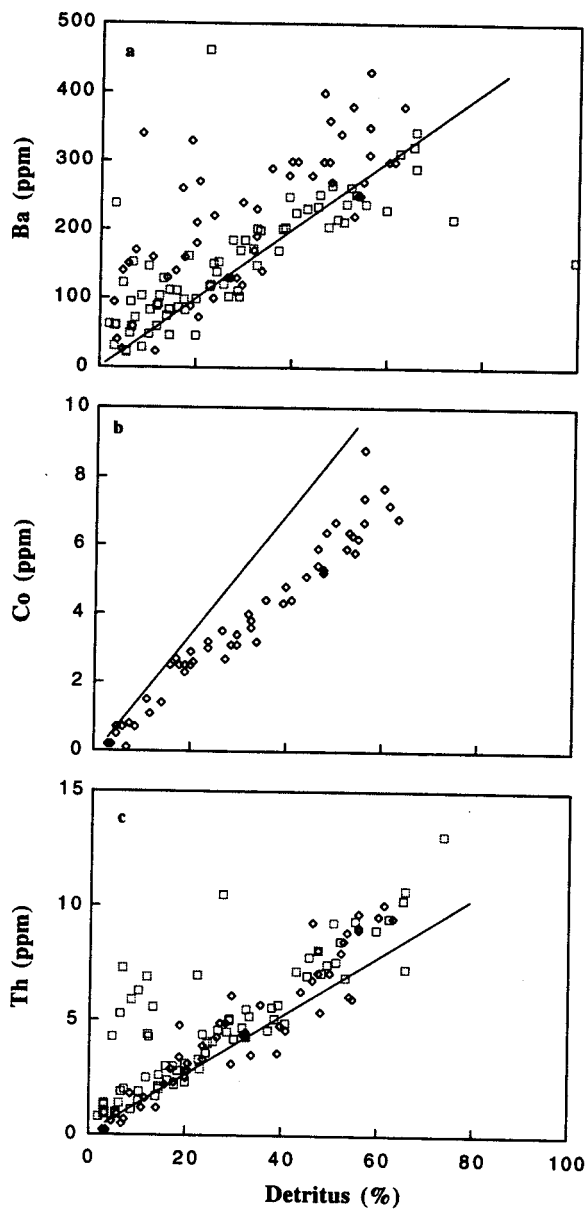
Figure 7. Relation between detritus and selected trace elements. Symbols and curves are the same as in Figure 6.
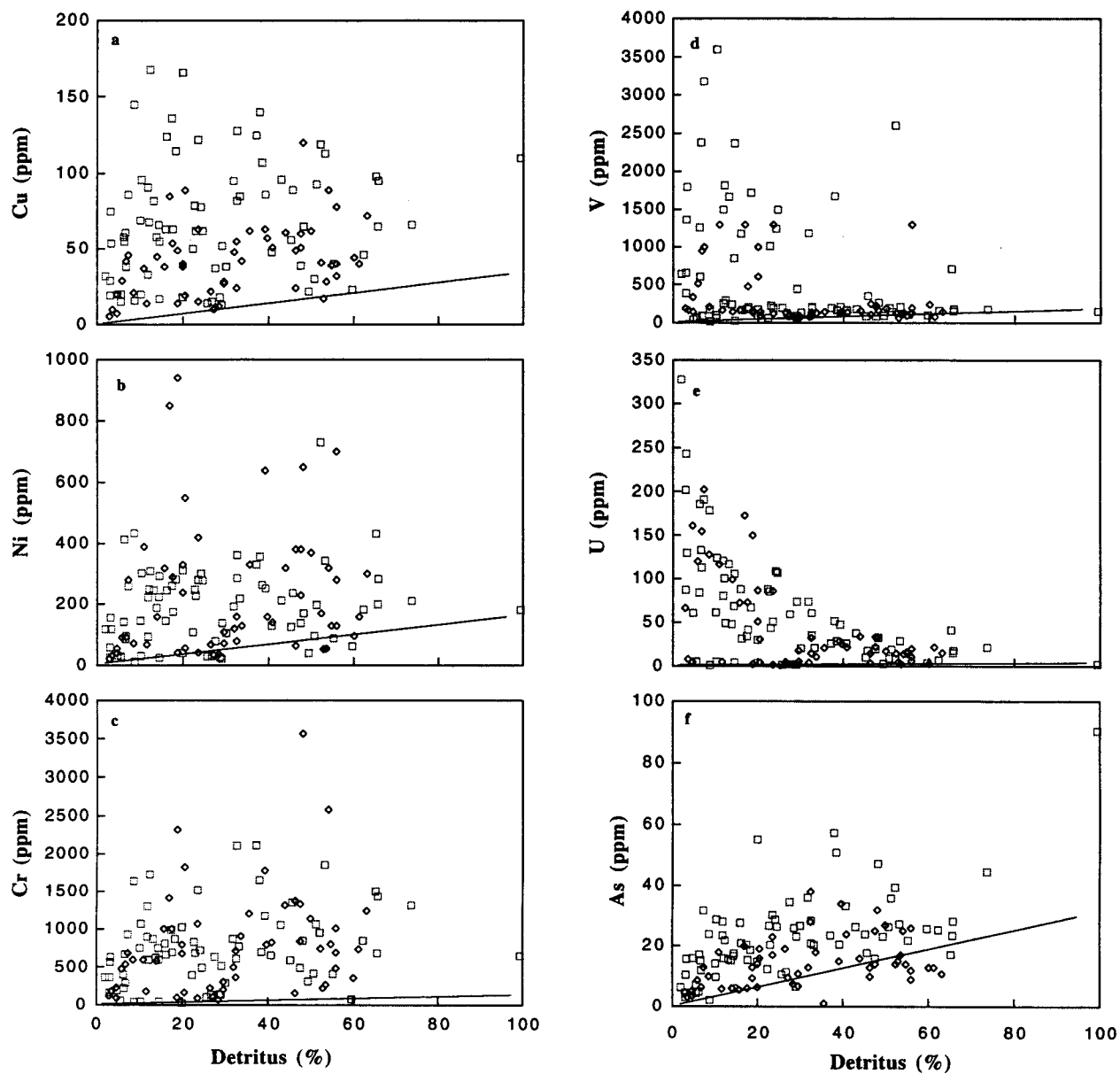
Figure 8. Relation between detritus and a selected group of trace elements that show a strong enrichment above the detrital contribution (Table 5). Symbols and curves are the same as in Figure 6. The detrital contribution of several trace elements at the Hot Springs Mine seems to be less than at the other sites. For example, an As minimum curve for the data (not shown) gives an As concentration in detritus of 10 ppm versus 32 ppm elsewhere.
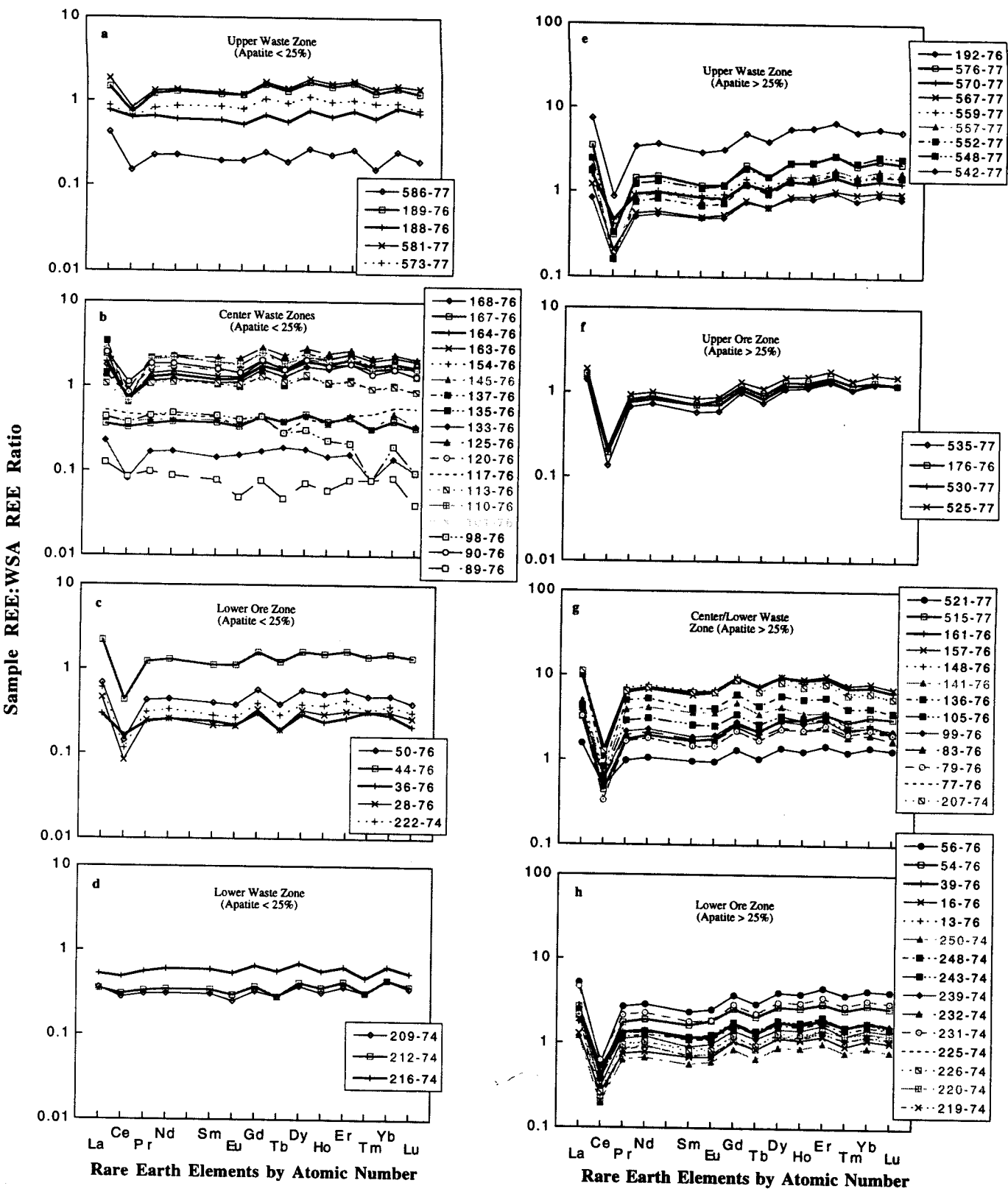
Figure 9. REE patterns of samples with less than 25% apatite (frames a - d) and greater than 25% apatite (frames e - h).
See Figure 2 for explanation of zones. Y-axis is three cycle in all frames. Note grouping in (g).
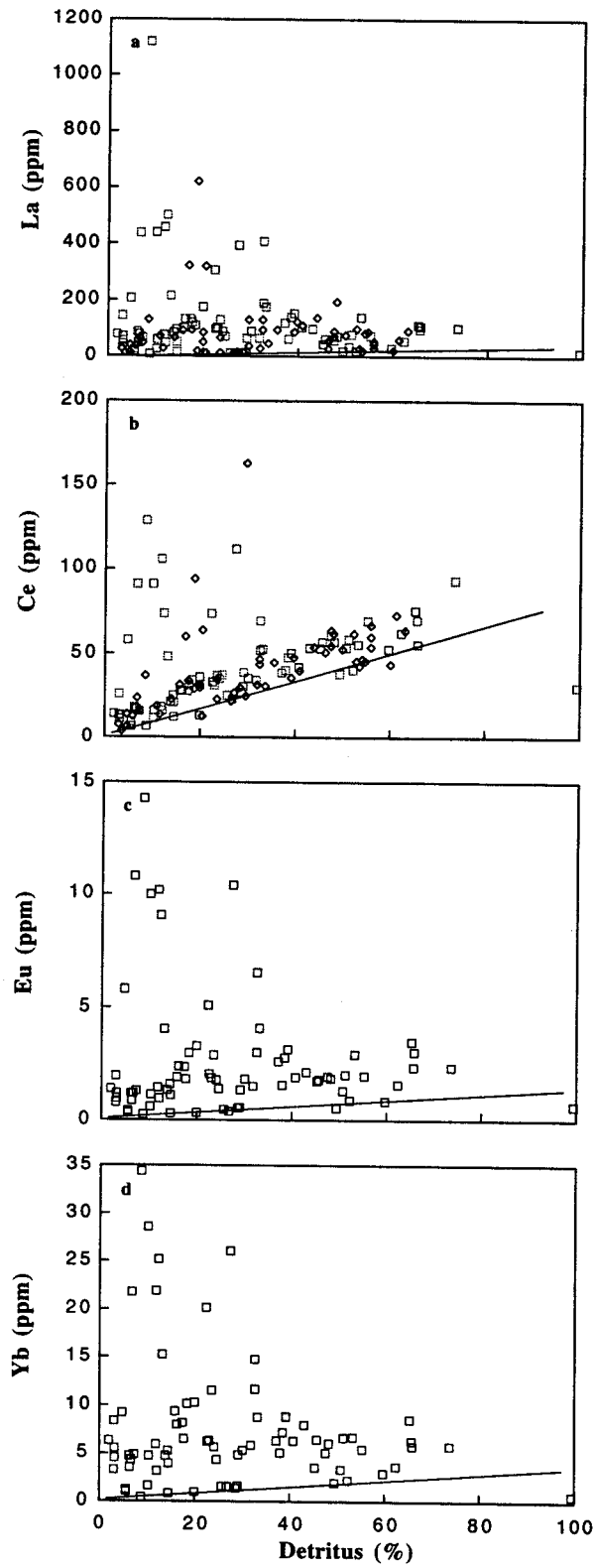
Figure 10. Relation between detritus and selected REE.
Symbols are the same as in Figure 6.
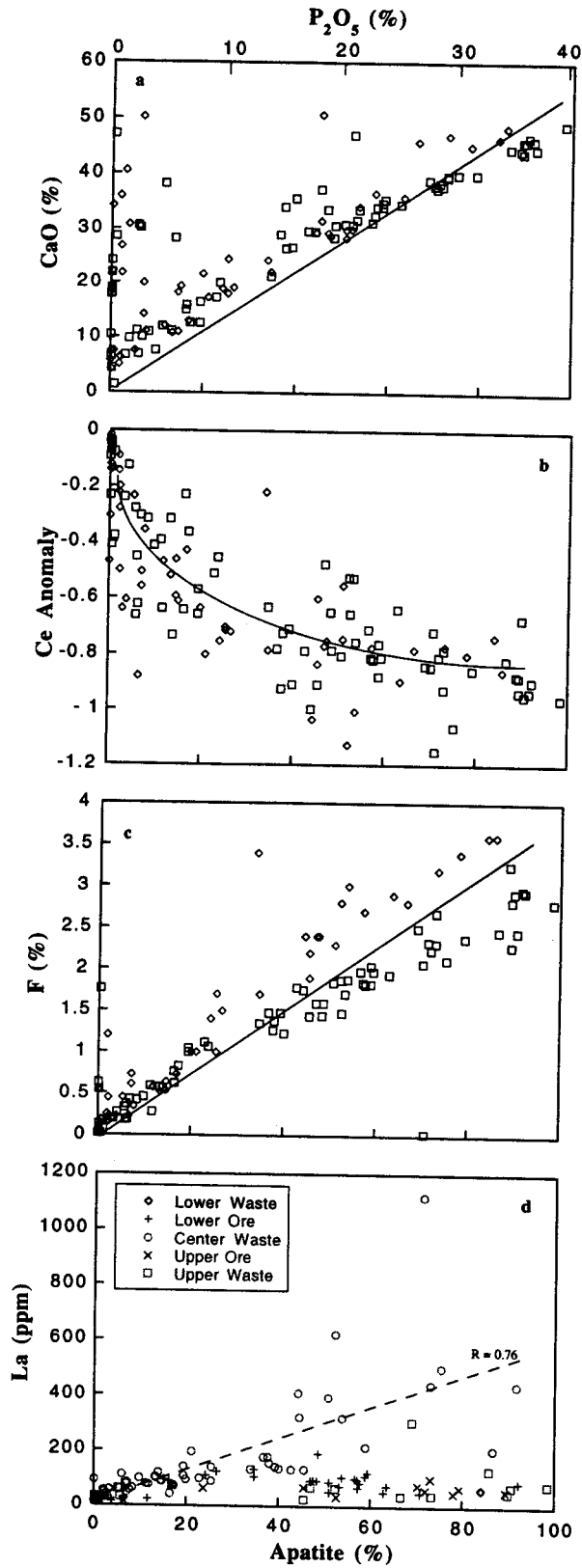
Figure 11. Relation between apatite and CaO (a), Ce anomaly (b), F (c), and La (d). Symbols are the same as in Figure 6 except for frame (d), in which samples from the ore and waste zones are shown. The broken curve is the least-squares best-fit for the center waste only.
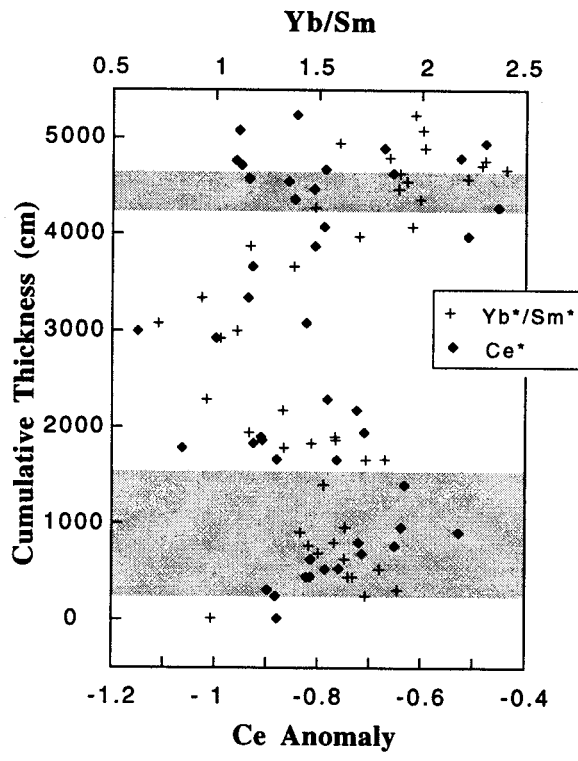
Figure 12. Relation between height above the base of the Meade Peak Member, the Ce anomaly, and normalized Yb:Sm ratios of samples with greater than 25% apatite. Ore zones are shown by shading (Figure 2).
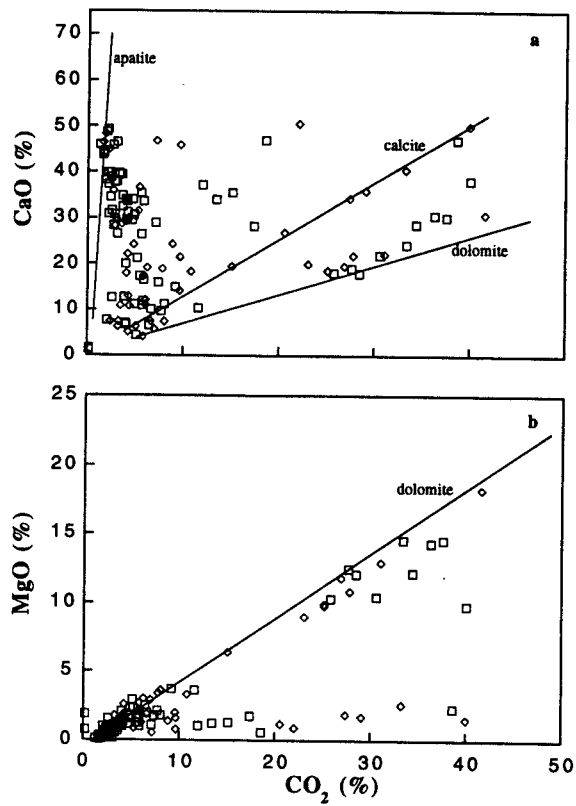
Figure 13. Relation between CO_2 and CaO (a) and MgO (b). Curves represent stoichiometric relations as defined in Table 2.
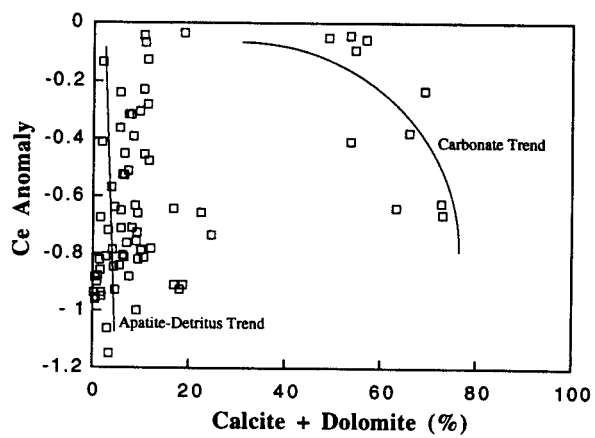
Figure 14. Relation between the sum of carbonate
minerals and the Ce anomaly. Note that the relation
divides samples into two distinct populations.
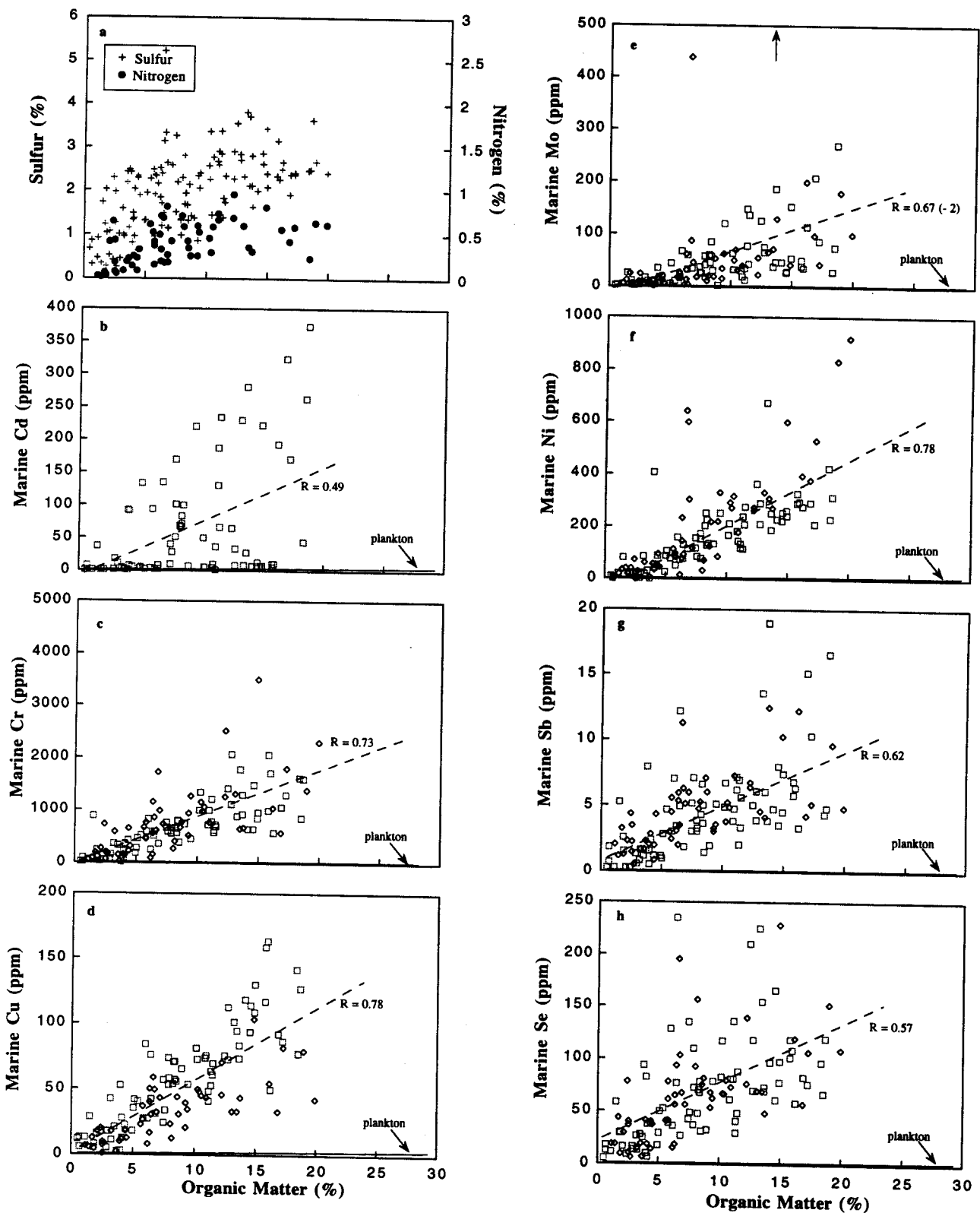
Figure 15. Relations between organic matter, sulfur, nitrogen, and selected trace elements. Solid curves give relations in modern plankton, broken curves give least-squares best fit along with standard deviation. A heteroscedastic distribution is evident in essentially all trace-element plots. Sample symbols are the same as in Figure 6, except for Frame a.
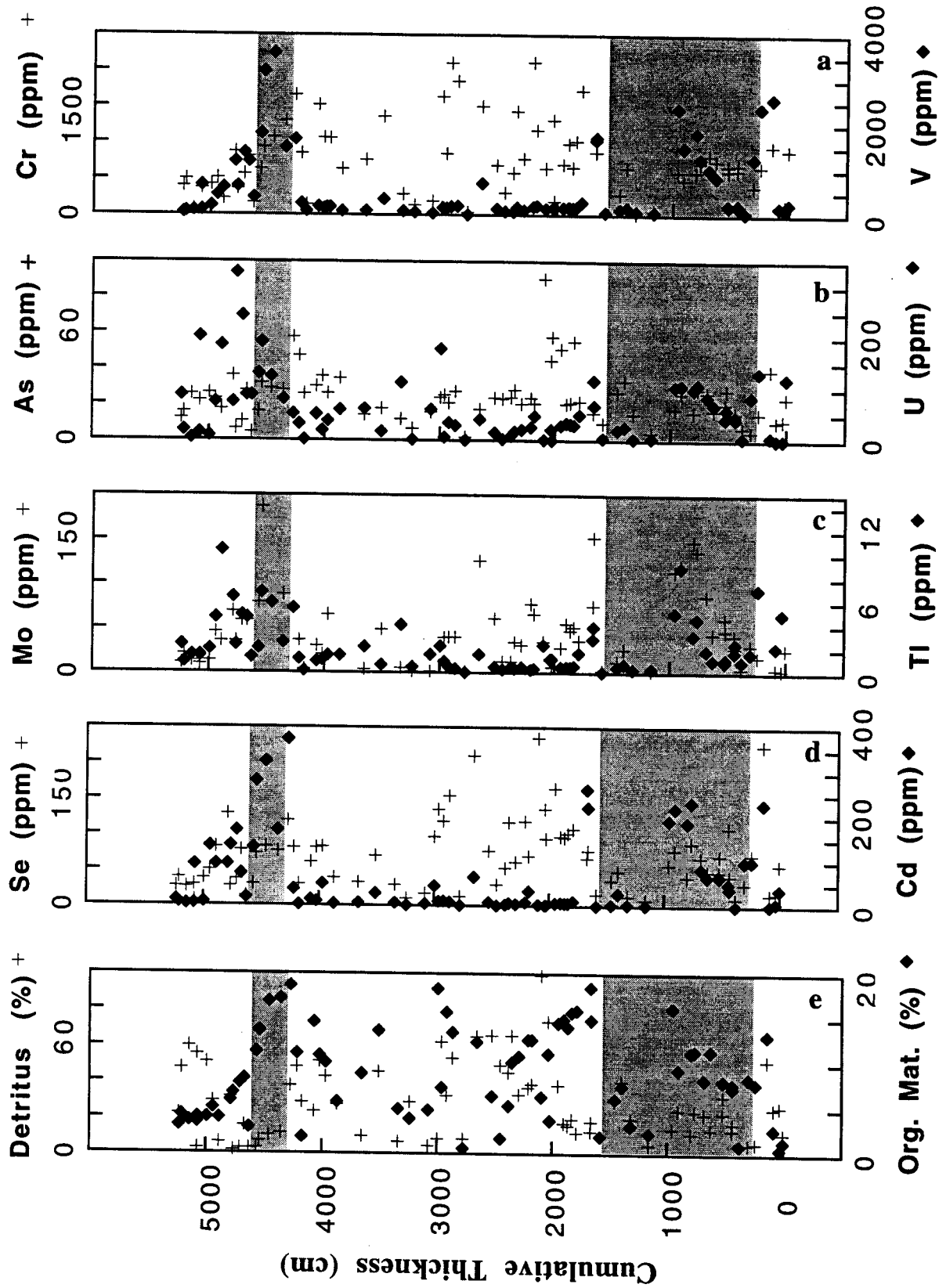
Figure 16. Distribution of selected components and trace elements versus depth, i.e., height above the base of the Meade Member of the Phosphoria Formation at the Hot Springs Mine. The approximate positions of the two ore zones, seen at other sites in SE Idaho, are shown by shading.
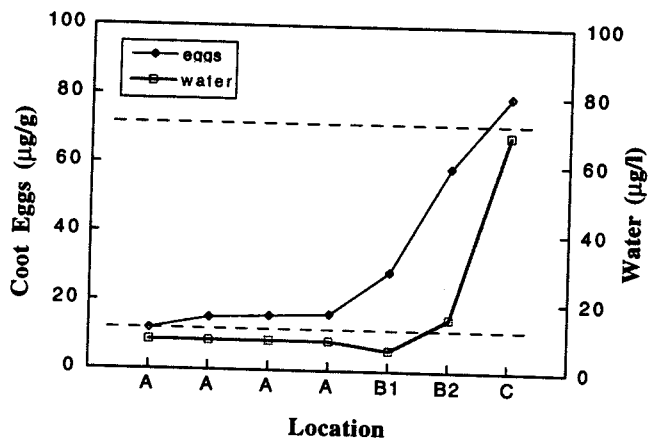
Figure 17. Preliminary results of Se in coot eggs and associated water. Site A is at the lower reservoir north-west of Conda: Sites B are at the upper Reservoir east of Smoky Canyon Mine; Site C is at South Pond, Rasmus-sen Valley. The upper broken curve gives the Se concen-tration above which 100% teratogenesis in embryos is ob-served; the lower broken curve gives the Se concentration above which the incidence of teratogenesis increases with increasing Se concentration. The two values are based on this and other studies. Se was analyzed by fluorescence-based micro-digestion. Water samples were unfiltered. The aim of the method is to ascertain the form of Se in different media. Although the data are preliminary, they compare well with data collected by various other methods used by the U.S. Fish and Wildlife Service.